

Lawrence Berkeley National Laboratory

Recent Work

Title

ESCA

Permalink

<https://escholarship.org/uc/item/8js0045r>

Author

Shirley, David A.

Publication Date

1972

ESCA

David. A. Shirley

January 1972

AEC Contract No. W-7405-eng-48

For Reference

Not to be taken from this room



DISCLAIMER

This document was prepared as an account of work sponsored by the United States Government. While this document is believed to contain correct information, neither the United States Government nor any agency thereof, nor the Regents of the University of California, nor any of their employees, makes any warranty, express or implied, or assumes any legal responsibility for the accuracy, completeness, or usefulness of any information, apparatus, product, or process disclosed, or represents that its use would not infringe privately owned rights. Reference herein to any specific commercial product, process, or service by its trade name, trademark, manufacturer, or otherwise, does not necessarily constitute or imply its endorsement, recommendation, or favoring by the United States Government or any agency thereof, or the Regents of the University of California. The views and opinions of authors expressed herein do not necessarily state or reflect those of the United States Government or any agency thereof or the Regents of the University of California.

ESCA*

David A. Shirley

Department of Chemistry and
Lawrence Berkeley Laboratory
University of California
Berkeley, California 94720

January 1972

I. INTRODUCTION

Since Hagstrom, Nordling, and Siegbahn¹ discovered in 1964 that chemical shifts in the binding energies of atomic core electrons could be detected by high-resolution energy analysis of photoelectrons ejected by characteristic x-rays, a great deal of interest has developed in the study of structural problems by electron spectroscopy. There are in fact a number of ways in which electron spectroscopy--and by this term we mean experimental methods employing the energy analysis of free electrons--can be applied in chemical physics and related fields. The Uppsala group of K. Siegbahn and co-workers has given the collective name ESCA--or Electron Spectroscopy for Chemical Analysis--to these methods. The subject of ESCA in the broad sense is scarcely in need of review at this time, nor could it be covered except in a very superficial manner in the space available here. There are three books available on this subject,^{2,3,4} and the reviewer is aware of at least six more volumes presently in preparation. Instead, this article deals with ESCA in the narrow sense; i.e., with x-ray photoelectron spectroscopy (XPS). The time is ripe for a comprehensive and critical review of chemical shifts in core-electron binding energies, which is by all odds the central topic of XPS. Accordingly the bulk of this article deals with these shifts. The remainder is devoted to the two special topics

of valence shell (or valence band) structure and multiplet splitting of core-orbital hole states--two areas in which, in the reviewer's opinion, the contributions of XPS are sufficiently extensive and well-understood to afford a reasonably definitive review at this time. Thus this article is selective rather than general, even within the relatively narrow confines of XPS. Several important topics were omitted either because they have recently been discussed adequately elsewhere or because they are too new and fragmentary to review at this time. Among these are instrumentation,^{2,3} two-electron effects (Auger, "shake-up", and "shake-off"),^{2,3,5} the reference-level question,⁶ and the recent work of Mateescu on charge distributions in norbonyl ion and related structures.⁷

The objectives of this article did not include the compilation of an exhaustive bibliography even on the topics that are discussed. While it is hoped that no key papers were overlooked, the reviewer hereby tenders apologies to any authors who have been slighted by omission.

This article's length necessitates an outline, which is given below.

- I. Introduction
- II. Chemical Shifts in Core Electron Binding Energies
 - II.A. General Comments
 - II.B. Theoretical Descriptions Based on the Calculation of Binding Energies
 - II.B.1. Methods Involving Both Initial and Final States
 - II.B.1.a. General Background
 - II.B.1.b. Results for Atoms and Ions
 - II.B.1.c. Results for Molecules

- II.B.2. Methods Involving the Initial State Only
 - II.B.2.a. Connection Between Hole-State and Frozen-Orbital Calculations
 - II.B.2.b. Comparison of Orbital Energy Differences with Experiment
- II.C. Quantum-Mechanical Methods Not Involving Binding-Energy Calculations
 - II.C.1. Potential Models
 - II.C.2. The ACHARGE Approach
 - II.C.3. Atomic Charge Correlations
 - II.C.4. Thermochemical Estimates
- II.D. Correlations of Binding-Energy Shifts with Other Properties
 - II.D.1. Correlations with Other Binding Energy Shifts
 - II.D.2. Correlations with Diamagnetic Shielding Constants
 - II.D.3. Correlations with "Pauling Charges" and Electronegativity
 - II.D.4. Correlations with "Group Shifts"
- III. Valence-Shell Structure
 - III.A. Introduction
 - III.B. Valence Bands in Metals
 - III.C. Valence Orbitals: Cross Sections
 - III.D. Valence Orbitals in Inorganic Anions
- IV. Multiplet Splitting
 - IV.A. Introduction
 - IV.B. Multiplet Splitting in Atoms

IV.C. Multiplet Splitting in Molecules

IV.D. Multiplet Splitting in Salts

IV.E. Multiplet Splitting in Metals

II. CHEMICAL SHIFTS IN CORE-ELECTRON BINDING ENERGIES

II.A. General Comments

When a characteristic x-ray photon of energy $h\nu$ ejects an electron from an atomic core orbital, the electronic kinetic energy is given by the relation

$$K = h\nu - E_B \quad , \quad (1)$$

where E_B is the binding energy. This relation is unambiguous for a gaseous sample, while for a solid sample it is true as stated only if E_B is the binding energy referred to the spectrometer vacuum level. To obtain the binding energy relative to the sample's vacuum level one must correct for the contact potential between the sample and the spectrometer, which is just the difference between their work functions,

$$\begin{aligned} K(\text{spect}) &= h\nu - E_B(\text{Fermi}) - \phi(\text{spect}) \\ &= h\nu - E_B(\text{vacuum}) - \phi(\text{spect}) + \phi(\text{sample}) \quad . \quad (2) \end{aligned}$$

Here ϕ denotes the work function, and $K(\text{spect})$ is the kinetic energy of an electron in the spectrometer. On entering the spectrometer an electron is accelerated by an energy $e[\phi(\text{sample}) - \phi(\text{spect})]$. While in principle this correction could be made for solid samples, $\phi(\text{sample})$ is seldom known in practice, and the

correction is seldom made. An element of uncertainty is thus introduced into the binding energy shifts in solids. For this reason detailed comparisons of binding-energy shifts with theory in this article is restricted to data for gaseous samples. This does not imply that shifts in solids cannot be interpreted similarly, but for purposes of evaluating theories of binding-energy shifts, which is our purpose here, gaseous-sample data are clearly preferable. That binding-energy shifts in solids parallel those in gases has been shown explicitly by Gelius, et al.,⁸ who compared experimental shifts for the same compounds as solids and gases, and implicitly by many workers, who found good correlations between shifts in solids and theoretical parameters for free molecules.

The basic physics of core-level binding-energy shifts can be understood in terms of shielding of the core electrons by electrons in the valence shell. When the charge in the valence shell changes, this shielding changes. A useful, albeit oversimplified, classical analogy is that of a charged conducting hollow sphere. If the charge is Q and the radius R , the potential outside the sphere is

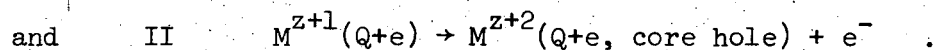
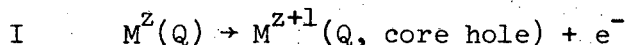
$$\phi(r) = \frac{Q}{r} \quad r > R, \quad (3)$$

while inside the sphere the potential has a constant value

$$\phi_Q = Q/R \quad r < R. \quad (4)$$

Now one component of the energy of a core electron in an atom is the potential energy term due to its interaction with valence electrons. Let us consider the

"chemical shift" in binding energy of a core electron between two charge states of the same atom with charges Q and $Q-e$ in the valence shell. That is, we compare the processes for element M



The notation is straightforward. If step I involved the loss of a core electron from ferrous ion, for example, $M^Z(Q)$ would be $\text{Fe}^{+2}(6)$, etc. The binding-energy shift for a core-electron would be in large part given by (minus) the shift in ϕ_Q . Thus

$$\delta E_B \cong -\delta V_Q \cong (-e) (-\delta\phi) \cong (-e) \frac{\delta Q}{R} = \frac{e^2}{R} \quad (5)$$

where $V_Q = -e\phi_Q$ is the potential energy of a core electron due to the valence shell and R is assumed to be constant for this estimate.

Three useful inferences can immediately be drawn from this crude model:

(1) For any two compounds, the binding-energy shifts of all the core-electron orbitals of a particular atom should be about the same. This follows because ϕ_Q is independent of r , for $r < R$.

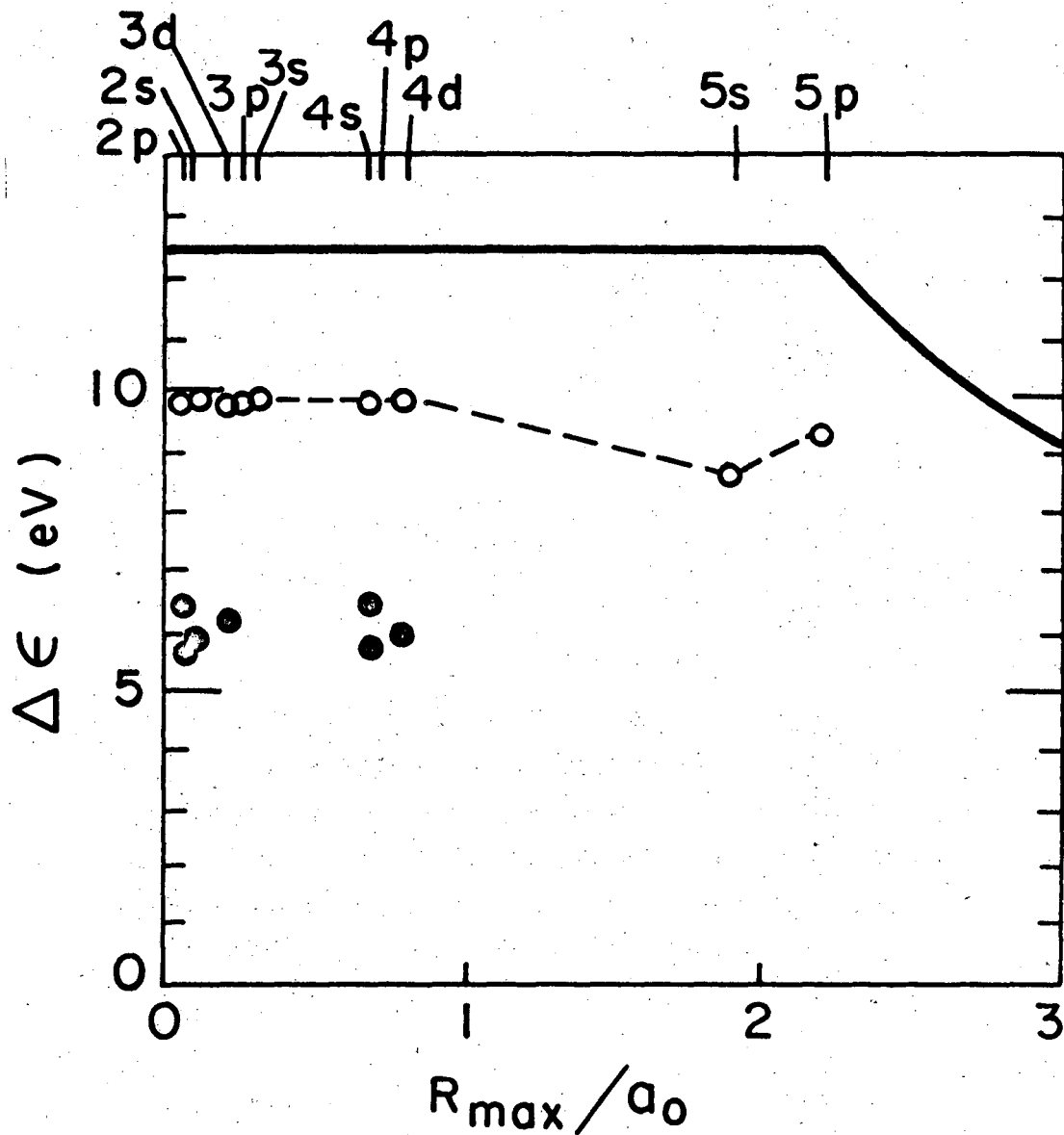
(2) The sensitivity of E_B (core electrons) to Q varies roughly as the inverse of the valence-shell radius, thus increasing toward the top and right side of the periodic table.

(3) For $R = 1\text{\AA}$, $\delta E_B \cong 14.4 \text{ eV}/|e|$, from Eq. (5). This gives an order-of-magnitude estimate for the sensitivity $\delta E_B/\delta Q$.

Fadley, et al.⁹ made a detailed study of shifts in iodine core levels to confirm these predictions. They also estimated shifts from Hartree-Fock orbital energies in free ions. The agreement of the three approaches (classical, Hartree-Fock, and experimental), shown in Fig. 1, provides evidence that the shifts are qualitatively well-understood. For 2s through 4d orbitals, calculated orbital-energy shifts from atomic I(5s² 5p⁵) to ionic I⁺(5s² 5p⁴) are essentially constant, as the classical model predicts. While measurements of binding-energy shifts between these states was not feasible, the total binding-energy shifts from KI to KIO₄ were measured. As Fig. 1 shows, these shifts are essentially the same for all the core orbitals, confirming point (1) above. Point (2) was confirmed by Hartree-Fock calculations on other halogens.⁹ The third prediction was also confirmed by the good agreement between the classical and Hartree-Fock results in Fig. 1. Finally the KI - KIO₄ shifts, corresponding to a change of 8 in the oxidation state of iodine, show a change of less than one electron in the iodine valence shell. This implies that an increase of 1 in oxidation state is accompanied by the loss of ~ 0.1 electron. The ease with which this qualitative conclusion could be drawn is indicative of the directness and power of this method in elucidating chemical structure.

Before proceeding to discuss methods for calculating the chemical shift in binding energy, which we shall denote as δE , a comment about notation is in order. The complete designation of a chemical shift requires specification of the two compounds as well as the parent atom and orbital. Thus

$$\delta E(\text{Cl}s; \text{CH}_4 - \text{CF}_4) = E_{\text{B}}(\text{Cl}s; \text{CF}_4) - E_{\text{B}}(\text{Cl}s; \text{CH}_4) = 11.0 \text{ eV}$$



XBL721-2228

Fig. 1. Core level binding-energy shifts for electrons in iodine, from Ref. 9. The solid curve is based on the classical model (Eqs. (3) and (4)), while the dashed line connects core-level orbital-energy shifts from I to I^+ , from Hartree-Fock theory. Filled circles represent experimental shifts from KI to KIO_4 . Abscissa is the value of the radial maximum for each orbital, in atomic units.

indicates that a carbon 1s electron is 11.0 eV more tightly bound in CF_4 than in methane. Even this designation is incomplete. This shift has been observed in gaseous sources.^{3,10} For solid sources the methane- CF_4 shift is about 1 eV larger.⁸ Thus the state of the sample should always be specified. For technical reasons the temperature and pressure should also be given.

A comment on philosophy is also in order. Binding-energy shifts arise from changes in electronic and nuclear charge distributions between one molecular species and another. They are therefore closely related to properties of great chemical interest. Moreover, binding-energy shifts are not only well understood in principle theoretically, but the actual numerical calculation of shifts is straightforward, if tedious. In addition, the origins of these shifts are intuitively obvious, and "back-of-the-envelope" estimates usually give fairly good results, in contrast to the situation that obtains for NMR chemical shifts or Mössbauer isomer shifts. Indeed, binding energy shifts are so well understood that they can be calculated in a number of different ways. Although different approaches may be compared in regard to rigor, accuracy, applicability, etc., it would be impossible to classify them in terms of overall merit because the value of a given method is determined largely by the problem at hand. Instead, the discussion below treats a variety of theoretical approaches to binding energies and shifts approximately in order of decreasing rigor. This ordering is precise only at the beginning, where the different approaches are related by a well-defined series of approximations.

II.B. Theoretical Description Based on the Calculation of Binding Energies

Chemical shifts in binding energies may be obtained by evaluating the binding energies and taking differences; or they may be estimated directly. The former, more rigorous, approach is discussed first.

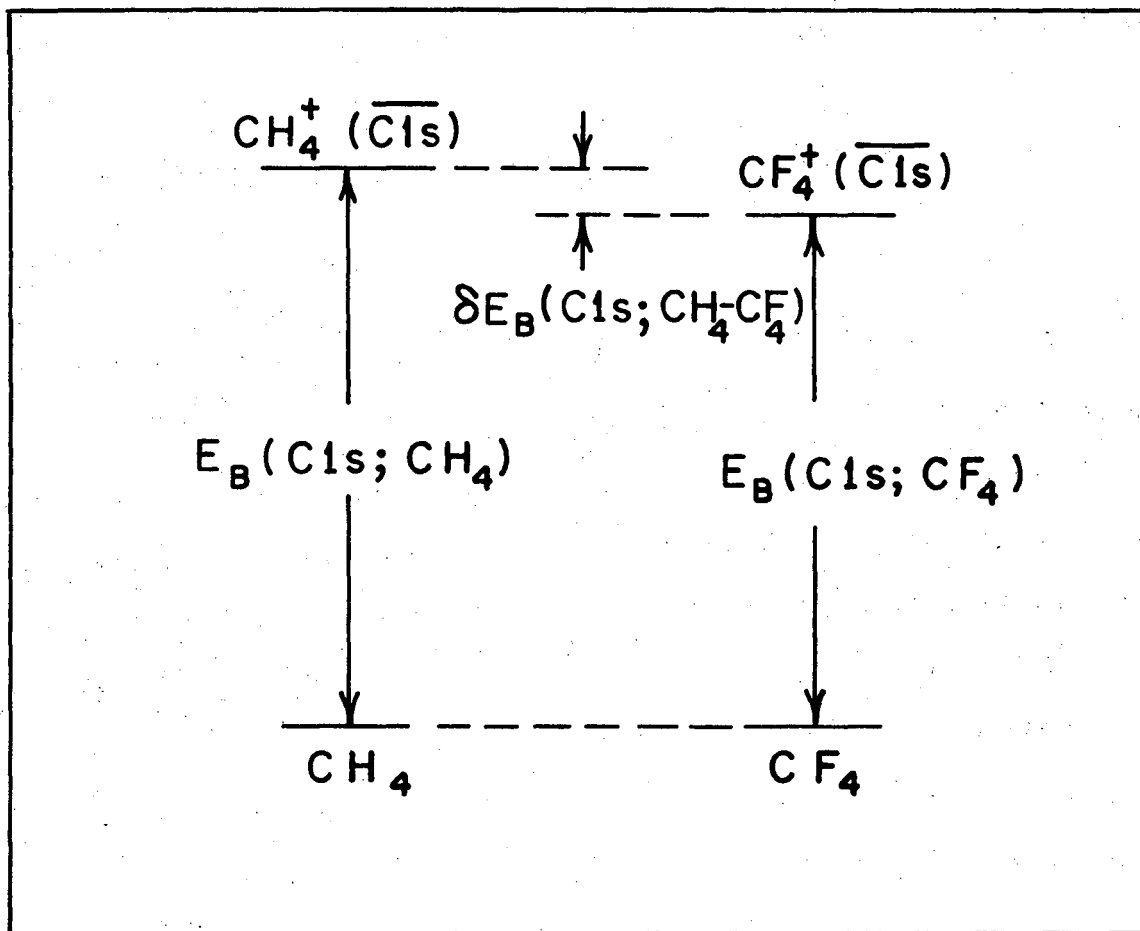
II.B.1. Methods Involving Both Initial and Final States

II.B.1.a. General Background. The energy relationships among the four states that determine the $\text{CH}_4 - \text{CF}_4$ chemical shift are indicated in Fig. 2. The total energies of all four states must be calculated in order to predict this shift rigorously. An exact calculation of the total energy of even simple multi-electron atomic systems is of course impractical, but self-consistent field (SCF) methods, with corrections, can yield rather accurate total energies. All of the binding energies discussed below were calculated either by the Hartree-Fock method or by the Dirac-Fock method. The former is based on the (nonrelativistic) Schrödinger Equation and the latter on the (relativistic) Dirac Equation. Relativistic effects are important for large binding energies, as the electron's velocity in the bound state is no longer negligible compared to the velocity of light. Because the properties of core electrons represent rather unfamiliar territory for most workers, it is useful to have a method for making rough estimates of the magnitude of the relativity correction. The relativistic kinematics of a free particle are described by the relation

$$E^2 = m^2 c^4 + p^2 c^2 = m^2 c^4 + \frac{m^2 c^2 v^2}{1 - v^2/c^2}$$

Expansion in powers of v/c yields (through order $(v/c)^5$)

$$E = mc^2 + \frac{1}{2}mv^2 \left[1 + \frac{3}{4}\left(\frac{v}{c}\right)^2 + \dots \right]$$



XBL721-2229

Fig. 2. Relationship of the four states that determine the CH₄ - CF₄ shift in the carbon 1s binding energy. Bars denote hole states of ions, and equality of initial-state energies indicates that both molecular species are at ground potential.

Thus the kinetic energy is increased, and (using the virial theorem) the total energy is decreased, by a fraction $\sim \frac{3}{4}(\frac{v}{c})^2$ because of relativity. As numerical examples let us consider atomic carbon and argon, with approximate 1s binding energies of 11 a.u. (~ 300 eV) and 120 a.u. (~ 3200 eV) respectively. The electron's rest mass is 511 keV. Thus

$$\delta E_B(\text{rel}) \approx \frac{3}{4} \left(\frac{v}{c}\right)^2 E_B \approx \frac{3}{2} \frac{E_B^2}{5.11 \times 10^5 \text{ eV}} \approx 0.01 \text{ a.u. for carbon}$$

$$\approx 1.2 \text{ a.u. for argon}$$

In terms of absolute binding energies the relativity correction is therefore fairly unimportant (0.1% or 0.3 eV) for the carbon 1s electron, while for the argon 1s case the correction is too large (1% or 30 eV) to ignore. Accurate values of the relativity corrections to the total energies of these two atoms have been given by Veillard and Clementi.¹¹ They are 0.01381 1.76094 au (argon). In both cases most of the correction may be assigned to the two 1s orbitals. Thus our rough estimate of $\delta E_B(\text{rel})$ are $\sim 50\%$ too large.

The Hartree-Fock Equations for n doubly occupied orbitals have the form (in atomic units)

$$\left[\left(-\frac{1}{2} \nabla^2 - \sum_k \frac{Z_k}{r_k} \right) + \sum_{j=1}^n (2J_j - K_j) \right] \phi_i = \epsilon_i \phi_i$$

Here ϕ_i is a one-electron orbital. The first term in parentheses accounts for an electron's kinetic energy plus its interaction with all nuclei. The Coulomb operator K_j have matrix elements

$$J_{ij} = \langle \phi_i(\mu) | J_j | \phi_i(\mu) \rangle = \langle \phi_i(\mu) | \langle \phi_j(\nu) | \frac{1}{r_{\mu\nu}} | \phi_j(\nu) \rangle | \phi_i(\mu) \rangle$$

$$K_{ij} = \langle \phi_i(\mu) | K_j | \phi_i(\mu) \rangle = \langle \phi_i(\mu) | \langle \phi_j(\nu) | \frac{1}{r_{\mu\nu}} | \phi_i(\nu) \rangle | \phi_j(\mu) \rangle ,$$

where μ and ν label electron coordinates. There are n Hartree-Fock equations in ϕ_i , with $i = 1, 2, \dots, n$. They must be solved iteratively until self-consistency is achieved, yielding a total determinantal wave function

$$\Psi = | \phi_1^2 \phi_2^2 \dots \phi_n^2 | .$$

The individual Hartree-Fock Equations are "pseudo-eigenvalue" equations. The left hand side of the Hartree-Fock Equation can be abbreviated to $\mathcal{F} \phi_i$, where \mathcal{F} is called the Fock Operator. The orbital energies ϵ_i are given by

$$\epsilon_i = \langle \phi_i | \mathcal{F} | \phi_i \rangle = \epsilon_i^0 + \sum_j (2J_{ij} - K_{ij}) . \quad (6)$$

The one-electron energy ϵ_i^0 is the expectation value of the one-electron operator $-\frac{1}{2} \nabla^2 - \sum_n Z_n / r_n$. The total Hartree-Fock energy of a system with n doubly-occupied orbitals is

$$E_{\text{HF}}^{(2n)} = 2 \sum_{i=1}^n \epsilon_i^0 + \sum_{i,j=1}^n (2J_{ij} - K_{ij}) . \quad (7)$$

To obtain the Hartree-Fock approximation to the adiabatic ionization potential of the k^{th} orbital of this system, another Hartree-Fock energy $E_{\text{HF}}^{(2n-k)}$ must be

obtained by solving the Hartree-Fock Equation with the k^{th} orbital singly occupied. An approximate value $E_{\text{HF}}^{(2n-k) \prime}$ can be estimated, however, simply by striking from Eq. (7) those terms that can be associated with a single electron in the k^{th} orbital, i.e.,

$$E_{\text{HF}}^{(2n-k) \prime} = \epsilon_k^{\circ} + 2 \sum_{i \neq k}^n \epsilon_i^{\circ} + \sum_{i, j \neq k}^n (2J_{ij} - K_{ij}) + \sum_{i \neq k}^n (2J_{ij} - K_{ij}) \quad (8)$$

This is the final-state energy that the system would have if there were no relaxation of the passive orbitals during ionization, that is, if the ionization were "sudden". The sudden ionization energy of the k^{th} orbital in the Hartree-Fock scheme,

$$E_{\text{HF}}^{(2n)} - E_{\text{HF}}^{(2n-k) \prime} = \epsilon_k^{\circ} + \sum_{i \neq k}^n (2J_{ik} - K_{ik}) + J_{kk} \quad (9)$$

is just equal to the orbital energy ϵ_k , as comparison of Eqs. (6) and (9) will show. This result was first shown by T. Koopmans.¹² It is known as Koopmans' Theorem. Because neglecting final-state relaxation (i.e., taking the integrals in Eq. (8) to having the same values as in Eq. (7)) always gives final-state energies that are too high, the sudden approximation overestimates binding energies. By contrast, neglect of relativity clearly tends to give estimates of ionization potentials that are too small. Further discussion of orbital-energy estimates of binding energies is given in Section A.2.

The use of the Hartree-Fock method to calculate the energy of a highly excited state (such as a $1s$ "hole" state) is subject to question. For the lowest state of each symmetry type the variational principle guarantees that the

Hartree-Fock energy gives an upper bound to the true energy of the system. For a higher state of a given symmetry type this holds only if McDonald's Theorem¹³ is satisfied; i.e., only if the state in question is orthogonal to all lower states of its symmetry type. For most systems a 1s hole state is so high in energy that there are many lower-lying states of the same symmetry, and orthogonalizing it to all of these states would be a formidable task. Bagus¹⁴ and Verhaegen, et al.,¹⁵ have pointed out, however, that the 1s hole state is unusual in that the 1s orbital has little overlap with the valence orbitals. Off-diagonal elements of the interaction matrix between the 1s-hole state and the lower states will therefore be small in comparison to differences in their energies. Thus the hole state would be changed little by orthogonalizing it to the lower states. In the calculations to date, hole states have simply been treated as if they satisfied McDonald's theorem.

II.B.1.b. Results for Atoms and Ions. Bagus¹⁴ made the first complete Hartree-Fock calculations on the hole states that can be formed by ejecting an electron from the closed shell configurations F^- , Ne, Na^+ , Cl^- , Ar, and K^+ . After making a relativity correction, he found that core-electron binding energies calculated from initial and final-state energies agreed better with experiment than did those estimated from ground-state orbital energies. His results for the s-type hole states of neon and argon are set out in Table I. In comparing his results with experiment, Bagus observed that the remaining errors in the binding energies were positive in some cases and negative in others. This was somewhat unexpected, because these errors arise almost entirely from differences between the electron correlation energies of the initial and final states. From a naive point of view the correlation energies might be expected

to be pairwise transferable. The initial state would then always have a larger correlation energy than the final state simply because it has more electrons, and the true binding energy would always be larger than the Hartree-Fock value corrected for relativity. In fact the opposite is often true. Bagus pointed out how this can be understood in terms of configuration interaction. The $\text{Ne}^+(1s^2 2s^2 2p^6)$ state, for example, can interact with configurations made by promoting only one electron to states with principle quantum number $n > 2$ (e.g., $1s^2 2s^2 2p^4 ns$). Thus its total energy is lowered more by electron correlation than is that of neutral neon in its ground state, because the configuration $1s^2 2s^2 2p^6$ can interact only with configurations formed by promoting two or more electrons to states with $n > 2$.

Even without corrections for correlation, Bagus' hole-state binding energies were accurate to 0.2%.

Rosén and Lindgren¹⁶ carried out relativistic Hartree-Fock-Slater (HFS) calculations on many atoms. They have given results for states in Cu, Kr, I, Eu, Hg, and U. Although HFS calculations are ordinarily more approximate than HF calculation because exchange effects are estimated by using the "Slater exchange potential"

$$v_{\text{ex}}(r) = - \left[\frac{81 \rho(r)}{32 \pi^2 r^2} \right]^{1/3}$$

However, these workers parameterized this potential as

$$v'_{\text{ex}}(r) = - \frac{c}{r} \left[\frac{81 r^n \rho(r)^m}{32 \pi^2} \right]^{1/3}$$

Table I. The ns Binding Energies of Neon and Argon (after Bagus¹⁴)

Final State ^a	$E_B(\text{expt})^b$	$\Delta E_B^{\text{rel}^d}$	$E_B(\text{sudden})^e$	$\Delta E_B(\text{sudden})^f$	$E_B(\text{adiabatic})$ $= E_{\text{hole}} - E_0$	$\Delta E_B(\text{adiabatic})^f$
Ne($\overline{2s}$)	1.7815		1.9303	- 0.1488 (- 4.049 eV)	1.8123	-0.0308 (-0.838 eV)
Ne($\overline{1s}$)	31.981(4) ^c	0.040	32.812	- 0.831 (-22.6 eV)	31.961	+0.020 (+0.54 eV)
Ar($\overline{3s}$)	1.0745		1.2773	- 0.2028 (- 5.518 eV)	1.2198	-0.1453 (-3.954 eV)
Ar($\overline{2s}$)	11.992(3) ^c		12.3219	- 0.330 (- 9.0 eV)	11.938	+0.054 (+1.5 eV)
Ar($\overline{1s}$)	117.83(2) ^c	0.54	119.15	- 1.32 (-35.9 eV)	117.97	-0.13 (-3.5 eV)

^aBar denotes hole relative to ground-state neutral atom initial state.

^bEnergies are in Hartrees (1 Hartree = 27.210 eV) unless otherwise indicated.

^cNew experimental value from Ref. 3. Error in last place is given parenthetically.

^dRelativity correction which has been added to Bagus' theoretical binding energies to give results in columns 4 and (6).

^eFrom orbital energies and relativity correction.

^fHere $\Delta E_B = E_B(\text{expt}) - E_B(\text{theo.})$.

00008700000

and did variational calculations to optimize c , n , and m . Their total energies obtained with optimized parameters appear to be essentially identical to the Hartree-Fock values. They calculated binding energies in two ways. Their "Method A" was based on "frozen" orbitals and therefore similar to the orbital energy approach (but not identical, as Koopmans' Theorem doesn't hold for the HFS approximation). In their "Method B", optimized HFS calculations were carried out on both the initial and the final states, and the binding energies were obtained by difference. The agreement of these binding energies with experiment varied considerable, but Method B tended to be within 1% of experiment and Method A within 2%. In many cases the agreement was much better than these figures. Results for several states with binding energies in the range of interest for ESCA studies are given in Table II.

The binding-energy calculations of Rosén and Lindgren are extended over the periodic table, and to discuss them in detail would be beyond the scope of this article. In seeking an explanation for the significant residual discrepancies between theory and experiment they invoked the Lamb shift for the inner shells of heavy atoms, and the magnitude of this effect appears to be about correct. For smaller binding-energy cases they discounted correlation effects because they expected correlation to increase the theoretical binding energies, which were already too large. In view of Bagus' discussion this interpretation should be reinvestigated.

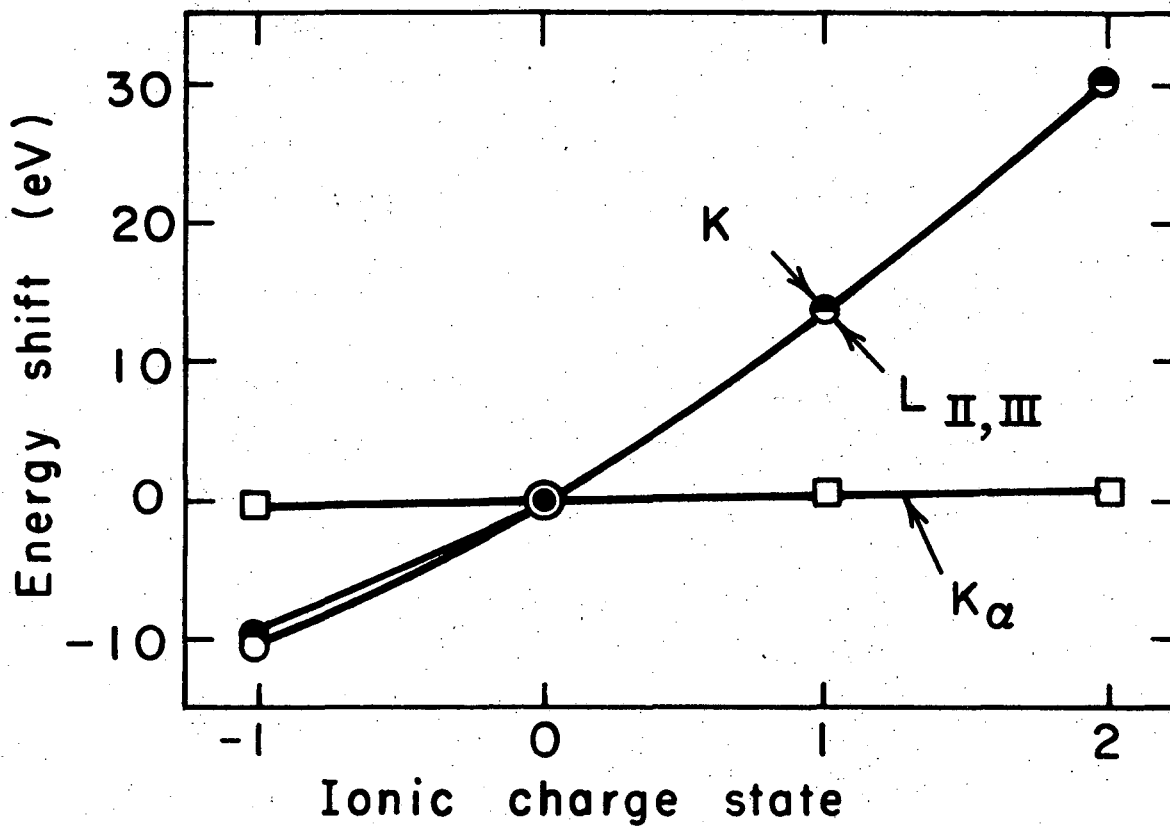
Gianturco and Coulson¹⁷ made both orbital-energy estimates (Method A) and hole-state calculations (Method B) of the binding energies of atomic and ionic sulphur. They did both HF and HFS calculations. Their results for neutral sulphur are given in Table III. The binding energies agree well with experiment, especially for the Hartree-Fock Method B case.

Table III. Sulphur Binding Energies (in eV) after Gianturco and Coulson¹⁷

State	Method A HF	Method A HFS	Method B HF	Method B HFS	Expt(x-ray)	Expt(ESCA)
1s	2503.6	2496	2474	2484	2476	2477
2s	245	239	233	238	231	233
2p	181	174	172	173	170	169
3s	23	22	22	23	21	--
3p	11.5	10	11	10	12	--

These authors also studied the variation of E_B with ionic state for the K and L shells of sulphur. They found average shifts of ~ 16 eV per ionization state in each case. This is expected, as Fadley et al.⁹ have discussed, because the shielding in both of these inner shells is essentially complete. In fact the simple argument that shielding by the M shell is less complete for the L shell than for the K shell correctly predicts the L-shell shifts to be slightly smaller than the corresponding K-shell shifts. The similarity of magnitudes of the two bodes ill for the sensitivity of shifts in the K_{α} x-ray emission lines, however, as Gianturco and Coulson noted. In fact the situation for the range of sulfur charge states (not oxidation states) that is chemically realizable, i.e., about -1 to +2, is much worse than might be inferred from their complete calculation for ionic charge states between -2 and +6, because the K_{α} energies shift little with charge for charge states near zero compared to the shifts in highly-ionized states. Again the physical reason for this is clear: as the charge in the sulphur ion increases through successive loss of the M electrons, the radial wave functions of those remaining are drawn in until they can no longer shield the L shell as effectively as the K shell. For charge states near zero, on the other hand, both K and L electrons are in more nearly true "core" orbitals, in which their energies are affected equally by the valence shell. The sensitivity advantage of ESCA shifts over K_{α} shifts is illustrated for this case in Fig. 3.

Verhaegen, et al.¹⁵ described an accurate calculation of the 1s and 2s binding energies of atomic neon. Their calculation is unique in that they evaluated explicitly the effects of relativity and correlation on the binding energies of the 1s and 2s orbitals. Table IV displays their results for these two cases.



XBL 721-2230

Fig. 3. Shift in K and L binding energies and in K α x-ray energy with charge state of free sulfur, after Gianturco and Coulson. Total binding energy (ESCA) shift is 40 eV: total x-ray shift is only 1.2 eV.

Table IV. Binding Energies in Neon (in eV) after Verhaegen, et al.¹⁵ and Bagus¹⁴

Method	$E_B(1s)$ (Ref. 15)	$E_B(1s)$ (Ref. 14)	$E_B(2s)$ (Ref. 15)	$E_B(2s)$ (Ref. 14)
Orbital Energy	891.7	891.7	52.5	52.5
HF Hole State	868.6	868.6	49.3	49.3
RHF Hole State	869.4	869.7	49.4	--
RHF Hole State plus Correlation	870.8	(871.1)	48.3	(48.2)
Experiment(Ref. 2)	870.2		48.4	

These workers accounted for relativity directly, by solving the Dirac-Fock (or relativistic Hartree-Fock, RHF) equation.

Verhaegen et al. extended core-level binding-energy calculations to a higher level of sophistication by including accurate corrections for correlation energy. It is necessary, in open-shell systems, to distinguish among three kinds of correlation energy which Öksüz and Sinanoğlu¹⁸ have classified as "internal", "polarization plus semi-internal", and "all-external". In internal correlations, two electrons correlate but shift to vacant Hartree-Fock orbitals. One electron in a pair shifts to a vacant Hartree-Fock orbital and one shifts out of the "Hartree-Fock sea" in semi-internal correlation, while in the "all-external" case both electrons shift to non-Hartree-Fock orbitals. Clearly only the last kind of correlation is available to closed-shell systems. Verhaegen, et al. noted that correlation effects will shift the energy of the atomic $\text{Ne}^+(\overline{1s})$ state relative to $\text{Ne}(^1S)$ by an amount

$$\Delta E_{\text{corr}} = -[\epsilon(1s, \overline{1s}) + \epsilon(1s, 2s) + \epsilon(1s, \overline{2s}) + 3\epsilon(1s, 2p) + 3\epsilon(1s, \overline{2p})] ,$$

where the pair correlation energies ϵ are all negative. This expression is based on the assumption that all the pair correlations are transferable. In fact this is essentially true for the (closed-shell) ground state, while the $1s$ hole state also has the possibility of semi-internal correlation. This was assumed to be negligible, however, because of the unusual nature of this highly-excited state. Using Nesbet's¹⁹ values for the pair correlation energies in $\text{Ne}(^1S)$, obtained by solving the Bethe-Goldstone equations, Verhaegen et al. found $\Delta E_{\text{corr}} = +0.0524$ au for this case. This direction, an increase in E_B because of correlation, is the normal one. For the $\text{Ne}^+(\overline{2s})$ case, however,

semi-internal correlation is important, lowering the energy by 0.0978 a.u., according to the calculations by Öksüz and Sinanoğlu. This is more than enough to offset the external contribution of 0.0542 au to the energy difference between $\text{Ne}^+(\overline{2s})$ and $\text{Ne}(1s)$, and the net contribution of correlation is to decrease the binding energy by 0.0436 a.u.

Table IV deserves careful scrutiny, because neon, with its closed shells, is the ideal test case for calculating core-electron binding energies. Furthermore, the results given for neon represent the first detailed attempt to include electron correlation effects. Bagus' results from Table I are included for comparison. There is a discrepancy of 0.3 eV (0.01 a.u.) in the RHF 1s binding energies before the correlation correction. The 0.6 to 0.9 eV discrepancy between theory and experiment is perplexing. The experimental accuracy is 0.1 eV, so the difference must be taken seriously. It is by no means obvious where the error lies, but the assumption, that the "unusual" nature of the 1s hole state justifies simplifying approximations in the calculation of this state's HF energy and its correlation energy, deserves further study.

II.B.1.c. Results for Molecules. Schwartz²⁰ reported the first hole-state calculations in molecules. He used a Gaussian orbital basis set for both excited and ground states, and tested his method of choosing orbitals by comparison of calculations on Ne with Bagus' results.¹⁴ Neither relativity nor correlation were explicitly considered. Calculations were made on BH_3 , CH_4 , NH_3 , H_2O , HF, and Ne. At that time experimental 1s binding energies were known only for CH_4 and Ne. Since then results for NH_3 and H_2O have become available. The calculated values, shown in Table V, are in excellent agreement with experiment. In fact the agreement is fortuitously good. The relativity correction will increase

Table V. Hole-State 1s Binding Energies in Molecules

Molecule	Hole	E_B (expt) ^a	E_B (theory)	E_B (theory, corrected) ^l
BH ₃	B1s	--	197.5 ^e	198.9
CH ₄	C1s	290.8 ¹⁰ , 290.7 ³	291.0 ^e , 290.7 ^f , 292.9 ^g , 298.0 ^h , 283.8 ^m	292.5, 292.2, 294.4, 299.5, 285.3
NH ₃	N1s	405.6 ³	405.7 ^e , 408.6 ^h , 400.9 ^m	407.3, 410.2, 402.5
H ₂ O	O1s	539.7 ³	539.4 ^e , 539.7 ^f , 540.8 ^h , 512.3 ^m	541.2, 541.5, 542.6, 513.1
HF	F1s	--	693.3 ^e	695.3
CO	C1s	296.2, 295.9 ³	295.9 ^f	297.4
CO	O1s	542.6, 542.1 ³	542.1 ^f	543.9
CH ₃ F	C1s	293.6, 293.5 ^c	296.3 ^g	297.8
	F1s	692.4 ¹⁰		
CH ₂ F ₂	C1s	296.4 ^b	299.3 ^g	300.8
	F1s	693.1 ^b		
CHF ₃	C1s	299.1, 298.8 ³	302.7 ^g	304.2
	F1s	694.1 ¹⁰		
CF ₄	C1s	301.8, 301.8 ³		
	F1s	695.0 ¹⁰		
C ₂ H ₄	C1s	290.7	298.1 ^h	299.6

(continued)

Table V (continued)

Molecule	Hole	E_B (expt) ^a	E_B (theory)	E_B (theory, corrected) ^l
NO	Nls, $^3\pi$	410.3 ³	411.17 ⁱ	412.7
	Nls, $^1\pi$	411.8 ³	412.52 ⁱ	414.1
	Ols, $^3\pi$	543.3 ³	542.1 ⁱ	543.9
	Ols, $^1\pi$	544.0 ³	542.5 ⁱ	544.3
O ₂	Ols, $^4\Sigma_g^-$	543.2, 543.1 ¹⁰	542.0 ^j	543.8
	Ols, $^2\Sigma_g^-$	544.3, 544.2 ¹⁰	542.6 ^j	544.4
furan	Ols	539.4 ^d	547.75 ^k	549.5

^aValues from Refs. 3 and 10 are so labeled. If no reference is given, shifts are from D. W. Davis, J. M. Hollander, D. A. Shirley, and T. D. Thomas, J. Chem. Phys. 52, 3295 (1970) and hydride reference values from Ref. 10 (C) or 3 (N,O). Accuracy is ± 0.1 to ± 0.2 eV.

^bD. W. Davis, D. A. Shirley, and T. D. Thomas, J. Chem. Phys. 56, 671 (1972).

^cRef. 8.

^dUppsala group, quoted by P. Siegbahn, Chem. Phys. Letters 8, 245 (1971).

^eRef. 20.

^fRef. 24.

^gFrom C. R. Brundle, M. B. Robin, and H. Basch, J. Chem. Phys. 53, 2196 (1970).

^hR. Moccia and M. Zandomenighi, Chem. Phys. Letters 11, 221 (1971).

ⁱP. S. Bagus and H. F. Schaefer III, J. Chem. Phys. 55, 1474 (1971).

^jP. S. Bagus and H. F. Schaefer III, J. Chem. Phys. 56, 224 (1972).

^kP. Siegbahn, Chem. Phys. Letters 8, 245 (1971).

(continued)

0 0 0 0 8 7 0 0 9 9 2

Table V (continued)

The following corrections for relativity plus correlation have been estimated by the reviewer:
B, 1.4 eV; C, 1.5 eV; N, 1.6 eV; O, 1.8 eV; F, 2.0 eV. See footnote 22 and Refs. 18, 21, and 23.
Ref. 26.

the binding energy by from 0.1 eV for CH_4 to 1.2 eV for Ne,²¹ while correlation will raise E_B by about 1.4 eV for each case.^{22,23} The values of E_B after these corrections are given in Table V.

Hillier, Saunders, and Wood²⁴ took a different approach to calculating $E_B(1s)$ for CH_4 , H_2O , and CO . They calculated the ground state using a double zeta basis set of Slater type orbitals, found the Koopmans' Theorem E_B , and then accounted for relaxation in the valence orbitals via a CI calculation on the ions using virtual molecular orbitals from the neutral-molecule calculations. It is difficult to evaluate the results of this work, but a few observations can be made. First, the basis set was small, and the total energies were high by up to 0.15 au (4 eV). The orbital energies were in error by only ~ 0.5 eV, however. The CI calculation presumably accounted for some correlation, but not $1s$ - $1s$ correlation, since only valence electrons were considered. Finally, relativity was neglected. The question of whether extra-atomic polarization effects differ enough from one molecule to another that hole-state calculations would predict shifts better than would orbital energies is unfortunately left open. The $1s$ shift between CO and H_2O is improved from 4.86 eV using orbital energies to 3.63 eV when relaxation is considered (the experimental shift is 2.94 eV). In contrast the $1s$ shift between CO and CH_4 is worsened (5.46 eV from orbital energies, 7.55 eV with relaxation, and 5.4 eV experimentally).

Brundle, Robin, and Basch²⁵ have carried out $1s$ hole-state calculation on CH_4 , CH_3F , CH_2F_2 , and CHF_3 . Their values of $E_B(1s)$ are about 4 eV higher than experiment after our (problematical) correction for relativity and correlation. These authors suggested that the correlation energy may be larger in the hole states than in the ground states of these molecules, thus tending

to decrease the theoretical binding energies toward the experimental values. This seems unlikely, but even if it were true, it would presumably obviate the basis upon which the hole-state calculations were made to begin with: namely, the "unusual" nature of the 1s hole state. The success of this calculation in predicting shifts will be discussed in a later section.

Gianturco and Guidotti²⁶ have cast doubt on hole-state calculations that simply follow the aufbau criterion of emptying a hole-state orbital in the ground-state basis set. In order to test the effect of basis-set flexibility, these workers employed very large basis sets: 39 Slater-type orbitals for CH₄, 32 for NH₃, and 29 for H₂O. The 1s binding energies obtained were low by 7.0 eV, 4.7 eV, and 27.4 eV respectively. They attributed this discrepancy to the failure of the SCF calculations to provide a true upper bound because of lack of orthogonality to lower states. As especially clear evidence of this effect they noted that while their calculations gave discrepancies of only a few eV for CH₄ and NH₃, a larger discrepancy was found for H₂O, for which they used a richer atomic basis set on the heavy atom, and in the ground state of which there are three filled a₁ molecular orbitals.

Moccia and Zandomeneghi²⁷ have offered a solution to the above problem. They used an approach called the strong orthogonal group function (GF) approximation.²⁸ They approximated the neutral-molecule wave function by an anti-symmetrized product of geminals constructed from sets of orbitals localized around the K shell. The K-hole state was then described by eliminating one electron from the K geminal. They stated that this choice of orbitals has the effect of preventing the exaggerated mixing of states of the same symmetry which tends to spoil hole-state calculations in molecules. Their GF binding energies were

too large in all four cases calculated-- CH_4 , NH_3 , H_2O , and C_2H_4 (see Table V). This was also taken as evidence that SCF GF results can be trusted not to collapse in the way that ordinary hole state calculations do. Clearly this whole question needs further study, especially since other workers have not found hole-state calculations to collapse in the way that Gianturco and Guidotti did.

Bagus and Schaefer²⁹ used a very large basis set of 18 Slater orbitals on each atom to calculate $E_B(1s)$ for transitions to the four hole states $\text{NO}^+(\overline{\text{N1s}}; 1\pi)$, $\text{NO}^+(\overline{\text{N1s}}; 3\pi)$, $\text{NO}^+(\overline{\text{O1s}}; 1\pi)$, and $\text{NO}^+(\overline{\text{O1s}}; 3\pi)$. Their results agreed very well with experiment for the $\overline{\text{O1s}}$ states and were about 2 eV high for the $\overline{\text{N1s}}$ states after estimated corrections for relativity and correlation were applied (Table V). These same authors³⁰ made hole-state calculations on O_2 . With a similar basis set of 18 Slater orbitals on each atom they obtained similar excellent agreement with experiment after corrections were applied: discrepancies of only 0.6-0.7 eV for the $\text{O}_2^+(\overline{1s}; 4\Sigma_g^-)$ state and 0.1-0.2 eV for the $\text{O}_2^+(\overline{1s}; 2\Sigma_g^-)$ state. An important result of this calculation is that it established the localized nature of the 1s hole in these final states. This topic has also been clarified in a lucid discussion on atomic relaxation energies by Snyder.³¹ The problem is this: in molecules possessing two or more equivalent atoms, proper symmetry of the total molecular state ($3\Sigma_g^-$ in O_2 , for example) is often regarded as being achieved by a simple aufbau approach. That is, molecular orbitals such as $1\sigma_g$ and $1\sigma_u$ are successively filled with electrons. It is then natural to imagine that a photoemission event in which an oxygen K electron is ejected will result in a final state described by the O_2 molecular orbital designations, with a hole in the σ_g or σ_u shell. In such a "delocalized" hole state each oxygen would have an electron population of $7\frac{1}{2}$. Such a state is unstable, however, relative to localization of the 1s hole. Snyder has stated

the reason for this result succinctly. After discussing relaxation of the passive orbitals in terms of atomic shielding constants, he noted, "...one expects the relaxation energy to be quadratic in the charge of the hole". He argued that distribution of a hole over n centers would produce a hole charge of $\frac{1}{n}$ on each center and thus approximately a total atomic relaxation energy $\frac{1}{n}$ times as large as that for a localized hole. For $N_2^+(\overline{1s})$ he showed that an improvement of about 7 eV in the atomic relaxation energy could be expected if the hole were localized. Bagus and Schaefer³⁰ made hole-state calculations with g or u symmetry imposed on the $1s$ hole states, finding $E_B(1s) = 554.4$ eV, in poor agreement with the experimental value of 543.1 eV. When the symmetry restriction was relaxed, the Hartree-Fock equations yielded two equivalent solutions at $E_B(1s) = 542$ eV, corresponding to a $1s$ hole on either oxygen atom. They pointed out that a total wave function of the proper Σ_g or Σ_u symmetry can be formed from these two localized hole states. The 12 eV relaxation energy is actually in quite good agreement with Snyder's estimate of 7 eV for a nitrogen atom, because it is clear from the results of Bagus and Schaefer that a great deal of molecular relaxation, or polarization of valence electrons toward the localized $1s$ hole, takes place. The gross atomic population that these workers found for the $O_2^+(\overline{1s}; {}^4\Sigma^-)$ state are given in Table VI.

P. Siegbahn³² made a hole-state calculation on the ion formed by ejecting an oxygen K electron from furan. This calculation is of interest because furan is by far the largest and least symmetrical molecule on which hole-state calculations have been attempted. The result is a lowering of the binding energy well over halfway from the Koopmans' Theorem value toward the experimental value, may be taken as encouraging, especially because Siegbahn used a smaller basis set for the ion calculation.

Table VI. Gross atomic populations for the localized $O_2^+(\overline{1s}; {}^4\Sigma^-)$ state (Ref. 30)

Shell ^a	Oxygen A	Oxygen B	Shell	Oxygen A	Oxygen B
$1s_A$	1.00	0.00	$\sim 3\sigma_g$	1.03	0.97
$1s_B$	0.00	2.00	$\sim 1\pi_\mu$	3.44	0.56
$\sim 2\sigma_g$	1.13	0.87	$\sim 1\pi_g$	0.26	1.74
$\sim 2\sigma_\mu$	0.92	1.08	Total	7.78	7.22

^aMolecular orbital designations are approximate.

Before going on to the less rigorous theories, let us review and criticize the present situation in hole-state calculations. In broad outline core-level binding energies are well-understood and can be quite accurately calculated for very small systems. At a slightly finer level of detail there are still several important open questions. In heavy atoms there are large discrepancies between theoretical and experimental binding energies, perhaps arising from quantum electrodynamic (Lamb Shift) effects. In neon, the best-studied case to date, for which both relativity and correlation have ostensibly been rigorously dealt with, a residual discrepancy of nearly 1 eV (0.1%) remains in $E_B(1s)$. In most of the hole state binding energy calculations to date on molecules, the results were within 4 eV of experiment after relativity and correlation corrections of questionable applicability had been made. Because the theoretical E_B 's tended to be larger than experimental values, an expansion of the basis set for the hole-state calculations would ordinarily be indicated. However, the 1s hole states lie above, and are not orthogonal to, other states of the same symmetry, so that these calculations are not protected by a variation principle. Thus basis-set expansion requires care. Although it has been argued that the "unusual" nature of these states obviates the need for orthogonalization, the arguments presented in the molecular case are not very rigorous or quantitative, and more work on this question is needed. On the positive side, it is now clear that core hole states in symmetric molecules are localized. Hole-state calculations predict shifts fairly accurately, and it appears that hole-state calculations can be extended to larger molecules.

II.B.2. Methods Involving the Initial State Only

II.B.2.a. Connection Between Hole-State and Frozen-Orbital Calculations.

As indicated in Eq. (9), the binding energy can be estimated as simply a one-electron orbital energy. We shall use the notation

$$E_B^k(KT) \equiv -\epsilon(k) \quad , \quad (10)$$

to represent the binding energy of the k^{th} orbital as estimated by a "sudden" approximation in which the passive orbitals are frozen, whether or not Koopmans' Theorem is rigorously applicable to the particular case under discussion. When this Theorem is applicable, $E_B^k(KT)$ is given by Eq. (9). Before discussing actual results obtained using $E_B(KT)$, it is instructive to relate $E_B(KT)$ to $E_B(\text{Hole})$, the theoretical binding energy obtained from hole-state SCF calculations. Of the available discussions of the relationship between $E_B(KT)$ and $E_B(\text{Hole})$, three are reviewed below. These three approaches differ in detail, and each affords a unique physical insight.

Hedin and Johansson³³ formulated the correction that must be applied to $E_B^k(KT)$ to bring it down to $E_B^k(\text{Hole})$ in terms of a polarization potential created by the presence of a hole in the k^{th} orbital. Specifically, they wrote the Hartree-Fock Hamiltonians for the ground state and k -orbital hole state in terms of the one-electron operator h and the operators V_i describing two-electron Coulomb plus exchange interaction as

$$H = h + V = h + \sum_i V_i \quad ,$$

$$H^* = h + V^* = h + V - V_k + V_p \quad , \quad (11)$$

where an asterisk denotes the hole state. Here V_p is a polarization potential,

$$V_p = \sum_{i \neq k} (V_i^* - V_i) \quad , \quad (12)$$

that describes the change in the Hartree-Fock potential accompanying the removal of an electron from the k^{th} orbital. Hedin and Johansson proved by a straightforward derivation that with the neglect of some small terms the true binding energy and orbital energy of the k^{th} orbital are related by (in our notation)

$$E_B^k(\text{Hole}) = E_B^k(\text{KT}) + \frac{1}{2} \langle k | V_p | k \rangle \quad , \quad (13)$$

where $|k\rangle$ is the k^{th} one-electron orbital. These authors suggest that this result can be understood physically by the hypothetical two-step process: (i) adiabatic relaxation of electrons in all other orbitals following the "switching off" of the charge of the electron in the k^{th} orbital, thereby storing energy $\frac{1}{2} \langle k | V_p | k \rangle$, followed by (ii) ejection of this electron, which would now have a binding energy given by Eq. (13) (using Koopmans' Theorem, now valid because no further relaxation can occur). This result was shown to be very nearly equivalent to Liberman's³⁴ suggestion that E_B is essentially the arithmetic mean of the orbital energies for the k^{th} orbital in the ground state and hole state, i.e.,

$$E_B^k(\text{Hole}) \cong \frac{1}{2} [E_B^k(\text{KT}) + E_B^k(\text{KT})^*] \quad . \quad (14)$$

Using this relation, which he derived using the similar approach of Brenner and Brown,³⁵ Liberman found $E_B(\text{argon } 1s) = 118.0 \text{ a.u.}$, in excellent agreement with the values in Table I.

Results from the polarization potential method, applied to Na^+ , are given in Table VII. The polarization potential model appears to work very well for core orbitals. From their results on Na, K, Na^+ , and K^+ , Hedin and Johansson concluded that on formation of a hole in a given shell the relaxation of more tightly bound shells is negligible, and that intrashell relaxation is small in comparison to the relaxation of outer shells. They also found that relaxation effects are only weakly dependent on Z. For "outer core" levels (e.g. the 2s level in Na^+) they found that $E_B(\text{Hole})$ gave no better agreement with experiment than did $E_B(\text{KT})$. This was attributed to the presence of only intrashell relaxation in these cases.

Manne and Aberg³⁶ have given an especially clear picture of the relationship between the Koopmans' Theorem "state" $\Psi_{\text{KT}}^k(N-1)$ formed (as an abstract concept: it does not exist in nature) by removing an electron from the k^{th} orbital of an N-electron system and the real final states of the system $\Psi_i^k(N-1)$. Since the latter form a complete set, they could write

$$\Psi_{\text{KT}}^k(N-1) = \sum_{i=0}^{\infty} \langle \Psi_i^k | \Psi_{\text{KT}}^k \rangle \Psi_i^k(N-1) \quad (15)$$

Now $\Psi_{\text{KT}}^k(N-1)$ and $\Psi_i^k(N-1)$ are, respectively, the initial and final states of the N-1 passive orbitals. By assuming the transition moment for photoemission to be energy-independent, they showed that the transition moment to each state i is proportional in magnitude to the above overlap integral. Thus the probability of the system going to final state i is proportional to the square of this integral, and the energy sum rule

$$E_B^k(\text{KT}) = E_B^k(\text{Hole}) + \sum_{i=1}^{\infty} |\langle \Psi_i^k | \Psi_{\text{KT}}^k \rangle|^2 (E_i - E^k(\text{Hole})) \quad (16)$$

Table VII. Polarization potential corrections to Na^+ binding energies
(after Hedin and Johansson³³)

Final State	$E_B(\text{expt})^a$	$E_B(\text{expt}) - E_B(\text{KT})^b$	$\frac{1}{2} \langle k V_p k \rangle$	$E_B(\text{Hole}) - E_B(\text{KT})$
$\text{Na}^{2+}(\overline{1s})$	40.000	0.762	0.822	0.828
$\text{Na}^{2+}(\overline{2s})$	2.924	0.166	0.102	0.105
$\text{Na}^{2+}(\overline{2p})$	1.741	0.056	0.113	0.117

^aAll energies are in a.u. (27.210 eV).

^bThe experimental values have been corrected for relativity and for solid-state effects.

follows. The lowest-lying hole state ($i = 0$ in Eq. (15)) has been separated here from the sum over final state of higher excitation. Such states have been observed as high (binding) energy satellite peaks in photoelectron spectra. By rearranging Eq. (16) it is evident that $E_B^k(KT)$ measures the average energy of the spectrum. Manne and Aberg calculated an average binding energy of 886 ± 1 eV from the Ne 1s spectrum reported by Krause et al.³⁷ This is in fair agreement with the Koopmans' Theorem value of 892 eV. Finally these authors pointed out that there is a strong analogy between the phenomena described by Eq. (16) and the Franck-Condon principle for electronic transitions to vibrational states within a vibrational manifold. We note that this analogy is especially close for molecular photoelectron spectra.

Snyder³¹ considered the problem of orbital relaxation in an atom from which an inner electron is ejected and discussed this effect in terms of atomic shielding constants. He gave an equation for the binding energy of an electron in the m^{th} shell, based on atomic shielding constants ideas above, in the equivalent of a "frozen orbitals" approximation:

$$E_B^m("KT") = -\frac{1}{m^2} (Z-s_m)^2 + \frac{2Z}{m^2} (Z-s_n) - \frac{2}{m^2} (0.85 N_{m-1} + \sum_{\ell=1}^{m-2} N_{\ell}) (Z-s_m) - \frac{2}{m^2} (2N_m - 2)(s_m - s'_m)(Z-s_m) - 2 \sum_{n>m} \frac{N_n}{n^2} (s_n - s'_n)(Z-s_n) \quad (17)$$

Here s_n is the shielding constant for the n^{th} shell,^{38,39} and the prime denotes the core-ionized state. The five terms in Eq. (17) denote respectively, kinetic and potential-energy interactions involving the nucleus, and repulsive interactions between an electron in the n shell and electrons in inner shells, in

the m shell, and in outer shells. This equation gave $1s$ binding energies for neon and argon that were within 3-4% of the Koopmans' Theorem values from Hartree-Fock calculations, as shown in Table VIII. Also listed for these cases are the derivatives of E_B ("KT") with Z , which gives the variation of binding energy for isoelectronic systems such as F^- , Ne, and Na^+ . Finally Snyder derived an expression for the relaxation energy in an ion with a $1s$ hole (and possessing electrons up to the $3s$, $3p$ shells)

$$\Delta E^{\text{relax}} = -(1.2 + 2.5 N_2 + 1.5 N_3) \text{ eV} \quad (18)$$

Here N_2 and N_3 are the populations of the $n = 2$ and 3 shells. This equation predicts ΔE^{relax} to be independent of Z . In fact the Z dependence is approximately $Z^{-1/2}$. The predicted magnitudes of ΔE^{relax} for Ne^+ and Ar^+ are within $\sim 5\%$ of the Hartree-Fock values.

As the above discussion indicates, the formal connection between E_B (KT) and E_B (Hole) is well-understood. For atomic systems the actual magnitudes of ΔE^{relax} can be calculated with good accuracy by alternate approaches, indicating that for these systems the mechanistic details of relaxation in the hole state are known. At a level of sophistication adequate for the discussion of chemical shifts in binding energies, however, atomic relaxation is inadequate, and molecular relaxation, in particular differential molecular relaxation, must be considered. Thus while this subsection makes a conceptual link between E_B (Hole), discussed earlier, and E_B (KT) discussed below, it does not provide a quantitative bridge that would provide a basis for using E_B (KT) in estimating chemical shifts. Such a bridge could take either of two forms: Differential molecular relaxation could be shown to be negligible, or the

Table VIII. Comparison of Energies from Shielding-Constant and Hartree-Fock Calculations^a

Final State	E_B ("KT")		ΔE_B ("KT")/ ΔZ		ΔE^{relax}	
	Shielding	HF	Shielding	HF	Shielding	HF
Ne ⁺ ($\overline{1s}$)	930.3	891.7	209.4	203.0	-21.2	-23.2
Ar ⁺ ($\overline{1s}$)	3313.9	3227.4	402.7	397.2	-33.2	-32.2

^aFrom References 14 and 31. All energies are in eV.

magnitude of molecular relaxation could be estimated for each case. Since in O_2^+ about ~ 5 eV of relaxation energy can apparently be attributed to extra-atomic relaxation (as discussed earlier), it seems probable that the differences of extra-atomic relaxation energies from one molecule to another could be a fair fraction of this figure. Thus the failure of $E_B(KT)$ to include this effect could perhaps account for up to 2 or 3 eV of scatter in comparison of experimental chemical shifts with theoretical shifts deduced by the use of orbital energies.

II.B.2.b. Comparison of Orbital Energy Differences with Experiment.

In this section experimental binding-energy shifts in gaseous molecules are compared with orbital energies. Although orbital energies are calculated, there is little reason to compare them with experimental binding energies, because they tend to be high by an amount in excess of the whole range of chemical shifts. The carbon 1s orbital in methane is about 305 eV, for example, while the binding energy of this orbital is 290.8 eV. The intercomparison of orbital energies from different calculations on the same compound is more meaningful, but even its value is limited. Although $\epsilon(1s)$ for a particular compound presumably has a unique value in the Hartree-Fock limit, its value is not governed by the variation principle. Thus while one might expect $\epsilon(1s)$ and the total energy E to be correlated far from the HF limit (i.e., for poor choice of basis sets) just on the ground that $2\epsilon_{1s}$ is a reasonably large fraction of $-E$, no such correlation is to be expected near this limit. Hence the goodness of an $\epsilon(1s)$ value cannot be judged by its magnitude, nor can the proximity of $\epsilon(1s)$ to the Hartree-Fock limit necessarily be judged by the value of E alone, without additional information about the particular SCF calculation in question. These

conclusions are illustrated by the values of E and $\epsilon(1s)$ for methane given in Table IX. It is difficult to compare results reported by different workers, because their basis sets differ in a variety of ways. Fortunately Gianturco and Guidotti²⁶ have studied the relationships of $\epsilon(1s)$ to E and to the basis set, by varying the basis set in a systematic way, for the molecular CH_4 , NH_3 , and H_2O . They found variations in $\epsilon(1s)$ of 1.2, 2.8, and 1.1 eV, respectively, for these three molecules. That $\epsilon(1s)$ and E are not strongly correlated is evident from the entries from Ref. 26 in Table IX. More evidence is given in the original paper, in which appear the results of 6, 5, and 9 SCF calculations, respectively, for these three molecules. It is particularly noteworthy that "double-zeta" basis sets give values of E that are fairly close to those obtained using large basis sets, but that the double-zeta $\epsilon(1s)$ results are considerably in error for NH_3 and H_2O . In fact for these two cases the double-zeta basis sets give worse results for $\epsilon(1s)$ than do minimal basis sets (Table X). In view of the ~ 1 eV error in $\epsilon(1s)$ that appears to attend the use of double-zeta basis sets, and particularly because this $\epsilon(1s)$ can apparently err in either direction, about 1 eV of scatter can be expected in theoretical chemical shifts based on orbital energies from ab initio calculations of double-zeta quality. Evidently similar scatter can be expected if shifts are estimated as differences between orbital energies from different sources, unless all the values of $\epsilon(1s)$ are obtained from calculations near the Hartree-Fock limit. On the other hand the results quoted in Table IX can be interpreted as indicating that a careful calculation of $\epsilon(1s; \text{CH}_4)$ with a well-chosen basis set will yield a reproducible value in the range 305.1 ± 0.1 eV.

Basch and Snyder⁴⁰ were the first to predict a large number of binding energy shifts, using orbital energies from ab initio (double zeta quality)

Table IX. Total and 1s-orbital energies for CH₄

Basis set ^a	-E(a.u.)	-ε(1s)(eV)	Ref.
Extensive GTO	40.1890	305.07	8
GTO	40.1812	304.9	20
GTO 2ζ	40.1303	305.22	24
GTO	40.1823	304.97	25
Large STO set	40.2045	305.15	26
ditto, minus C 3d's	40.1866	304.76	26
2ζ	40.1845	305.30	26
minimal STO	40.1153	305.95	26

^aSTO = Slater type orbital, GTO = Gaussian type orbital. More detailed descriptions of basis sets are (in most cases) given in the references.

Table X. Energies for CH₄, NH₃, and H₂O, after Gianturco and Guidotti²⁶

Molecule	Basis Set	-E(a.u.)	-ε(1s)(eV)	Δε(1s) ^a
CH ₄	extensive	40.2045	305.15	--
CH ₄	2ζ	40.1845	305.30	+0.30
CH ₄	minimal	40.1153	305.95	+0.80
NH ₃	extensive	56.1861	423.52	--
NH ₃	2ζ	56.1675	422.34	-0.18
NH ₃	minimal	56.0051	422.65	-0.87
H ₂ O	extensive	76.0384	560.05	--
H ₂ O	2ζ	76.0052	558.73	-1.32
H ₂ O	minimal	75.7030	559.53	-0.51

^aThis difference gives an estimate of the expected variation in chemical shifts that are estimated from orbital energies derived from the smaller basis sets.

calculations on thirty small molecules. Davis et al.⁴¹ measured shifts for some of these molecules, finding good agreement. Several other experimental shifts and orbital energy differences for small molecules are also available.^{3,8,25,42-44} We have listed in Table XI, and plotted in Figs. 4(a)-(c), those cases for which both experimental and theoretical figures are available. In most cases for which two experimental values are available the agreement is very good. Average experimental values are used in the figures. In all three cases plotted--C, N, and O--straight lines of unit slope have been drawn through the points. Perfect agreement between δE_B (expt) and $\Delta \epsilon$ would correspond to all the points' lying on the lines. In fact in only one case (NH_3) is the orbital-energy value off by over 1.0 eV. Several points are 1.0 eV off the lines, but the average error is only ~ 0.5 eV. Thus orbital energies appear to provide reasonably accurate values of binding energy shifts, reliable to the ~ 1 eV level. In view of the foregoing discussion about the expected scatter of ~ 1 eV in the theoretical values of $\epsilon(1s)$, this is about the best agreement that could be anticipated. Before further improvement can be expected in the agreement between $\Delta \epsilon(1s)$ and δE_B , basis sets of better than double-zeta quality will probably be required. As evidence that a large basis set can give good results, the $\text{CH}_4 - \text{CF}_4$ shift of 12.11 eV predicted by Gelius, et al.⁸ by the use of a large basis set agrees well with experimental value of 11.0 eV, especially if the former is corrected downward to 11.6 eV to correct for the scale factor of 1.05 between $\epsilon(\text{Cl}s)$ and $E_B(\text{Cl}s)$. Gelius et al. found a slope of $\Delta \epsilon / \delta E = 1.09$ by fitting a line through the seven points that they calculated with large basis sets.

In summary, chemical shifts predicted from differences in orbital binding energies based on ab initio Hartree-Fock calculations agree with experiment to

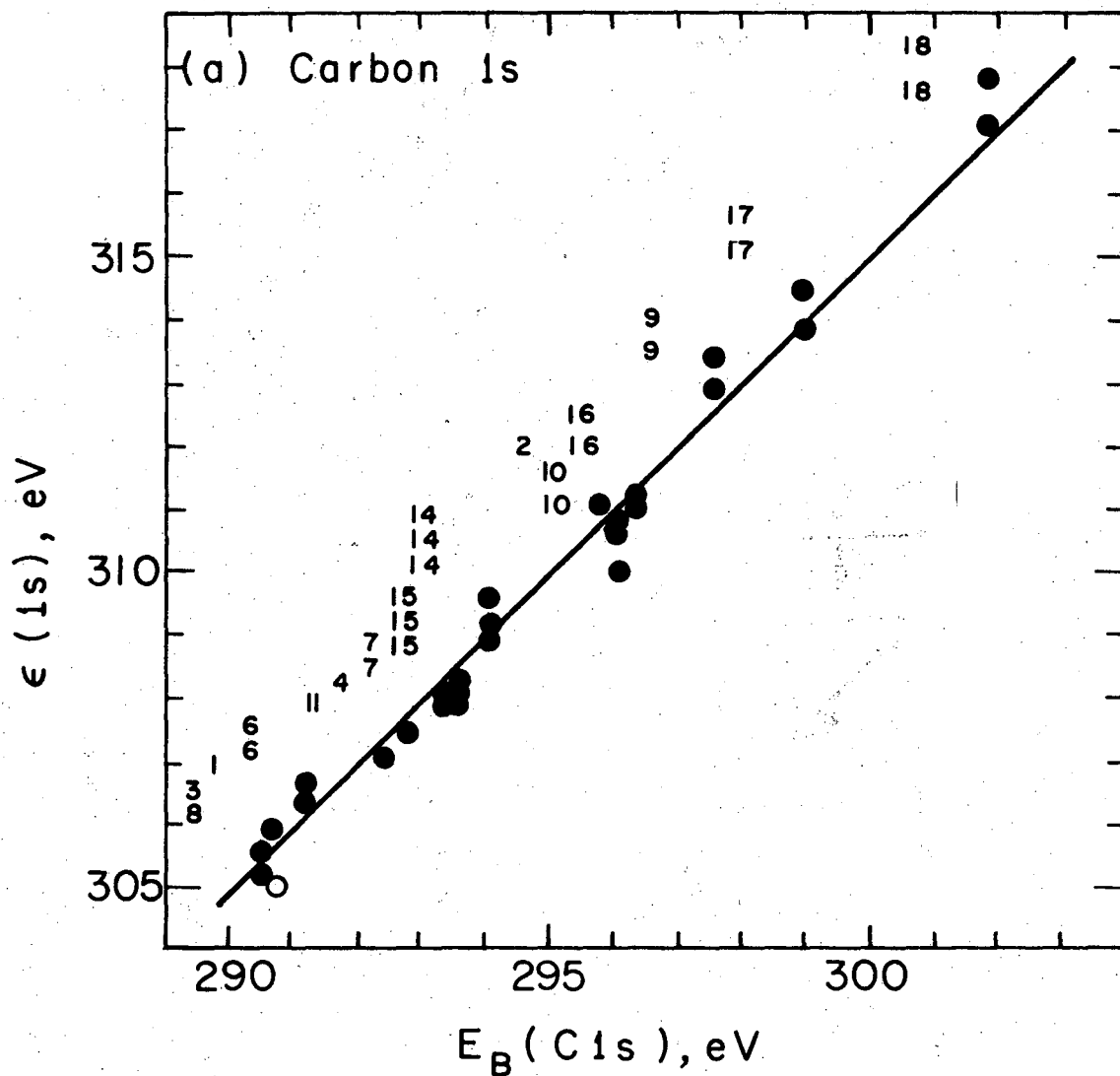
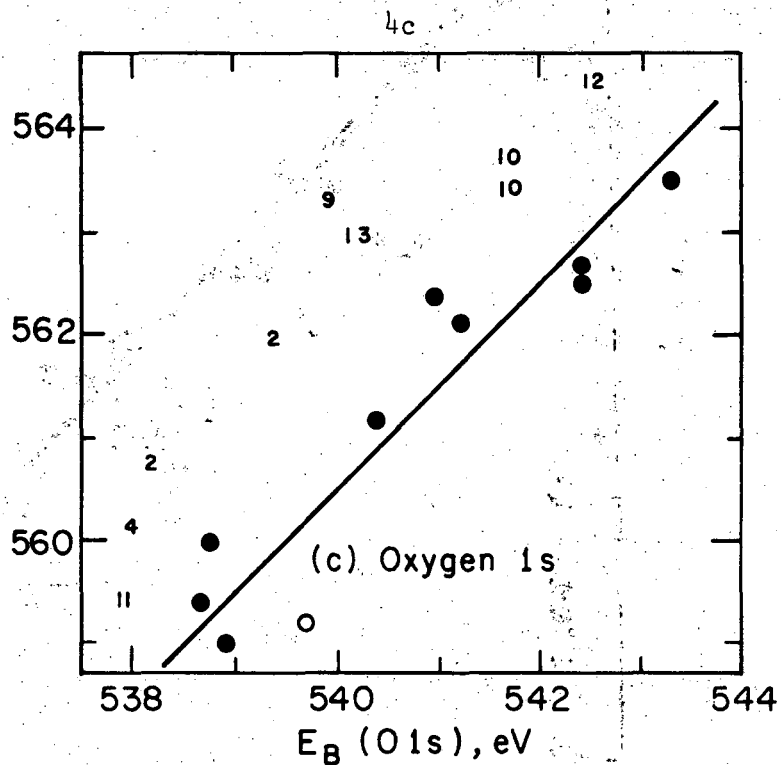
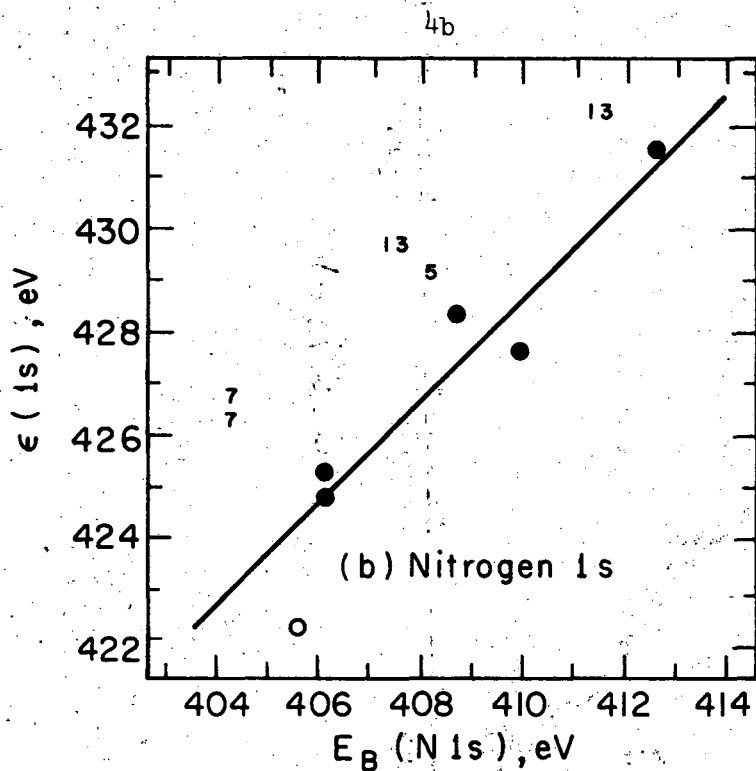


Fig. 4a. Orbital energies versus binding energies for carbon 1s electrons in gaseous carbon-containing molecules. Open circle denotes methane, while other compounds are numbered as in Table XI. Compound numbers stand in the same relative positions as do the points. Multiple entries denote more than one theoretical value. Line has unit slope.



XBL 721 - 2232

Fig. 4b. Nitrogen data, plotted as in Fig. 4a. Open circle denotes ammonia. Two points for N_2O (13) denote inequivalent nitrogens.

Fig. 4c. Oxygen data, plotted as in Fig. 4a. Open circle denotes water. Two points for HCO_2H (2) denotes inequivalent oxygens.

Table XI. $\delta E_B(1s, \text{expt})$ and $\Delta\epsilon(1s)$ for small molecules (eV)^a

No.	Molecule	carbon		nitrogen		oxygen		fluorine	
		δE_B	$\Delta\epsilon$	δE_B	$\Delta\epsilon$	δE_B	$\Delta\epsilon$	δE_B	$\Delta\epsilon$
1	C ₂ H ₄	-0.1	0.9						
2	HCO ₂ H	4.99(10)	6.0			0.67(5)	2.0		
						-0.95(5)	0.8		
3	cyclo- propane	-0.23	0.5						
4	C ₂ H ₄ O	2.01(5)	2.4			-1.05(5)	0.2		
5	N ₂			4.3 ^b , 4.35(20)	5.4				
6	C ₂ H ₂	0.4	1.56 ^c , 1.4						
7	HCN	2.6(2)	3.00 ^c , 2.8	0.55(20)	2.53 ^c , 3.0				
8	C ₂ H ₆	-0.2	0.2						
9	CO ₂	6.8 ^b , 6.84(5)	7.86 ^d , 8.3			1.1 ^b , 1.44(5)	3.2		
10	CO	5.2 ^b , 5.4	5.01 ^d , 5.67 ^c , 5.5			2.4 ^b , 2.94(10)	3.43 ^c , 3.3		
11	CH ₃ OH	1.6 ^b , 1.9(2)	2.0			-0.8 ^b , 0.80(10)	-0.2		
12	O ₂					3.4 ^b , 3.84(6)	4.3		
13	N ₂ O			2.9 ^b , 3.17(10)	6.1	1.5 ^b , 1.54(10)	2.9		
				6.9 ^b , 7.04(5)	9.3				
14	H ₂ CO	3.3 ^d	4.55 ^c , 3.90 ^d , 4.1						

(continued)

 0330570001
-49-

Table XI (continued)

No.	Molecule	carbon		nitrogen		oxygen		fluorine	
		δE_B	$\Delta\epsilon$	δE_B	$\Delta\epsilon$	δE_B	$\Delta\epsilon$	δE_B	$\Delta\epsilon$
15	CH ₃ F	2.8(2)	3.18 ^c , 2.89 ^d , 3.0 ^e , 4.9 ^f						
16	CH ₂ F ₂	5.55(5) ^g	5.93 ^d , 6.1 ^e					0.73(5) ^g	1.2 ^e
17	CHF ₃	8.1 ^b , 8.3(2)	8.81 ^d , 9.4 ^e , 15 ^f						
18	CF ₄	11.1 ^b , 11.0(2)	12.11 ^d , 12.8 ^e					2.6(2) ^g	3.6 ^e

^aReference compounds are hydrides, except for F(1s), which is referred to CH₃F. Unless otherwise annotated, $\Delta\epsilon$ (1s) and δE_B (1s) values are from Refs. 40 and 41, respectively.

^bRef. 3.

^cRef. 42.

^dRef. 8.

^eRef. 25.

^fRef. 43.

^gRef. 44.

~ 1 eV or better, when basis sets of double-zeta quality are used. Better basis sets will probably improve this agreement, because at the double-zeta level the orbital energies are still not near their optimum values. Finally, the scale for $\Delta\epsilon$ should probably be 1.05 that for δE_B , because orbital energies tend to be about 5% larger than binding energies.

II.C. Quantum-Mechanical Methods Involving Binding-Energy Calculations

The foregoing theoretical approaches are valuable in elucidating the foundations of binding-energy shifts, but ab initio calculations presently constitute a rather cumbersome approach to the actual calculation of shifts for molecules of any size. Fortunately the physical origins of the shifts are well enough understood that they can be calculated directly, using models based on electrostatic potential energy considerations. These models can be subdivided further into those that entail (or require) an accurate evaluation of the local potential and those that do not.

II.C.1. Potential Models

It was realized very early that binding-energy shifts arose almost entirely from differences in the electrostatic potential energies of core electrons.⁴⁵ However, the first detailed theoretical analyses that demonstrated this result quantitatively were given relatively recently and independently by Basch⁴⁶ and Schwartz.⁴² The analysis given by Schwartz is summarized below to provide a basis for the potential-model approach.

The orbital energy of a 1s electron on nucleus n can be conveniently expressed by rewriting Eq. (6) as

$$\begin{aligned} \epsilon_{1s} = & \langle 1s(1) | -\frac{1}{2} \nabla_1^2 - \frac{Z_n}{r_{1n}} | 1s(1) \rangle + J_{1s1s} - \sum_{m \neq n} Z_m \langle 1s(1) | 1/r_{1m} | 1s(1) \rangle \\ & + \sum_{i=\text{local}} (2J_{1si} - K_{1si}) + \sum_{i=\text{distant}} (2J_{1si} - K_{1si}) \quad (19) \end{aligned}$$

Here it has been assumed that the molecular orbitals have been expressed in terms of a "localized molecular orbital" basis set $\{L_i\}$.⁴⁷ The last two sums are then taken over the "local" orbitals L_i that connect atom n and over the "distant" orbitals that do not. Schwartz showed that to a very good approximation $K_{1si} = 0$ for the distant orbitals. By direct calculation he found values of 2×10^{-4} a.u. or less for the three $1s$ -distant orbital exchange integrals in CH_3F . He also showed that, to within 10^{-4} a.u., the distant Coulomb integrals J_{1si} are equal in magnitude to $1/Z_n$ times the electrostatic attraction integral between nucleus n and the distant orbital L_i , and that $\langle 1s(1) | Z_m/r_{1m} | 1s(1) \rangle = Z_m/R_{nm}$, where R_{nm} is an internuclear distance. Finally the one-electron interaction with nucleus n , $\epsilon_{1s,n} \equiv \langle 1s(1) | -\frac{1}{2} \nabla_1^2 - \frac{Z_n}{r_{1n}} | 1s(1) \rangle$, was shown to vary by only a few ten-thousandths au from one molecule to another. In view of these results, shifts in the orbital energy can be related to shifts in the external electrostatic potential evaluated at the nucleus by the approximate expression

$$\Delta(-\epsilon_{1s}) \cong \Delta V_{\text{ext}} + e^2 \Delta \sum_{i=\text{local}} \left[2 \langle L_i(1) | 1/r_{1n} | L_i(1) \rangle - 2J_{1si} + K_{1si} \right] \quad (20)$$

The last term is just the difference between the actual interaction energy of electrons in the local orbitals with the $1s$ electron and the value that this

interaction energy would have if the $1s$ orbital were collapsed to the nucleus and exchange were absent. The results given by Schwartz for CH_4 and CH_3F show that for the $1s$ orbitals in these molecules the second term in Eq. (20) amounts to only 0.23 eV, or less than 10% of the measured shift. From calculations on 15 molecules, he found $\Delta(-\epsilon_{1s}) = 1.11 \Delta V_{\text{ext}}$ on the average. This coefficient exceeds unity as expected (i.e., because the radial extent of the $1s$ orbital makes the Coulomb and exchange integrals in ϵ_{1s} more sensitive to environment than the $1/r$ integrals in V_{ext}). Since orbital energies exceed experimental binding energy shifts by a few percent, ΔV might be expected to predict these shifts better than $\Delta(-\epsilon)$ would.

Basch⁴⁶ gave a similar derivation, differing mainly in that he allowed $1s$ orbitals to collapse into their nuclei for the purpose of approximating certain Coulomb integrals involving these orbitals as one-electron integrals. With this approximation, he found that the "potential" relation, $\Delta(-\epsilon) \cong \Delta V$, is valid if the quantity

$$\langle 1s(1) | -\frac{1}{2} \nabla_1^2 - Z_n/r_{1n} | 1s(1) \rangle + J_{1s1s} - \sum_i K_{1si}$$

does not change appreciably with environment. He established the validity of the potential relation by direct calculation, for the fluorinated methanes, of $\Delta\epsilon$, ΔV , and $\Delta V'$, where the quantity

$$V' = \sum_{m \neq n} \frac{Z_m}{R_{mn}} + 2 \sum_i \langle i | 1/r_{1n} | i \rangle = \sigma_{\text{av}}^d(n) \quad , \quad (21)$$

is just the diamagnetic shielding coefficient at nucleus n . V' differs from V only in that it contains a term in the sum for the $1s$ orbital. Equation (21)

establishes a connection between binding-energy shifts and nmr parameters, as the agreement among Basch's value of $\Delta\epsilon$, ΔV , and $\Delta V'$, set out in Table XII, shows.

Comparison of shifts in potential and orbital energies as determined from ab initio calculations are helpful in understanding the origins of shifts, but beyond that their value is limited. Most molecules are too large for ab initio calculations to be feasible, and in those cases for which ab initio calculations can be made the orbital energies themselves are readily available and may as well be used directly to estimate shifts. The real reason for establishing the relation between $\Delta\epsilon$ and ΔV is that V , but not ϵ , can be reliably estimated for larger molecules by the use of intermediate level molecular-orbital theories such as the CNDO⁴⁸ model. Gelius, et al.⁸ have studied the potential model using both CNDO and ab initio wave functions. For several small carbon-containing molecules they have done ab initio calculations using large basis sets and have given values for $\Delta\epsilon$, $q_c(g)$, the gross atomic charge on carbon atom, and V , the molecular potential arising from the surrounding atoms. The discussion below is largely based on their results, which are set out in Table XIII; although it differs in detail, the conclusions are consistent with those of Gelius, et al.

These workers compared experimental shifts δE_B with calculated parameters, finding a good fit to the relation

$$\delta E_B = 18.3 q_c(g) + V + 3.0 \text{ eV} \quad (22)$$

In order to compare $\Delta\epsilon$ with $\Delta q_c(g)$ and ΔV , we have tested for a relation of the form

Table XII. Orbital Energy and Potential Shifts for Cls Electrons,
after Basch⁴⁶

Method	CH ₄	CH ₃ F	CH ₂ F ₂	CHF ₃	CF ₄
Experiment	(0.0)	2.8 eV	5.6	8.3	11.0
$\Delta\epsilon(1s)$	(0.0)	3.0	6.1	9.4	12.7
$\Delta V(1s)$	(0.0)	3.0	6.2	9.6	13.1
$\Delta V'(1s)$	(0.0)	3.0	6.2	9.5	13.0

Table XIII. Molecular Parameters for Carbon Compounds

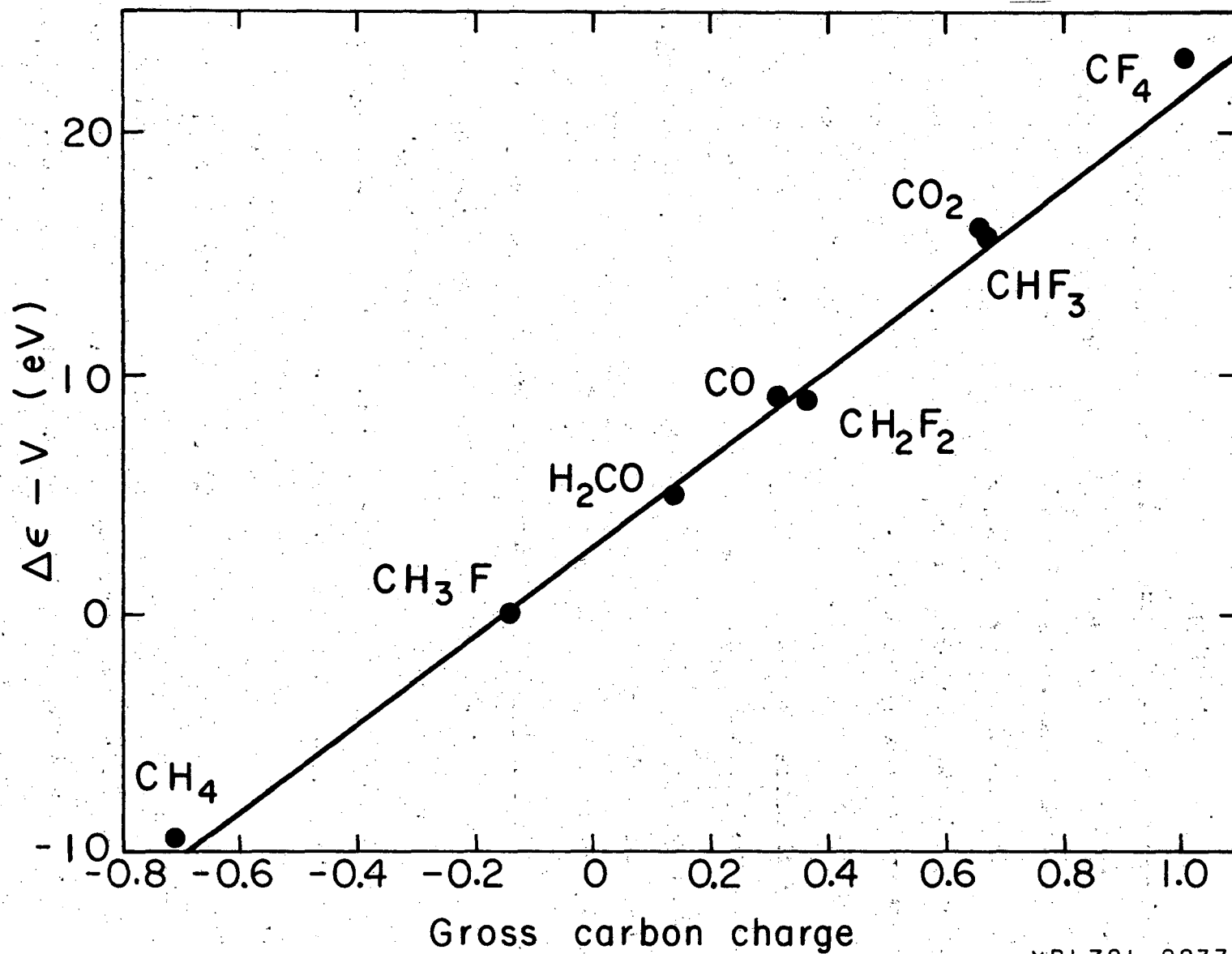
Molecule	$\Delta\epsilon_{1s}^a, \text{eV}$	Carbon atomic charge		Molecular potential ^c	
		<u>ab initio</u> ^a	CNDO ^b	<u>ab initio</u> ^a	CNDO ^b
CH ₄	0	-0.71	-0.049	9.40	0.65
CH ₃ F	-2.89	-0.13	0.180	2.73	-1.85
CHF ₃	8.81	0.67	0.613	-6.86	-6.67
CF ₄	12.11	1.01	0.708	10.99	-8.82
CO	5.01	0.32	0.042	-4.13	-0.53
CO ₂	7.86	0.66	0.536	-8.14	-6.64

^aRef. 8.^bRef. 49.^cPotential energy of 1s electron from extra-atomic origins, in eV.

$$\Delta\epsilon = kq_c(g) + V + b \quad , \quad (23)$$

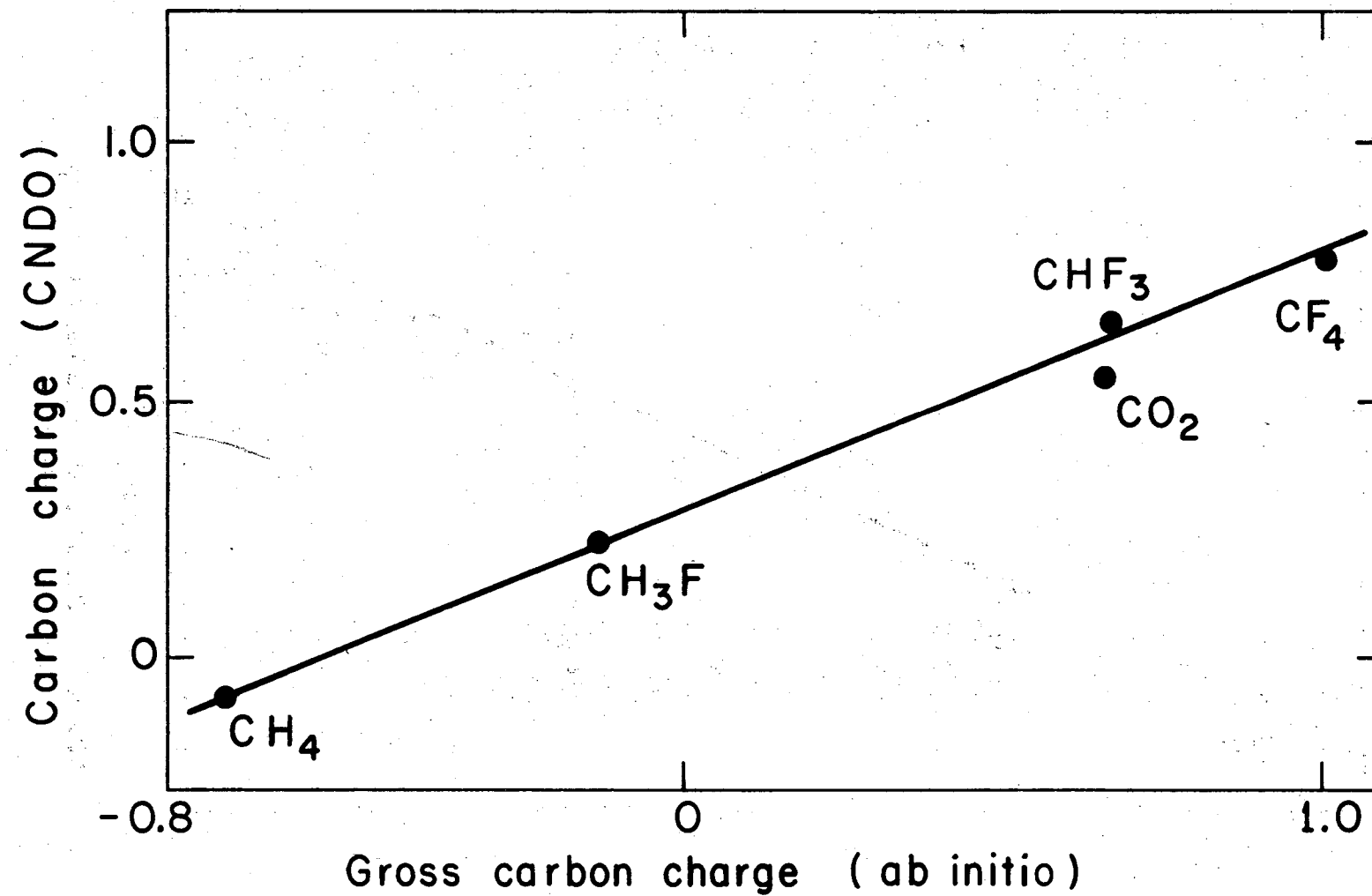
by plotting $\Delta\epsilon - V$ against $q_c(g)$, in Fig. 5. These quantities show a very nearly linear relationship, but a slight curvature is also apparent. A line with parameters $k = 18.3$ and $b = 3.0$ fits the points quite well, thereby justifying the linear variation of $\Delta\epsilon$ with $q_c(g)$.

It is useful to examine the relationship between $q_c(g)$ and V as calculated from ab initio wave functions and the comparable quantities from CNDO theory. The latter have been given by Ellison and Larcom⁴⁹ and have also been calculated by D. W. Davis.⁵⁰ They are also listed in Table XIII. The agreement between either $q(\text{ab initio})$ and $q(\text{CNDO})$ or $V(\text{ab initio})$ and $V(\text{CNDO})$ is poor, but this means little by itself because the two values of q are defined differently. The ab initio gross atomic charges are based on a Mulliken population analysis⁵¹ and thus include "overlap population", while the CNDO theory allows for no overlap. As a result the range of atomic charge is over a factor of two larger on the ab initio theory. This is compensated in part by a smaller value of k in Eq. (23) and in part by a larger range of the extra-atomic potential V . Thus the near agreement of k for the two sets of charges (18.3 vs 23.5⁸) does not imply that the charges themselves agree that well. However, plots comparing the charges (Fig. 6a) or the potentials (Fig. 6b) separately show linear relationships for both cases, thereby supporting the validity of relations like Eq. (23) for either ab initio or CNDO parameters. The CO points, and perhaps the CO₂ points, lie substantially removed from straight lines through the substituted methane results in both Figs. (6a) and (6b). In fact the CNDO model predicts the CO shift poorly. This result is expected. The CNDO theory gives essentially a point-charge treatment of shifts in $E_B(1s)$, and multiple bonds are not well described by point-charges.



XBL721-2233

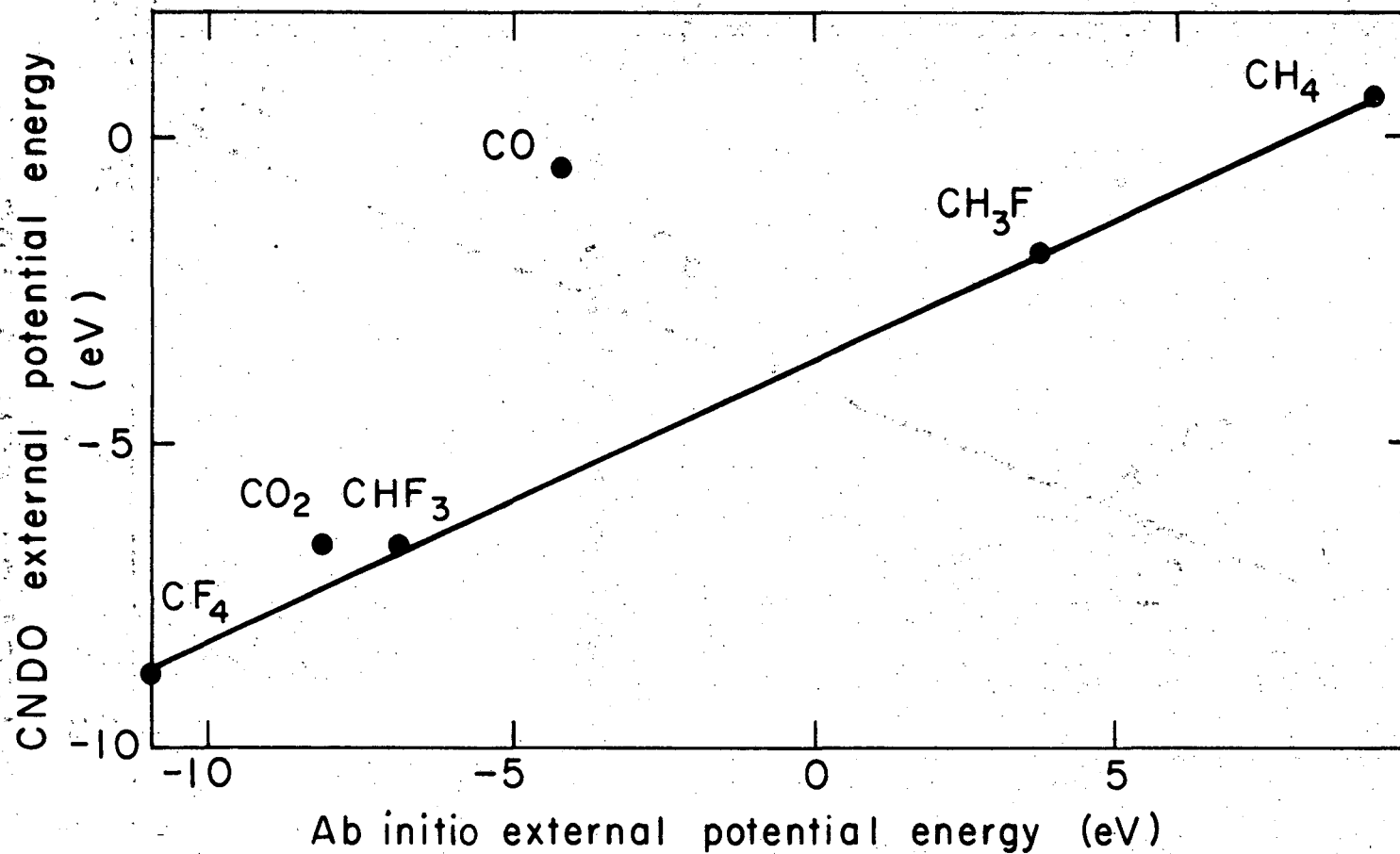
Fig. 5. Plot of energy parameters for C(1s) in several compounds, against gross carbon atomic charge, to test linearity. Data were taken from Ref. 8.



XBL721-2234

Fig. 6a. The CNDO carbon charge (Ref. 49) versus the ab initio gross carbon charge (Ref. 8). Multiply-bonded CO and CO₂ do not follow trend.

00008700006



XBL721-2235

Fig. 6b. The Cls external potential energies from CNDO (Ref. 49) and ab initio (Ref. 8) calculations. Note that CO and CO₂ are again off the line, as in Fig. 6a, but above it this time. Thus the deviations are partially compensated in the sums $kq + v$.

The above discussion suggests that a potential model based on CNDO theory might predict shifts in good agreement with experiment, with some reservations about multiply-bonded systems. Several approaches have been taken to test this possibility. The Uppsala group^{3,52} wrote the binding energy shifts as (in our notation)

$$\delta E_i = kq_i + V_i + \ell \quad , \quad (24)$$

where $V_i = e^2 \sum_j q_j / R_{ij}$ is the "molecular potential" term. Here a charge q_j is assigned to the j^{th} atom, and it is taken as being located at the nucleus. They calculated q_i and V_i for a number of molecules, using CNDO theory, and least-squares fitted experimental shifts δE_i to determine k and ℓ . They made fits for compounds of C, N, O, F, and S. The quality of fit varied from one element to another, and in some cases there was too little variation in q_i to determine k very well. However the fits tended to be rather good for most compounds in a group, with some points, such as CO in the C(1s) group and N_2 in the N(1s) group, falling well off the line. An important result of these fits is that the values of k were quite close to those of the corresponding atomic (1s-valence) one-center repulsion integrals. In the format: element symbol, k from fit, k from repulsion integrals, the results were: C, 21.9, 22.0; N, 21.5, 26.4; O, 25.8, 30.7; F, 27.6, 35.1; S, 13.8, 16.5.

Ellison and Larcom⁴⁹ have suggested that the above relation could be altered to give separate kq terms for host-atom s and p electrons, by writing

$$\delta E_i = k_s q_{is} + k_p q_{ip} + V \quad , \quad (25)$$

with $q_i = q_{is} + q_{ip}$ and a reference chosen such that $l = 0$. By carrying out a two-parameter (k_s and k_p) fit, they found that they could correctly predict the C(1s) shift in CO as well as the other C(1s) shifts reported by Davis, et al.⁴¹ They found $k_s = 17.5$ and $k_p = 24.5$ for C(1s), and, for several oxygen compounds, $k_s = 18.0$, $k_p = 26.4$. It should be noted, however, that the carbon compounds are fitted better by a two-parameter expression only because CO is among them. If CO is excluded one parameter does essentially as well. Furthermore, a two-parameter fit excluding CO gives values of k_s and k_p for C(1s) that are very close to one another. In view of this, of the similarity of the 1s-2s and 1s-2p repulsion integrals, and the deviations shown by CNDO parameters for CO (as indicated in Fig. 6), the value of a two parameter fit seems questionable.

Davis, Shirley, and Thomas^{44,53} have used CNDO theory in a way that differs from either of the above approaches. Without any empirical curve-fitting they simply calculated the expected C(1s) and F(1s) shifts for a series of fluorinated benzenes and methanes. The results are quite encouraging. Before discussing them, however, a couple of observations should be made, lest the results appear better than they really are. First, rather simple molecules²³¹¹ were chosen. Second, comparisons of C(1s) shifts are made only within each group (substituted benzenes and methanes). The two scales disagree by 0.9 eV, indicating that the CNDO approach can handle subtle shifts within groups of compounds with similar bonding better than intergroup shifts. Finally a subtlety was introduced into the calculations of V. One can treat electrons in atomic orbitals on neighboring atoms as if they were simply point charges, and evaluate the electrostatic potential they create as q_j/R_{ij} . This is exact for a spherical charge distribution on center j , hence for s orbitals and closed shells. The foregoing estimates of V were made by this "point charge"

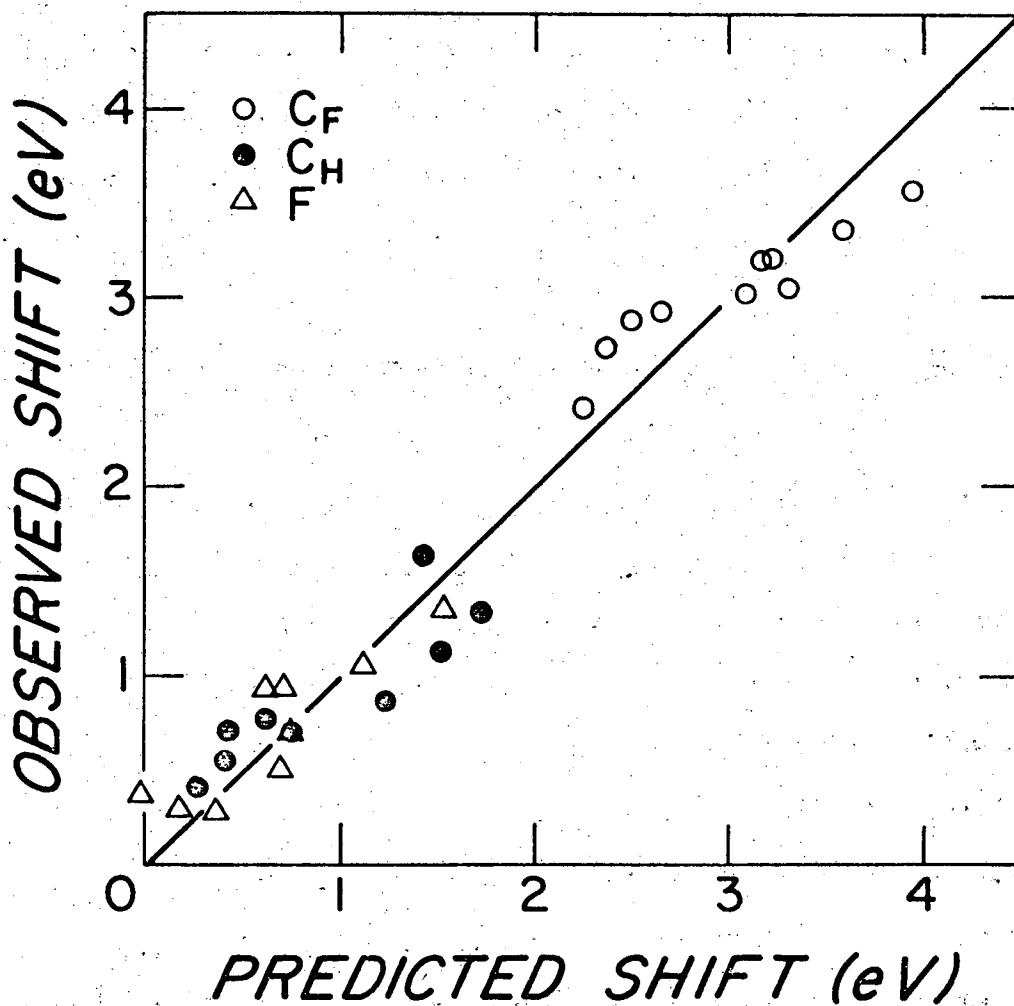
method, and Davis et al. also used this approach. However, they also made another estimate, based on the "p-p'" method. In this second calculation the external potential at nucleus i arising from orbitals on center j was evaluated by actual calculation of $1/r$ integrals. These integrals have different values for p_σ and p_π orbitals. Ordinarily in CNDO theory only integrals of the form $\langle p_{\sigma j} | 1/r_{ij} | p_{\sigma j} \rangle$ or $\langle p_{\pi j} | 1/r_{ij} | p_{\pi j} \rangle$ would be considered. This is all right if the coordinate axes are chosen normal to the line from i to j . If not, invariance to coordinate transformations requires the retention of off-diagonal elements $\langle p_j | 1/r_{ij} | p'_j \rangle$, where p and p' are, for example, p_x and p_y .

The CNDO potential model predicts the fluoromethane shifts very well, as Table XIV shows. The shifts predicted by the p-p' modification agree better with experiment than do any other theoretical estimates. Even the F(1s) shifts are predicted well, in contrast to the ab initio results in Table XI.

For fluorine-substituted benzenes the CNDO potential model also predicts shifts quite well.⁵³ For this case the p-p' method overestimates the shifts somewhat, while the point-charge methods gives excellent results, as shown in Fig. 7. None of the 28 shifts deviates by over 0.4 eV from the experimental value. Apparently this model can predict shifts quite well within a series of related compounds. Its narrow range of applicability is a drawback, however, as is the ambiguity of whether the point-charge or p-p' modification is preferable.

II.C.2. The ACHARGE Approach

Davis et al.⁵³ introduced a different approach for interpreting binding energies, called the "atomic charge" analysis, or ACHARGE. In some respects ACHARGE is quite similar to the above analyses, but philosophically it is quite



XBL 723-504

Fig. 7. Observed C(1s) and F(1s) binding-energy shifts in fluorobenzenes, relative to C_6H_6 (for C1s) and C_6H_5F (for F1s), plotted against CNDO "point-charge" potential-theory estimates, from Ref. 53. Here C_F and C_H denote energies of peaks assigned to the aggregate of all carbons bonded directly to F or H.

Table XIV. CNDO Shifts in Fluorinated Methanes (Ref. 44).

Molecule	Shifts in $E_B(\text{Cls})^a$			Shifts in $E_B(\text{Fls})^b$		
	point charge	p-p'	Expt. ^c	point charge	p-p'	Expt.
CH_3F	2.58	2.97	2.8(2)	--	--	--
CH_2F_2	4.99	5.58	5.55(5)	1.07	0.82	0.73(5)
CHF_3	7.32	8.54	8.3(2)	2.09	1.60	1.7(2)
CF_4	9.52	11.14	11.0(2)	3.11	2.37	2.6(2)

^aShifts in eV, relative to methane.

^bRelative to CH_3F .

^cError in last place is given parenthetically.

different. The idea in ACHARGE is to work backward; i.e., to learn chemistry from binding energies rather than using known chemical facts to explain the spectra. The ACHARGE approach is based on assuming point charges to exist on all the atoms in a molecule, measuring a complete set of core-level shifts, and deriving a consistent set of values of the charges from the shifts. ACHARGE is not a molecular-orbital model, but gives rather an experimental population analysis. The derived charge values agree very well with CNDO charges, presumably because CNDO is essentially a point-charge theory.

In ACHARGE an equation of the form

$$\delta E_i = k_i q_i + e^2 \sum_{j \neq i}^n \frac{q_j}{R_{ij}}$$

is written for each of the n atoms in a molecule. The parameter k_i , which has the same value for all atoms of a given element, is essentially the two electron repulsion integral for a free atom of that element. If the molecule does not contain hydrogen there exist n equations linear in the charges q_i (for hydrogen-containing molecules some assumption about q_H must be made). If there are equivalent atoms, these equations can be condensed by gathering terms in each q_i and eliminating redundant equations, obtaining finally m linear equations, with $m \leq n$. In matrix form these may be written

$$\vec{\delta} = A\vec{q}, \quad (26)$$

where $\vec{\delta}$ and \vec{q} are vectors whose components are the sets $\{\delta E_i\}$ and $\{q_i\}$, and A is an $m \times m$ matrix. A diagonal element of A has the form

$$A_{\ell\ell} = k_{\ell} + e^2 \sum_{\ell'} (1/R_{\ell\ell'}) \quad , \quad (27)$$

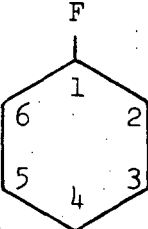
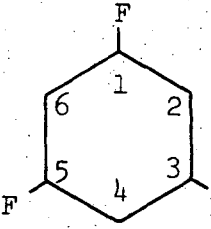
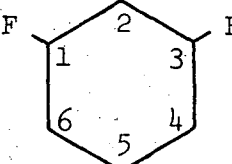
where the sum is taken over all other sites equivalent to the ℓ^{th} site. Only the ℓ^{th} site itself contributes a linear equation to Eq. (26), equations arising from the sites labeled by ℓ' were redundant and were lost in contracting from n to m equations. The off-diagonal elements have the form

$$A_{\ell p} = e^2 \sum_{p'} (1/R_{\ell p'}) \quad , \quad (28)$$

with the sum taken over sites that are equivalent among themselves but different from ℓ . The matrix A is usually non-symmetric.

In studying fluorinated benzenes Davis et al. used $k_c = 22 \text{ eV}/|e|$ for carbon and $k_F = 32.5 \text{ eV}/|e|$ for fluorine. For a given molecule the charges on all hydrogens were assumed equal. An additional equation was obtained by requiring overall charge neutrality. Finally, for each molecule all carbons bound to the same ligand (hydrogen or fluorine) were taken to have the same $1s$ binding energy, because inequivalent carbons with the same ligand appeared only as unresolved components of the same $C(1s)$ peak in the photoelectron spectrum. Using this model, measured shifts $\delta E(C1s)$ and $\delta E(F1s)$, and molecular geometries, Davis et al. deduced atomic charges for several fluorinated benzenes that agreed very well with CNDO charges. Their results for four molecules are given in Table XV, together with the CNDO values. In spite of the approximate nature of the ACHARGE model it yields charges that are consistent with the basic physical and chemical properties of fluorobenzene. For example, withdrawal

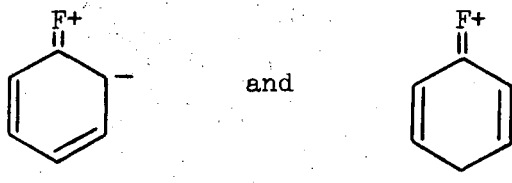
Table XV. Atomic charges in fluorinated benzenes (after Ref. 53).

Compound	Atom ^a	q (ACHARGE)	q (CNDO/2)	Compound	Atom	q (ACHARGE)	q (CNDO/2)	
	C ₁	23 ^b	24		C _{1,3,5}	27	28.5	
	C _{2,6}	-4	-5		C _{2,4,6}	-13	-14	
	C _{3,5}	1	3		F	-18	-19	
	C ₄	0	-1		H	4	4	
	F	-19	-20					
	\bar{H}	0	0		C _{1,3}	25	26	
					C ₂	-9	-12	
C_6F_6	C	14	15.5		C _{4,6}	-4.5	-7	
	F	-14	-15.5		C ₅	2	5	
					F	-18	-20	
					\bar{H}	0.5	2	

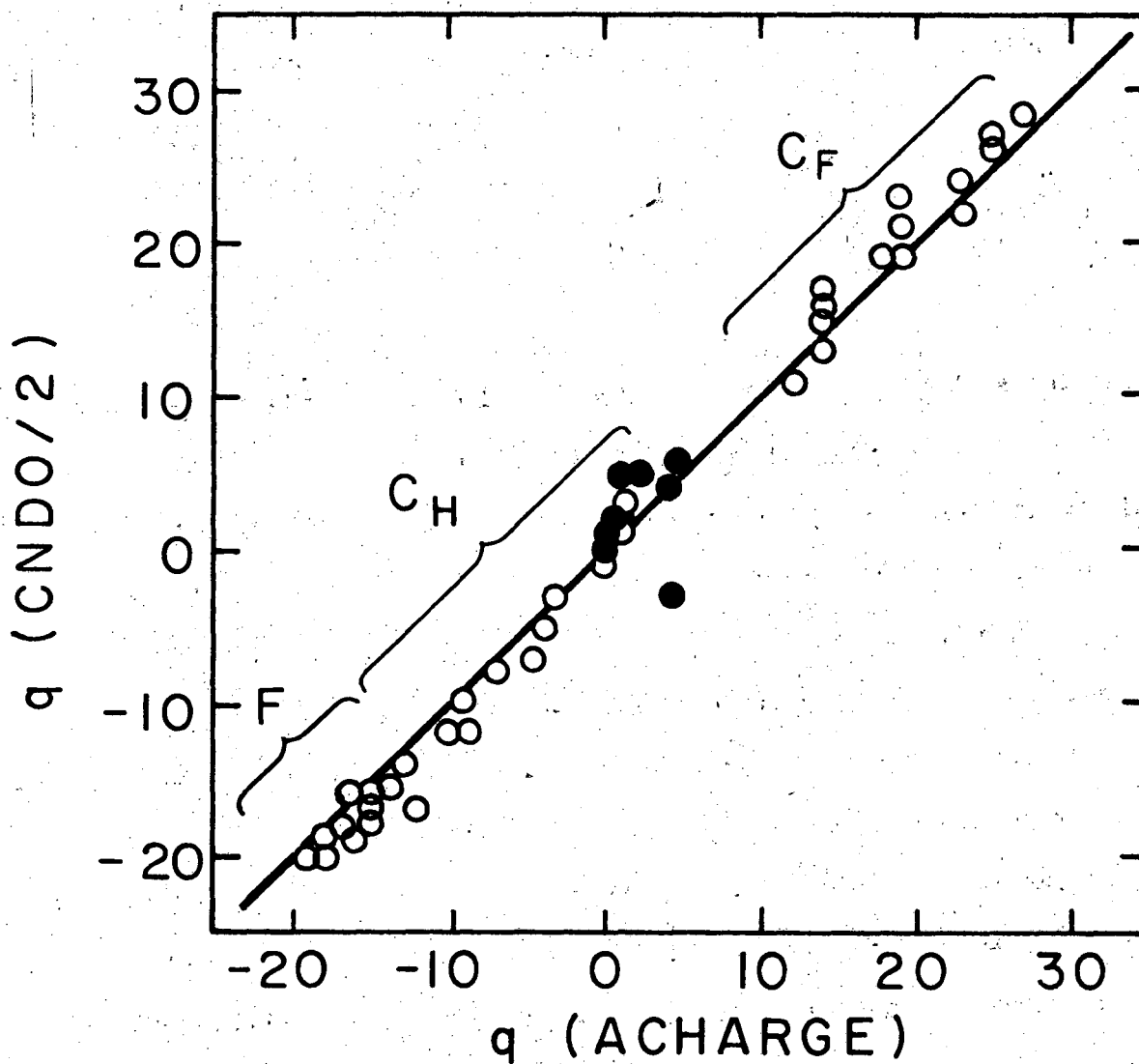
^aHere \bar{H} denotes average of all hydrogen charges.

^bCharges are given in units of $10^{-2} |e|$.

of electronic charge from the ring by fluorine is manifest as a negative charge on the fluorine atom and polarization of the C-F bond. On a more detailed level the ortho-meta-para alternation in charge, usually invoked to explain the preferential ortho-para orientation of electrophilic substituents, is evident. This alternation is explained classically by the tautomeric forms



Although Davis et al. presented consistent evidence for ortho-meta-para charge alternation derived from different arguments, the effect is small. Larger effects of this nature were found in multiply-substituted cases in which the charge shifts caused by two or more fluorines could reinforce one another. In *m*-difluorobenzene, for example the carbon in position 2 is ortho to two fluorines, and consequently its charge is $-0.09 |e|$, or about twice that of an ortho carbon in fluorobenzene. Carbons 2, 4, and 6 in 1,3,5-trifluorobenzene are each ortho to two fluorines and para to another. Each of these carbons therefore carries the large negative charge of $-0.13 |e|$, in the ACHARGE analysis. Further chemical arguments of the nature can be made on the basis of the atomic charges derived from shifts in other fluorinated benzenes. These arguments are essentially the same that would be made by using CNDO charges, since the two sets of charges agree so well, as shown in Fig. 8.



XBL 721-2236

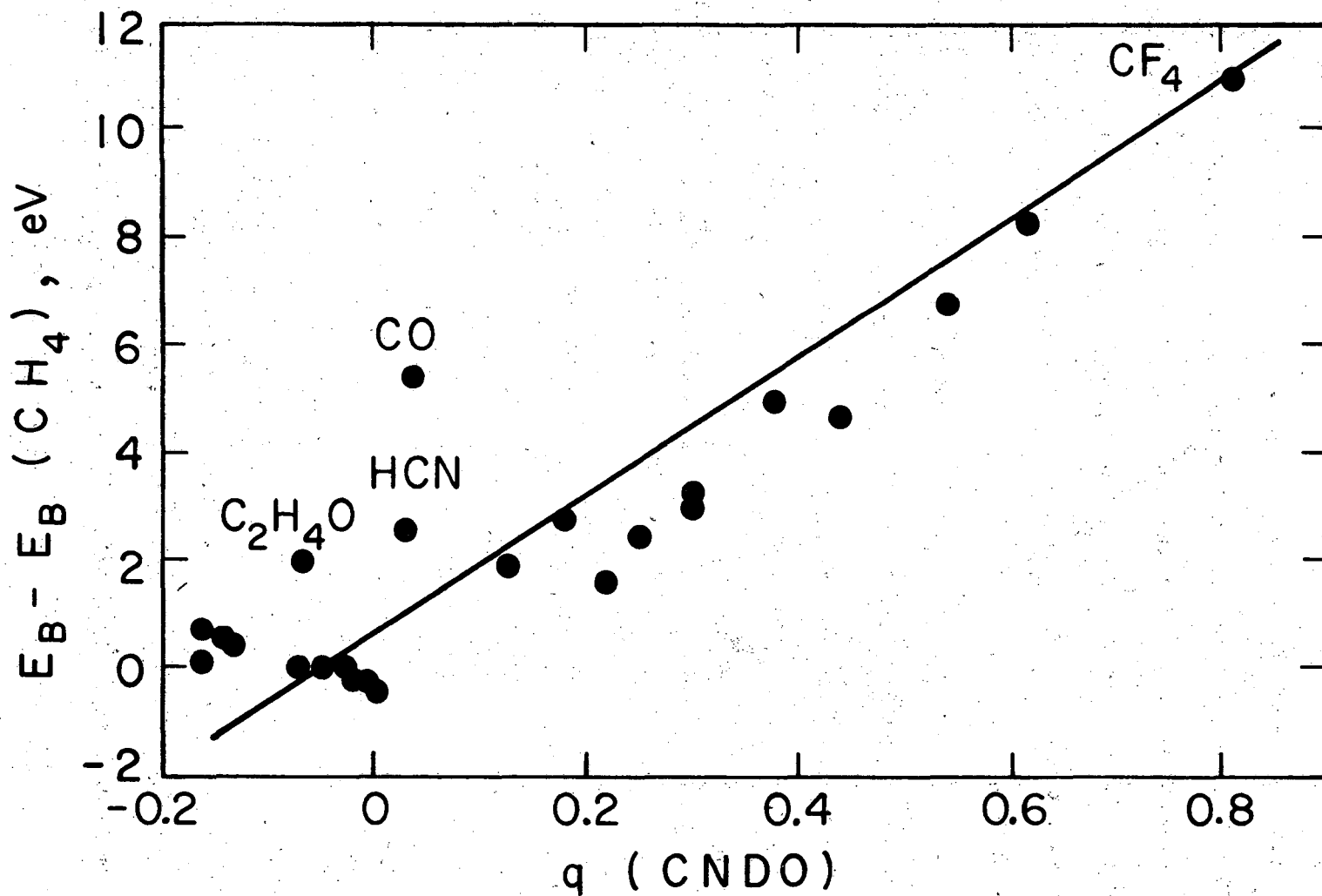
Fig. 8. Comparison of atomic charges in fluorinated benzenes, as derived from CNDO theory and from the ACHARGE analysis (Ref. 53). Filled circles are average charges on hydrogens. Open circles represent fluorines, and carbons bonded to hydrogen or fluorine, as labeled.

II.C.3. Atomic Charge Correlations

In the early days of ESCA studies, particularly before molecular calculations were widely applied to the estimation of shifts, the shifts were interpreted as arising primarily from the atomic charge on the host atom, without a detailed account being made of contributions from the remainder of the molecule. These interpretations usually took the form of plots of binding energy versus atomic charge. The correlations were usually quite good on a rough scale, but poor on a finer scale.

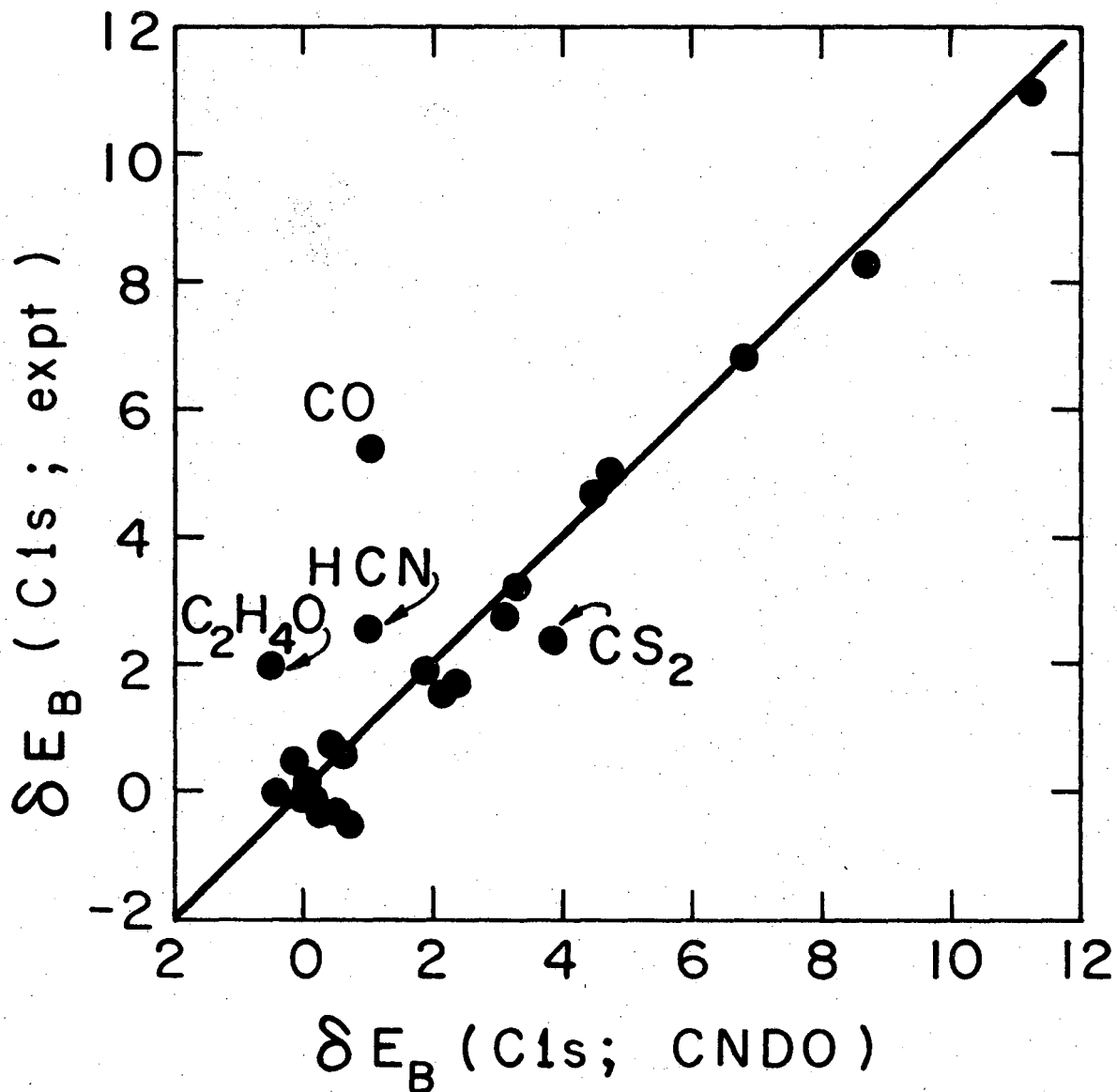
Figure 9 shows binding energies of C(1s) electrons from a number of small gaseous hydrocarbon molecules, plotted against host-atom CNDO charges. The data were taken from Refs. 3 and 41. The trend is obvious, but individual points scatter by 1-2 eV typically. This is to be expected: neglect of the environment cannot destroy the trend of δE over a large range of charge. The slope of a line "through" the points in Eq. (8) is only 13 eV/|e|. This is in accord with the earlier observation⁵⁴ that the molecular potential should decrease this slope by less than a factor of two. The slope without the environment would be given by the one-center, two-electron integral, $k_c \cong 22$ eV/|e| in this case.

Figure 10 shows a comparison of experimental and predicted binding-energy shifts for the same compounds as in Fig. 9. The theoretical values are calculated using the CNDO potential model, as described above. Comparison with Fig. 9 shows that inclusion of the potential makes an important difference. Comparison of Figs. 4a and 10 shows that for most cases the CNDO-potential model predictions are nearly as good as ab initio orbital-energy values, but that for the somewhat unusual molecules CO, C₂H₄O, HCN, and CS₂ the ab initio values are distinctly superior (see also Fig. 7 and the related discussion).



XBL 721-2237

Fig. 9. Experimental C(1s) binding-energy shifts for small gaseous molecules plotted against host-atom charge from CNDO theory, after Refs. 3 and 31. The straight line connects the methane and CF_4 points.



XBL721-2238

Fig. 10. Experimental C(1s) shifts, relative to methane, vs shifts calculated on CNDO theory using the molecular potential, for the same compounds plotted in Fig. 9. Compare also with ab initio results in Fig. 4a.

If comparisons are restricted to structurally similar compounds such as the fluorinated benzenes, so that the inability of CNDO theory to deal with unusual compounds would not be a factor, the correlation of δE_B with host-atom charge might be expected on the above arguments to break down. That it does is evident in Fig. 11, wherein measured C(1s) shifts for these compounds⁵³ are plotted against CNDO charges. The points are distributed in two groups, composed of carbons bonded to hydrogens and to fluorines. While the latter group have higher charges and higher binding energies than the former, and the two groups would fit rather well onto Fig. 9, the correlation of δE_B with $q(\text{CNDO})$ within each group is essentially nonexistent. The reason for this does not lie in the inadequacies of CNDO theory, for, as Fig. 7 shows, the CNDO potential model deals with these shifts rather well. Instead, the poor correlation in Fig. 11 must arise from neglect of the external potential. From this result and the foregoing discussion it is clear that binding energy-charge correlations are approximately valid over large charge ranges but have little application to subtle shifts.

Extended Hückel molecular orbital (EHMO) theory has been used extensively in discussing binding-energy shifts. The δE_B -atomic charge correlations are of varying quality, but typically they show an overall increase of E_B with q , with considerable scatter. There is a rather basic deficiency in EHMO theory: it does not account plausibly for electron repulsion. For this reason bond polarities are enormously exaggerated whenever EHMO theory is applied to compounds in which atoms of different electronegativities are bonded together. Atomic charges from EHMO calculations are therefore unrealistic and can be regarded only as empirical parameters. This deficiency showed up early

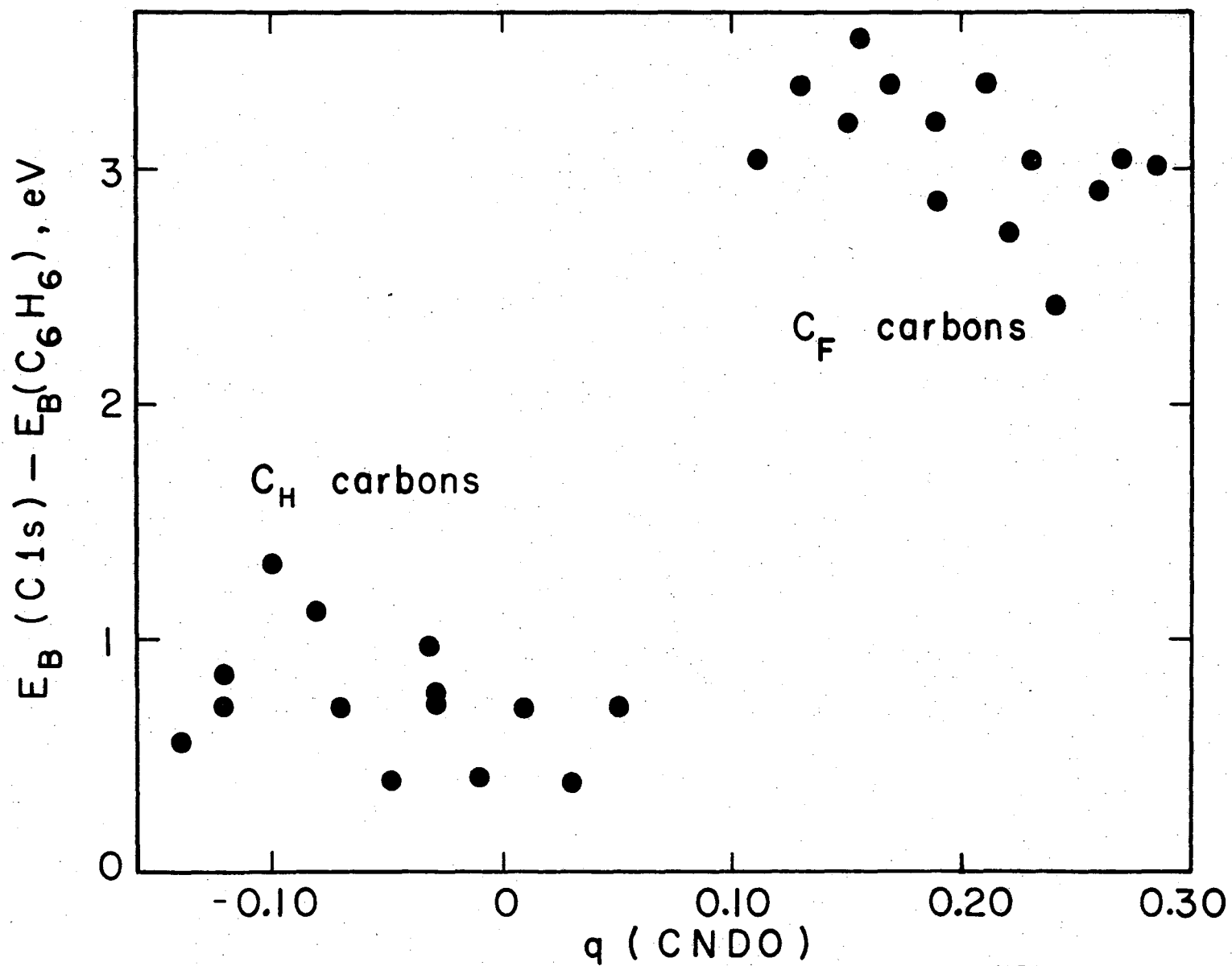


Fig. 11. Carbon 1s binding energy shifts, relative to benzene, for fluorinated benzenes, plotted against CNDO charges. Data were taken from Ref. 53.

41000700014

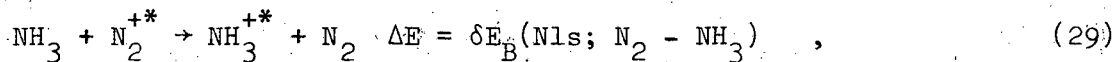
XBL721-2239

in E_B vs q correlations as an absurdly small slope, $\Delta E_B/\Delta q$.⁵⁴ More recently Schwartz⁵⁵ has shown that an improved correlation can be obtained using EHMO theory between observed binding energies and computed average potentials at the host nucleus. The "slope", $-\Delta E/\Delta V$, is still much too small, however. The computed $\text{CH}_4 - \text{CHF}_3$ potential energy difference is 29.9 eV, for example, while the experimental shift is only 8.3 eV.

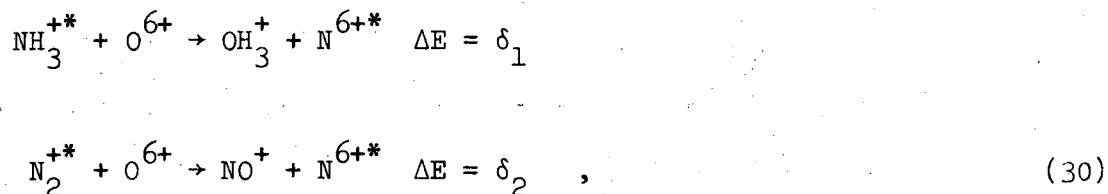
II.C.4. Thermochemical Estimates

Before discussing empirical correlations it is useful to consider a method for estimating core-electron binding energy shifts that was introduced by Jolly, et al.⁵⁶⁻⁵⁹ This method is based on the similarity of compounds that have isoelectronic valence orbitals and equally-charged cores. It has the virtue of using empirical thermochemical data to predict core-level binding-energy shifts, although it could equally well employ total energies calculated by SCF computations on molecular ground states. As this last remark implies, relaxation of passive orbitals is automatically taken into account, as only ground states are finally compared.

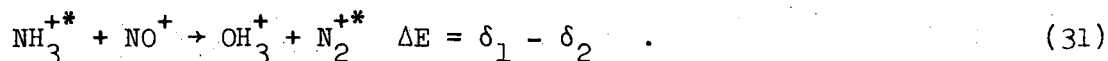
Jolly et al. pointed out that the N(1s) binding-energy shift from molecular nitrogen to ammonia is given by the reaction



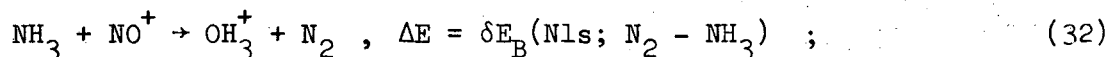
where an asterisk denotes a molecule with a nitrogen 1s electron missing. There are no thermochemical data available, in most cases, for such highly excited species as NH_3^{+*} . However, OH_3^+ , which is isoelectronic in its valence orbitals and in which O has a core (nucleus plus 1s shell) of the same charge as N in NH_3^{+*} , is well known. These cores may be exchanged via the reactions



which can then be added to give



Now if $\delta_1 - \delta_2 \cong 0$, i.e., if the energy of exchanging the O^{6+} and N^{6+*} cores is essentially insensitive to the chemical environment, Jolly pointed out that addition of (29) and (31) yields a reaction

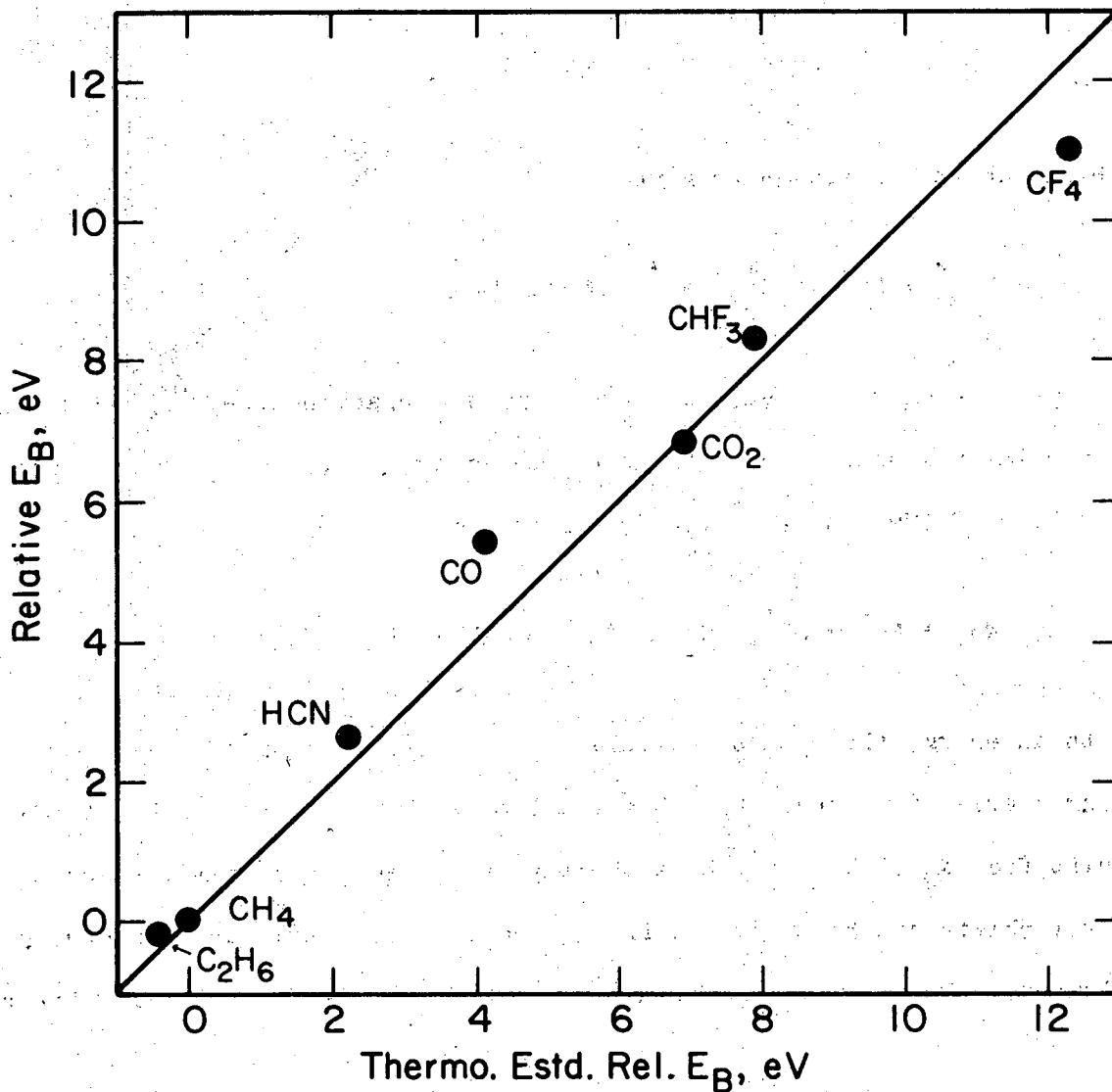


with an energy that can be calculated from the energies of formation of the four species involved. But this reaction energy is just the Nls binding-energy shift from N_2 to NH_3 , which is thereby predicted. From similar equations core level shifts can be predicted from thermochemical data for compounds of other elements. For example the methane- CF_4 shift can be derived using the reaction



Estimated and measured shifts for several gaseous carbon compounds^{57,59} are shown in Fig. 12.

This thermochemical approach is very valuable because it gives good results. Clearly it can be expanded to employ SCF total energies or energies of formation, as well as thermochemical data. Because of the potential

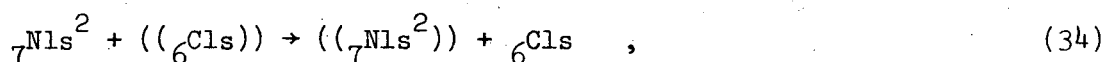


XBL 718-7209

Fig. 12. Experimental and thermochemically estimated Cls binding energy shifts in gaseous carbon compounds, after Jolly, et al. 37,59

usefulness of the method, it seems worthwhile to study its theoretical basis a bit further. The core-exchange step represented by Eq. (30) seems particularly in need of justification. In the following abbreviated discussion⁶⁰ this step is justified in the Hartree-Fock formalism.

Consider the core-exchange "half-reaction"



wherein a 5+ core consisting of a nitrogen nucleus plus a filled 1s shell replaces a 5+ core consisting of a carbon nucleus plus a half filled 1s shell. The double parentheses denote the molecular environment, which has identical electronic configurations on the two sides, although the radial wave functions may vary slightly. The nuclear positions are assumed identical. The total energy of the nitrogen compound may be written in Hartree-Fock notation as

$$\begin{aligned} E_N(\text{cpd}) = & 2 \epsilon_0^N(1s) + J_N(1s1s) + 2 \sum_{i \neq 1s}^n [2J_N(1s i) - K_N(1s i)] \\ & - 2 \sum_{m \neq N} Z_m \langle \text{N}1s(1) | 1/r_{1m} | \text{N}1s(1) \rangle - 2 \sum_{i \neq 1s}^n Z_N \langle \phi_i(1) | 1/r_{1N} | \phi_i(1) \rangle \\ & + \sum_{m \neq N} \frac{Z_m Z_N}{R_{mN}} + \dots \end{aligned} \quad (35)$$

where J and K are Coulomb and exchange integrals, ϕ_i is a molecular orbital, and R_{mN} is the internuclear distance from the host N nucleus to any other. The

system is assumed to possess n doubly-occupied orbitals. Because interactions between any two particles or orbitals outside the N $1s^2$ core should be only negligibly affected by core exchange, only those terms that directly involve the $1s$ core particles (N nucleus and $1s$ electrons) are written explicitly in Eq. (35). Expressions for the energies of the other three entities in Eq. (34) can be arrayed conveniently as

$$\Delta E = 2 \epsilon_0^N(1s) - 2 \epsilon_0^{N'}(1s) - \epsilon_0^c(1s) + \epsilon_0^{c'}(1s) + J_N(1s1s) - J_{N'}(1s1s) \quad \left. \vphantom{\Delta E} \right\} \quad \text{(I)}$$

$$+ \sum_i^n \{ 2[2J_N(1s i) - K_N(1s i)] - [2J_c(1s i) - K_c(1s i)] \quad \left. \vphantom{\sum} \right\} \quad \text{(II)}$$

$$- 2Z_N \langle \phi_i(1) | 1/r_{1N} | \phi_i(1) \rangle + 2Z_c \langle \phi_i(1) | 1/r_{1c} | \phi_i(1) \rangle \quad \left. \vphantom{\sum} \right\}$$

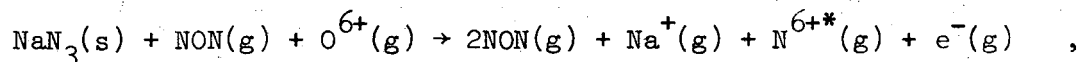
$$+ \sum_{m \neq N} Z_m \left[\frac{Z_N - Z_c}{R_{mN}} - 2 \langle N1s(1) | 1/r_{1m} | N1s(1) \rangle + \langle C1s(1) | 1/r_{1m} | C1s(1) \rangle \right] \quad \left. \vphantom{\sum} \right\} \quad \text{(III)}$$

(36)

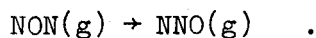
Here primes denote cores. Term III should in principle vanish identically. In fact the calculations and arguments presented by Schwartz⁴² in his justification of potential models can be used to show that both I and III are negligibly small. Term II is not so simple. If the orbitals i are expressed in terms of a "localized" orbital basis set,⁴⁷ and the sum over i is split into sums over local and distant orbitals, the former can be shown, by Schwartz's calculations, to be negligibly small. The sum over local orbitals is non-zero, however. The attraction of the N $1s^2$ core is systematically greater for these

orbitals than that of the $6C$ $1s$ core. This is a result both of incomplete shielding by the $1s$ electrons and of the contributions of the exchange integrals (the two effects reinforce one another). Each local orbital contributes a term of the order of -0.1 a.u. to ΔE . This term is similar in nature to the terms under the sum in Eq. (20). It is different in detail, however, and somewhat larger. Still the same arguments⁴² should apply to show that term II in Eq. (36) varies with environment an amount similar to the variation of the sum in Eq. (20). Thus the thermochemical model is justified to about the same level of approximation as the potential model.

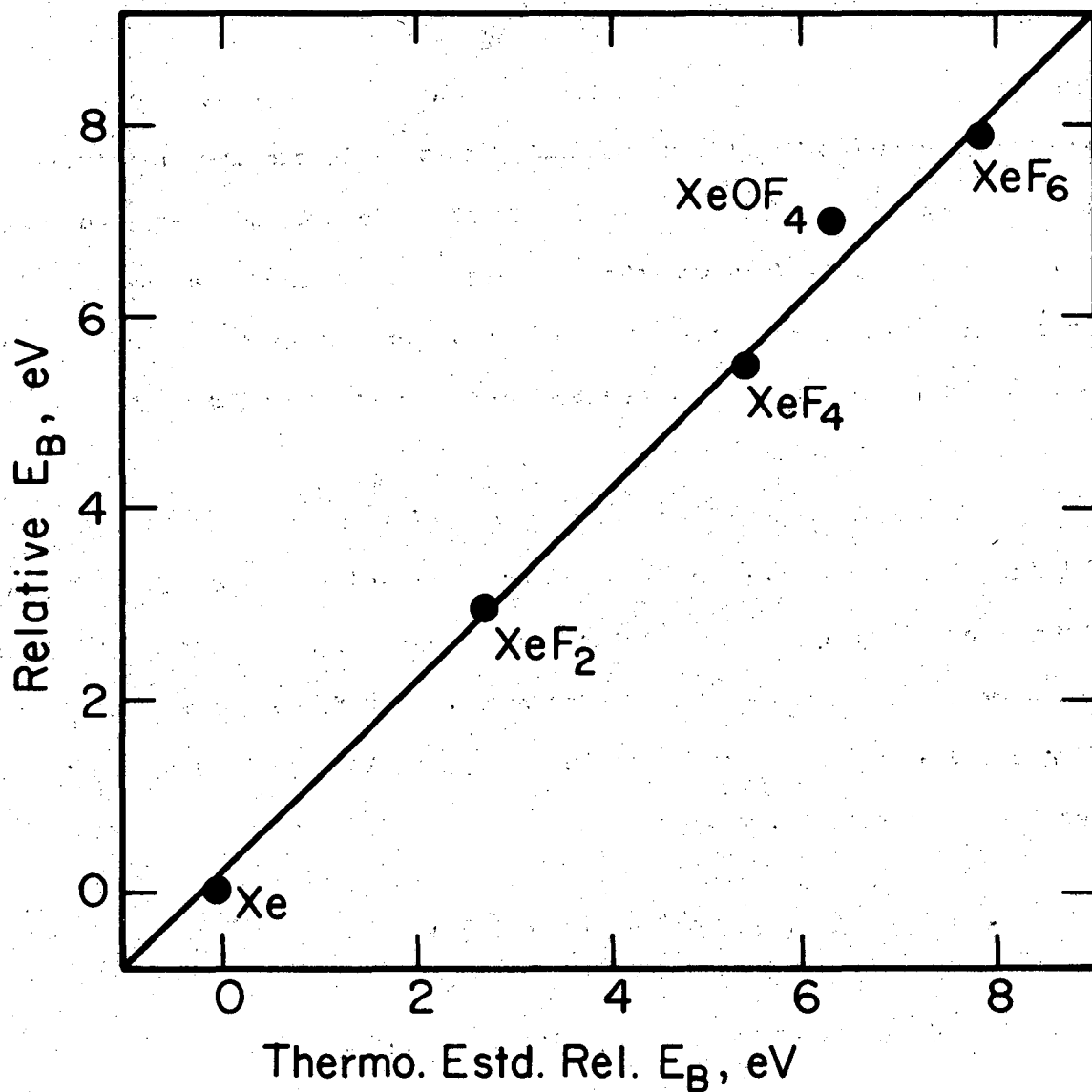
Jolly et al. have used the thermochemical model to estimate heats of formation from core level shifts and thus to predict the possible stabilities of hypothetical compounds. From the $1s$ binding energy of the middle nitrogen in sodium azide, together with the known heats of formation of $NaN_3(s)$ and $Na^+(g)$, and an estimated sublimation energy for NON , Jolly and Hendrickson⁵⁶ used the hypothetical reaction



to predict $\Delta H^\circ = -100$ kcal/mole for the isomerization



Using similar reasoning Jolly⁵⁹ was able to predict bond energies of essentially zero for the hypothetical molecules ArO_3 and ArO_4 . The thermochemical model can be applied to molecules that are too large for accurate Hartree-Fock calculations at present. For example, Hollander and Jolly^{57,59} made very good estimates of $Xe(3d_{5/2})$ shifts in xenon fluorides, as shown in Fig. 13. The success of these



XBL 718-7212

Fig. 13. Experimental and thermochemically estimated xenon core level binding-energy shifts, after Refs. 57 and 59.

predictions establishes the validity of the thermochemical approach for core levels other than 1s levels.

II.D. Correlations of Binding-Energy Shifts with Other Properties

There is of course no sharp distinction between prediction and correlation except for approaches that are completely rigorous in the first case or completely without theoretical justification in the latter. Thus most of the correlations discussed below could be turned around and used to predict shifts, and they are all theoretically understood to a greater or lesser degree. The common thread that links these methods is their ability in each case to illuminate some aspect of atomic or molecular structure by connecting two quantities--binding energy shift and another property--whose relationship might not be obvious. The correlation discussed below represent but a miniscule sample of the very wide range of possibilities. In fact the statement, "Each chemist can correlate binding-energy shifts with his favorite property", is essentially true. Because of its direct connection to the molecular charge distribution, the shift in core-level binding energy is related to practically every parameter of chemical interest.

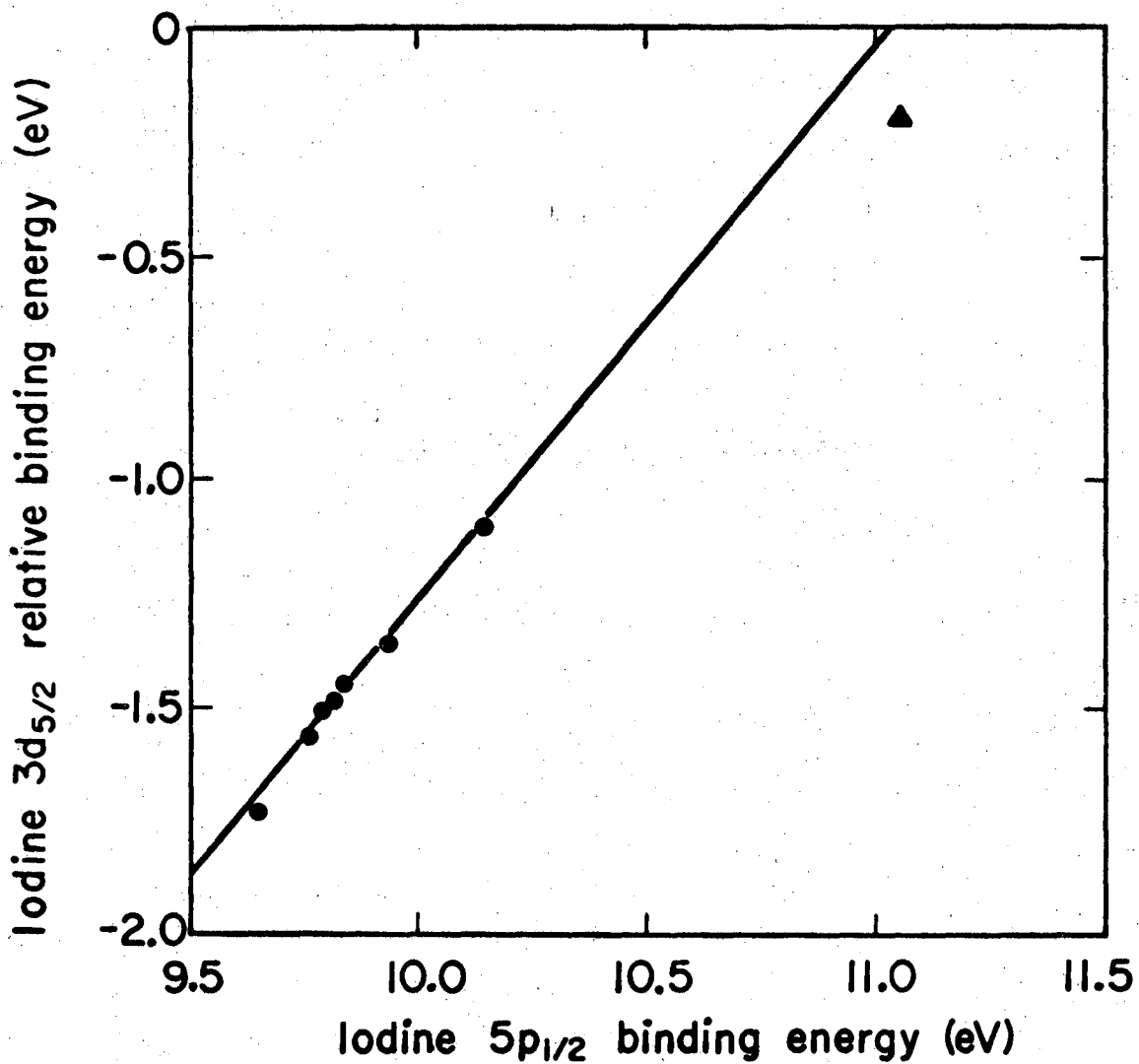
II.D.1. Correlations with Other Binding Energies Shifts

Perhaps the most obvious quantity with which the binding-energy shifts of a given core orbital may be compared is the shift of a different core orbital in the same atom. The physical insight afforded by a constant such as the conducting-sphere model lends to the expectation that all "deep" core levels in a given atom should show equal shifts upon a given change in environment. Fadley, et al.⁹ found that this is true for iodine, as discussed in Section II.A. and shown in Fig. 1. Similar behavior has been observed for core levels in

other atoms: if two core levels are described by wave functions whose radial extents are significantly smaller than that of the valence shell, these core levels will show very similar binding-energy shifts.

The above conclusions were valid--and even useful--in the early days of ESCA. Indeed an early disappointment of the method was the realization that the magnitudes of binding energy shifts depended only on the principle quantum number, and not on the orbital angular momentum, of the valence electrons. Now, however, the field has moved to a higher level of sophistication, both experimentally and theoretically, and in favored cases some sensitivity to details of orbital composition can be obtained. In a recent very careful study of shifts in the binding energy of the iodine $3d_{5/2}$ orbital in alkyl iodides and HI, Hashmall, et al.⁶¹ found a strong correlation with iodine $5p_{1/2}$ binding energies from UV photoemission studies,⁶² as shown in Fig. 14. There are two significant features about this figure. First, the slope of the line through the alkyl iodide points is 1.22 ± 0.05 , or significantly greater than unity. Thus binding-energy shifts are greater for the more core-like $3d_{5/2}$ orbitals than for the outer $5p_{1/2}$ orbitals. This result was actually anticipated in Fig. 1, wherein the orbital energies for core levels in ionic iodine were found to shift with charge state by essentially the same amount for 1s through 4d orbitals and somewhat less for the $n = 5$ orbitals (in two cases the 5p shifts were anomalously high because of the small basis sets). A more reliable estimate of this effect can be obtained directly from the Coulomb and exchange integrals that involve valence and core electrons. An estimate of this type is shown in Fig. 15, in which the function (see Eq. (6))

$$2J(ns, Np) - K(ns, Np) = F^0(ns, Np) - (1/6)G^1(ns, Np) \quad ,$$



XBL717-3928

Fig. 14. Correlation of iodine 3d_{5/2} and 5p_{1/2} binding energies in alkyl iodides (circles) and HI (triangle) after Hashmall, et al.⁶¹

was plotted for each s orbital, $n = 1, \dots, N$, and for each halogen as a free atom. Here N is the principle quantum number of the valence shell, and F^0 and G^1 are Slater integrals. The values of F^2 and G^1 were given by Mann.⁶³ The above function is essentially equal to the "slope" $k = \partial E_B / \partial q$ that appears in the potential models (Eq. 24). The abscissa in Fig. 15 is the radial maximum, R_{\max} , of the ns shell. In each case there is a large decrease in k from the penultimate to the outermost shell. Thus the slope observed in Fig. 14 is expected, and it can be at least partially attributed to a variation of the $I 5p_{\sigma}$ orbital population, in the alkyl iodides, with induction through the C-I bond.⁶¹

The other interesting feature of Fig. 14 is the deviation of the HI point from the straight line through the alkyl iodide data. Hashmall, et al. attributed this to hyperconjugation. The lone-pair $p_{1/2}$ orbitals are relatively large and can be destabilized by interaction with σ orbitals on the alkyl groups (not in the C-I bond itself). This effect is negligible, however, for the $3d_{5/2}$ orbitals. It is absent, of course, in HI. Thus the horizontal displacement of 0.14 eV of the HI point is a measure of the hyperconjugative destabilization energy of the $5p_{1/2}$ orbitals, and the role of the core-level shifts is to calibrate the inductive effect. This case provides an example of how detailed bonding information can be extracted from core-level shifts. Further application of this type can be expected.

II.D.2. Correlation with Diamagnetic Shielding Constants

There is in general no direct relation between core-level binding-energy shifts and NMR frequencies, but Basch⁴⁶ showed that δE_B should be closely related to the diamagnetic shielding constant σ_{Av}^d , which is given by the relation

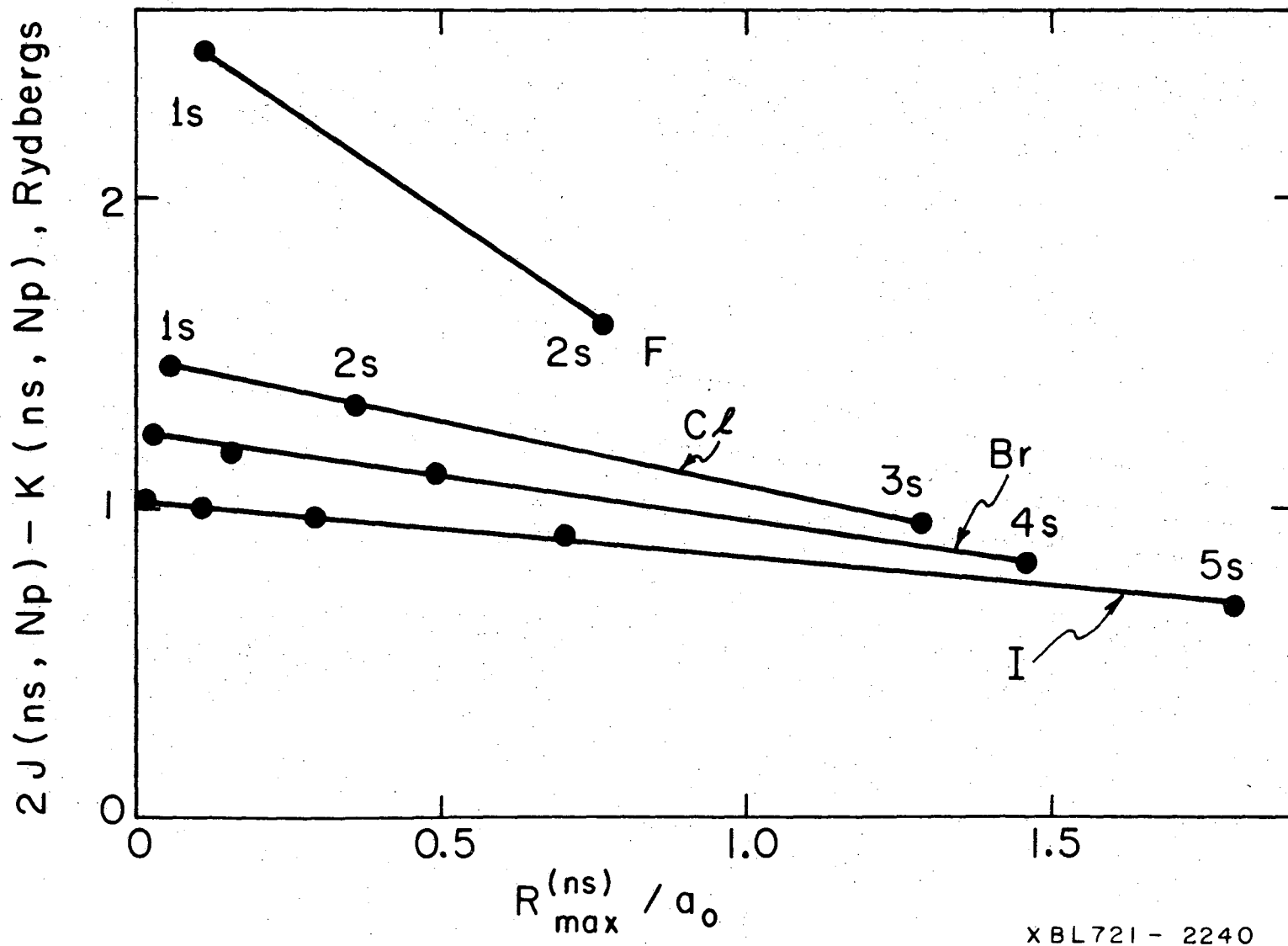


Fig. 15. Sensitivity of s-electron binding energies to valence-electron population, for s electrons in halogens. Note decrease from next-to-last to outer shell.

XBL721 - 2240

0 3 0 0 6 7 0 5 3 2 0

$$\sigma_{Av}^d(\nu) = 2(e^2/3mc^2) \sum_i \langle \phi_i(1) | 1/r_{1\nu} | \phi_i(1) \rangle \quad (37)$$

This expression gives the shielding constant at nucleus ν . The sum is taken over doubly-occupied one-electron orbitals ϕ_i . The potential energy of a core ls orbital k on nucleus ν due to other electrons and nuclei is similar:

$$V_\nu = 2 e^2 \sum_{i \neq k} \langle \phi_i(1) | 1/r_{1\nu} | \phi_i(1) \rangle - e^2 \sum_{n \neq \nu} Z_n/R_{\nu n} \quad (38)$$

Although the sums over ϕ_i are different in the two cases, shifts in $\sigma_{Av}^d(\nu)$ and V_ν are comparable because the $i = k$ term varies negligibly with environment. One can therefore define a potential energy

$$\begin{aligned} V'_\nu &= 2 e^2 \sum_i \langle \phi_i(1) | 1/r_{1\nu} | \phi_i(1) \rangle - e^2 \sum_{n \neq \nu} Z_n/R_{\nu n} \\ &= 3mc^2 \sigma_{Av}^d(\nu) - e^2 \sum_{n \neq \nu} Z_n/R_{\nu n} \end{aligned} \quad (39)$$

so that to a very good approximation

$$-\delta E_B = \Delta V_\nu = \Delta V'_\nu = 3mc^2 \Delta \sigma_{Av}^d(\nu) - e^2 \Delta \left[\sum_{n \neq \nu} Z_n/R_{\nu n} \right] \quad (40)$$

Here the first equality follows from the potential model, the second from the constancy of the $i = k$ term in Eq. (39), and the third by definition. Basch demonstrated the accuracy of Eq. (40) by direct calculation for the fluorinated methanes. Thus a link has been established between ESCA shifts and NMR shifts.

Several workers have observed correlations of δE_B with ^{13}C chemical shifts,⁶⁴ but Eq. (40) has as yet been little used. The problem is that a measured NMR shift δ is sensitive to paramagnetic shielding as well as to σ_{Av}^d . Thus a smooth variation of δE_B with δ can only be expected in restricted groups of compounds for which σ^p varies smoothly with σ^d . However, Eq. (40) can be used, together with measured values of δE_B , to test theoretical estimates of σ_{Av}^d . For example, Flygare and Goodisman⁶⁵ proposed the following approximate equation:

$$\sigma_{Av}^d(\nu) \cong \sigma_{Av}^d(\nu, \text{free atom}) + (e^2/3mc^2) \sum_{n \neq \nu} Z_n/R_{n\nu} \quad (41)$$

They found that this relation gave excellent predictions of $\sigma_{Av}^d(\nu)$ in a number of molecules. At first this might be surprising, because Eq. (41) can be interpreted as representing a model in which the molecule is taken as a collection of atoms, each with a spherically symmetrical electronic charge distribution and zero net charge. As Flygare and Goodisman pointed out, however, the first term in Eq. (41) is relatively large, and the second term actually does give a reasonably good representation of the effects on σ^d of electrons outside the host atom. Thus Eq. (41) should always be approximately correct, and good enough to give a fair estimate of σ^d . As a means of estimating core-level binding-energy shifts, however, the assumptions behind Eq. (41) represent too low an order of approximation. After combining Eq. (39) and Eq. (41) and taking the shift between two compounds, we have

$$-\delta E_B \cong \Delta V'_\nu = 3mc^2 \Delta \sigma_{Av}^d (\text{free atom}) \cong 0 \quad (42)$$

Thus in this approximation all binding-energy shifts would be zero! Basch thus demonstrated that the existence of such shifts is possible only because of inaccuracy in Eq. (41).

This approach may be turned around, and measured core-level shifts can be used to assess the accuracy of Eq. (41) for a given case. Substituting in values for physical constants, we have

$$\Delta\sigma^d(\nu)(\text{ppm}) = -0.65 \Delta E_B(\nu)(\text{eV}) \quad , \quad (43)$$

as the range over which $\sigma_{Av}^d(\nu)$ can deviate from estimates based on the Flygare-Goodisman estimate, Eq. (41). In Eq. (43) ΔE_B is the maximum range of binding energy shifts for core levels of atom ν . In carbon, for example, ΔE_B is 11 eV, so the Flygare-Goodisman estimates for carbon could never be in error by over $\sim 7-8$ ppm.

The next obvious step is to use measured binding-energy shifts to check proposed values of σ_{Av}^d . For example Ditchfield, Miller, and Pople⁶⁶ have calculated σ^d values for ^{13}C in a number of carbon-containing molecules. For methane and methyl fluoride they gave values of $\sigma^d(\text{CH}_4) = 296.2$ ppm and $\sigma^d(\text{CH}_3\text{F}) = 320.2$ ppm, or a difference of 24.0 ppm. The binding-energy shift of 2.8 eV would give a shift of -1.8 ppm, while the $\Sigma Z/R$ term in Eq. (40) would add about 56 ppm to σ^d . Thus the difference between the values of σ^d for these two molecules must in fact be about 50 ppm, or twice the difference proposed by Ditchfield, et al. These authors gave $\sigma^d(\text{CH}_2\text{F}_2) = 376.5$ ppm, or 80.3 ppm above $\sigma^d(\text{CH}_4)$. From $\delta E_B = 5.6$ eV (Table V) and Eq. (40) a difference of ~ 110 ppm is obtained. Thus the σ^d values of Ditchfield, et al. seem reliable to ~ 30 ppm or 10%. This is reasonable, since their σ^d values were calculated for the center of mass.

II.D.3. Correlation with "Pauling Charges" and Electronegativity

Pauling⁶⁷ suggested that the fractional ionic character of a bond between atoms A and B can be estimated from the expression

$$I = 1 - \exp[-0.25(X_A - X_B)^2] \quad , \quad (44)$$

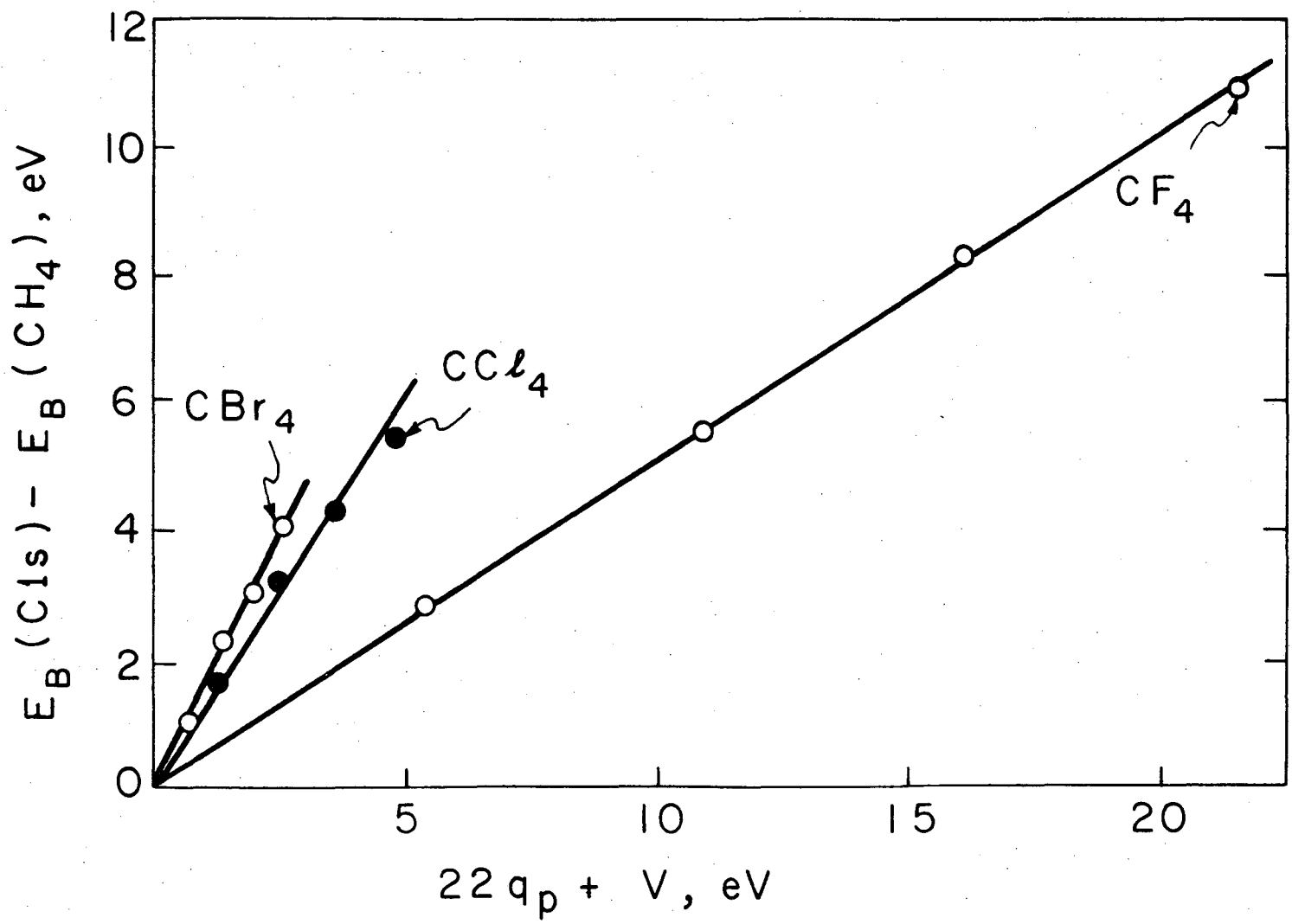
where X_A and X_B are electronegativities. Using the values $X_H = 2.1$, $X_C = 2.5$, $X_{Br} = 2.8$, $X_{Cl} = 3.0$, and $X_F = 4.0$, the percent ionic characters for the carbon-ligand bonds are: C-H, 4; C-Br, 2; C-Cl, 6; C-F, 43. From these bond ionicities charges can be calculated for all the atoms in halogenated methanes. These will be referred to as "Pauling charges", q_p . Both Thomas¹⁰ and Siegbahn et al.³ found linear correlations between $\delta E_B(\text{Cls})$ and $q_p(\text{C})$ for halogenated methanes, provided that only a single halogen (F, Cl, or Br) was considered. That is, $\delta E_B(\text{Cls}; \text{CH}_{4-n}\text{X}_n)$ varies linearly with $q_p(\text{C})$ as n is varied from 0 to 4. Values of q_p calculated from Eq. (44) are given in Table XVI, together with measured C(1s) shifts.^{3,10,44} The slopes of the δE_B vs q_p correlations differed by about a factor of two among the different halogens.^{3,10} Before accepting this as evidence for the inadequacy of Eq. (44), we should plot δE_B against $kq_p + V$ rather than just q_p , to take the molecular potential into account, as discussed in Section B. Such a plot is shown in Fig. 16. For this plot k_c was taken as $22 \text{ eV}/|e|$ and V was estimated on a point-charge model as

$$V = e^2 \sum_{\text{ligands}} q_p(\text{ligand})/R(\text{carbon-ligand}) \quad , \quad (45)$$

with q_p estimated from Eq. (44) and R taken as 1.1\AA for C-H, 1.4\AA for C-F, 1.8\AA for C-Cl, and 2.0\AA for C-Br throughout. The factor of two variation in slopes

Table XVI. Pauling charges and Cls shifts in halogenated methanes^{3,10,44}

Compound	X = Br		X = Cl		X = F	
	$q_P(C)$	$\delta E_B(Cl_s)$	$q_P(C)$	$\delta E_B(Cl_s)$	$q_P(C)$	$\delta E_B(Cl_s)$
CH ₄	-0.16	(0)	-0.16	(0)	-0.16	(0)
CH ₃ X	-0.10	1.0 eV	-0.06	1.6 eV	0.31	2.8
CH ₂ X ₂	-0.04	2.2	0.04	3.1	0.78	5.6
CHX ₃	0.02	3.0	0.14	4.3	1.25	8.3
CX ₄	0.08	4.0	0.24	5.5	1.72	11.0



XBL721 - 2241

Fig. 16. Binding energies of Cls electrons in halogenated methanes, plotted against a potential function, deduced from parameters in Table XVI and in text.

0 0 0 0 0 0 7 0 0 0 2 3

is still present, and the answer to this discrepancy must be sought elsewhere. Fortunately Fig. 16 tells us where to look. Because δE_B is plotted against potential energy rather than an empirical parameter, the points in Fig. 16 should all lie on a straight line of unit slope passing through the origin. In assessing why they don't, one is obliged to question q_p , because both $k_c = 22$ and V are on theoretically firm ground. Siegbahn, et al.³ indicated that increasing the electronegativity of Br from 2.8 to 3.3 would yield (through Eq. (44)) values of q_p for the brominated methanes that would bring them into agreement with the fluorinated methanes. Thomas¹⁰ preferred to abandon Eq. (44) and to use a relation such as that proposed by Gordy⁶⁸ for relating ionic character to electronegativity,

$$I = (X_A - X_B)/2 \quad (46)$$

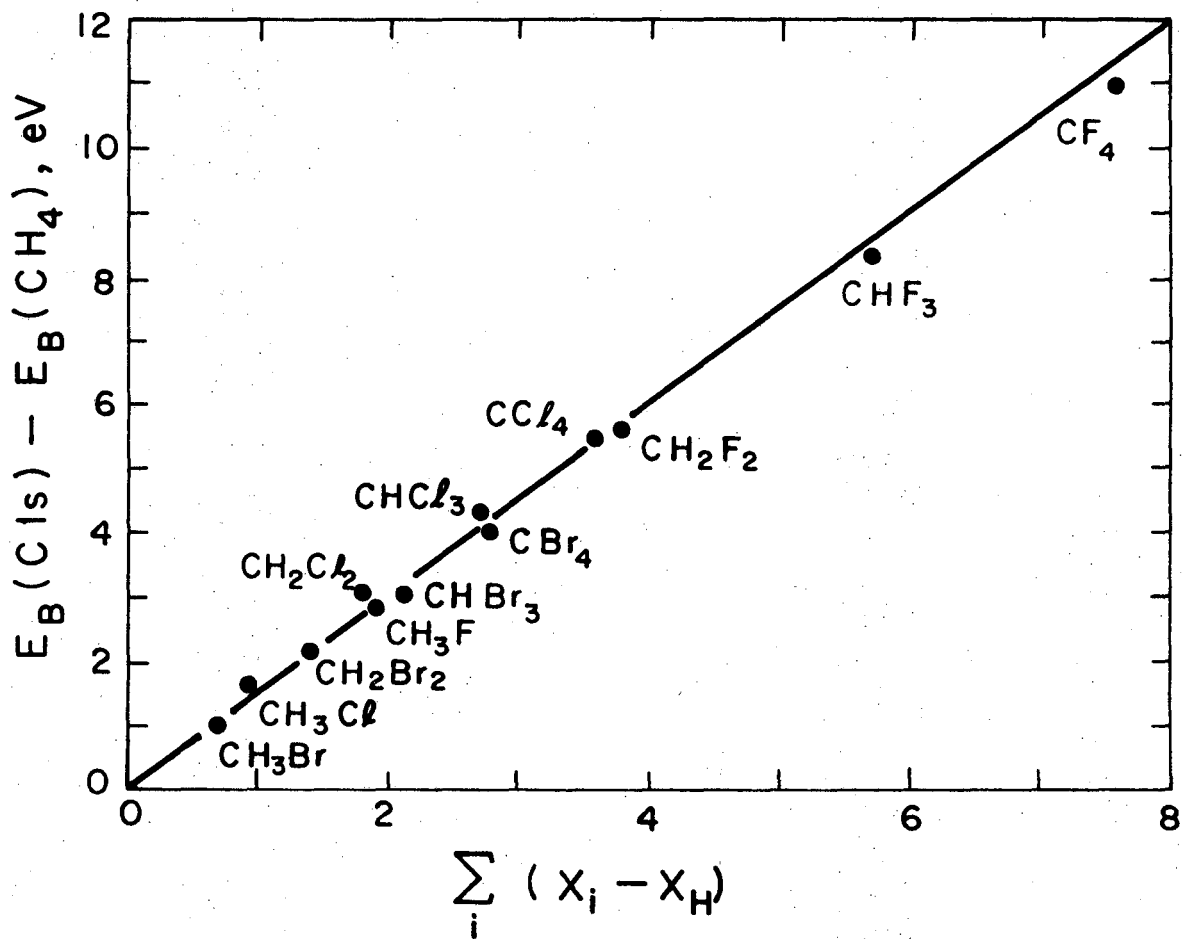
This would give

$$q_G(C) = \sum_i (X_i - X_C)/2 \quad (47)$$

as the carbon charge, with the sum taken over the four ligands for each molecule. Finally, in the "charge correlation" approximation, the Cls binding energy shift for a halogenated methane, relative to methane, should be given by¹⁰

$$E_B(\text{Cls}) - E_B(\text{CH}_4) = (\text{const}) \sum_i (X_i - X_H) \quad (48)$$

A plot testing this relation is shown in Fig. 17. Four points have been added to the plot given by Thomas.



XBL 722-317

Fig. 17. Binding energies of Cls electrons in halogenated methanes, versus total ligand electronegativity difference, after Thomas (Ref. 10). Four points have been added, from Refs. 3 and 4.

In reviewing the above results it should be noted that the excellent empirical correlation of binding energy with electronegativity, shown in Fig. 17, does not support the validity of q_p as calculated from Eq. (44) or q_G from Eq. (47). In both cases the range of charges on carbon in the fluorinated methanes is too large. Figure 16 illustrates this for q_p . For q_G the range is even larger, in fact unreasonably large, as Thomas¹⁰ observed. Since neither of the proposed relationships between ionicity and electronegativity gives charges that are consistent with binding-energy shifts, it is of some interest to derive charges that are consistent from a point-charge model and ascertain their relationship to electronegativity. Writing for a halomethane CX_4

$$E_B(\text{Cl}s; CX_4) = kq_C(CX_4) + \frac{4e^2}{R_{CH}} q_X(CX_4) = \left(k - \frac{e^2}{R_{CX}}\right) q_C(CX_4) \quad , \quad (49)$$

and similarly

$$E_B(\text{Cl}s; CH_4) = \left(k - \frac{e^2}{R_{CH}}\right) q_C(CH_4) \quad , \quad (50)$$

for methane, it is clear that even with k , R_{CX} , and R_{CH} known, the binding-energy shift can give only Δq_C . Unique values of q_C are obtained for the compounds CH_4 , CBr_4 , CCl_4 , and CF_4 , however, if the constraint is imposed that the ionic character of an AB bond be an even function of $(X_A - X_B)$. Using $k_C = 22 \text{ eV}/|e|$ and the bond distances given above, we find $q_C(CH_4) = -0.20$, $q_C(CBr_4) = 0.15$, $q_C(CCl_4) = 0.26$, and $q_C(CF_4) = 0.79$ as the set of charges that will satisfy these criteria. These charges can be predicted by the linear equation

$$I = 0.129 (X_A - X_B) \quad , \quad (51)$$

for the carbon-ligand bonds. Cls shifts relative to methane are then predicted by the potential model

$$\Delta E_B = k\Delta q_C + \Delta V$$

$$= (22)(0.129) \sum_{i=1}^4 (X_X(i) - X_H) - e^2(0.129) \left[\sum_{i=1}^4 \left(\frac{X_X(i) - X_C}{R_{CX}} \right) - \frac{4(X_H - X_C)}{R_{CH}} \right] \quad (52)$$

Shifts based on this equation are plotted, together with experimental shifts, in Fig. 17. This approach combines the advantages of preserving the excellent agreement found by Thomas (Fig. 17) and of giving both a quantitative relationship between ΔE_B and a reasonable set of charges on the carbon atom. Comparison with Fig. 6a supports this last point. The charge $q_C(\text{CF}_4) = 0.77$ predicted by Eq. (51) lies between the value 0.76 of CNDO theory and the ab initio value 1.01, which may be exaggerated by the overlap terms. Either Eq. (44) or Eq. (47) gives a carbon charge in CF_4 that is much too large (1.72 or 3.0).

Equation (51) can hardly be regarded as the final answer to ionicities in halomethanes. Some specific problems remain. For example, the F(1s) shift between CH_3F and CF_4 is 2.6^{10} eV, while this model predicts 5 eV. This shift is sensitive to q_F , which Eq. (51) would predict to be the same for these two molecules, whereas some saturation must take place in electron transfer from C to F. Still the charges predicted by Eq. (51) provide a good starting point for further improvements and extension to more complex molecules.

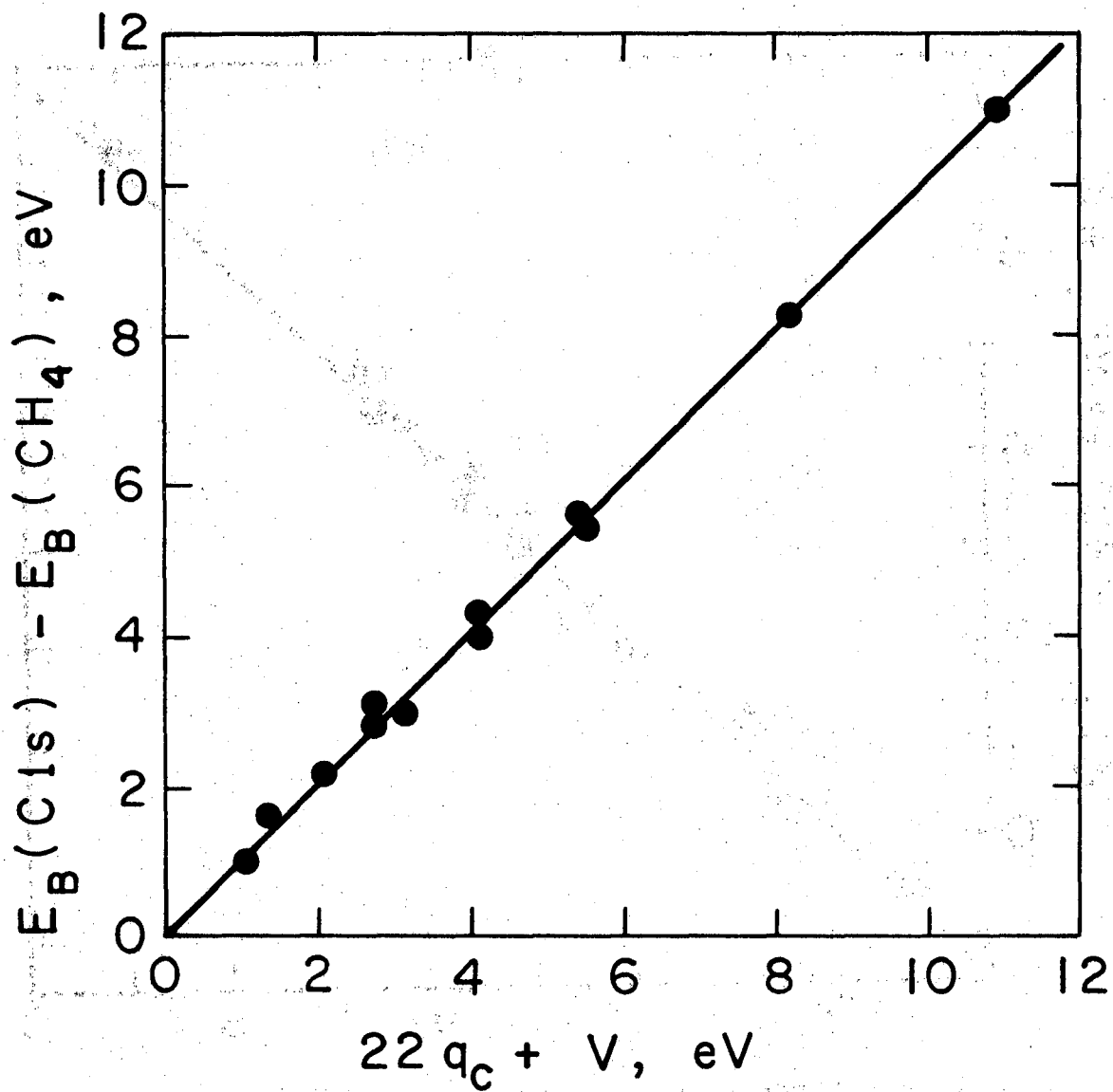
II.D.4. Correlations with "Group Shifts"

The foregoing discussion leads naturally to the concept of "group shifts", wherein the various groups bonded directly to the host atom cause additive shifts in core-level binding energies. Thus for the halomethanes the C(1s) shifts relative to CH₄ can be written

$$\Delta E = \sum_{\text{group}} (\Delta E_{\text{group}} - \Delta E_{\text{H}}) \quad (53)$$

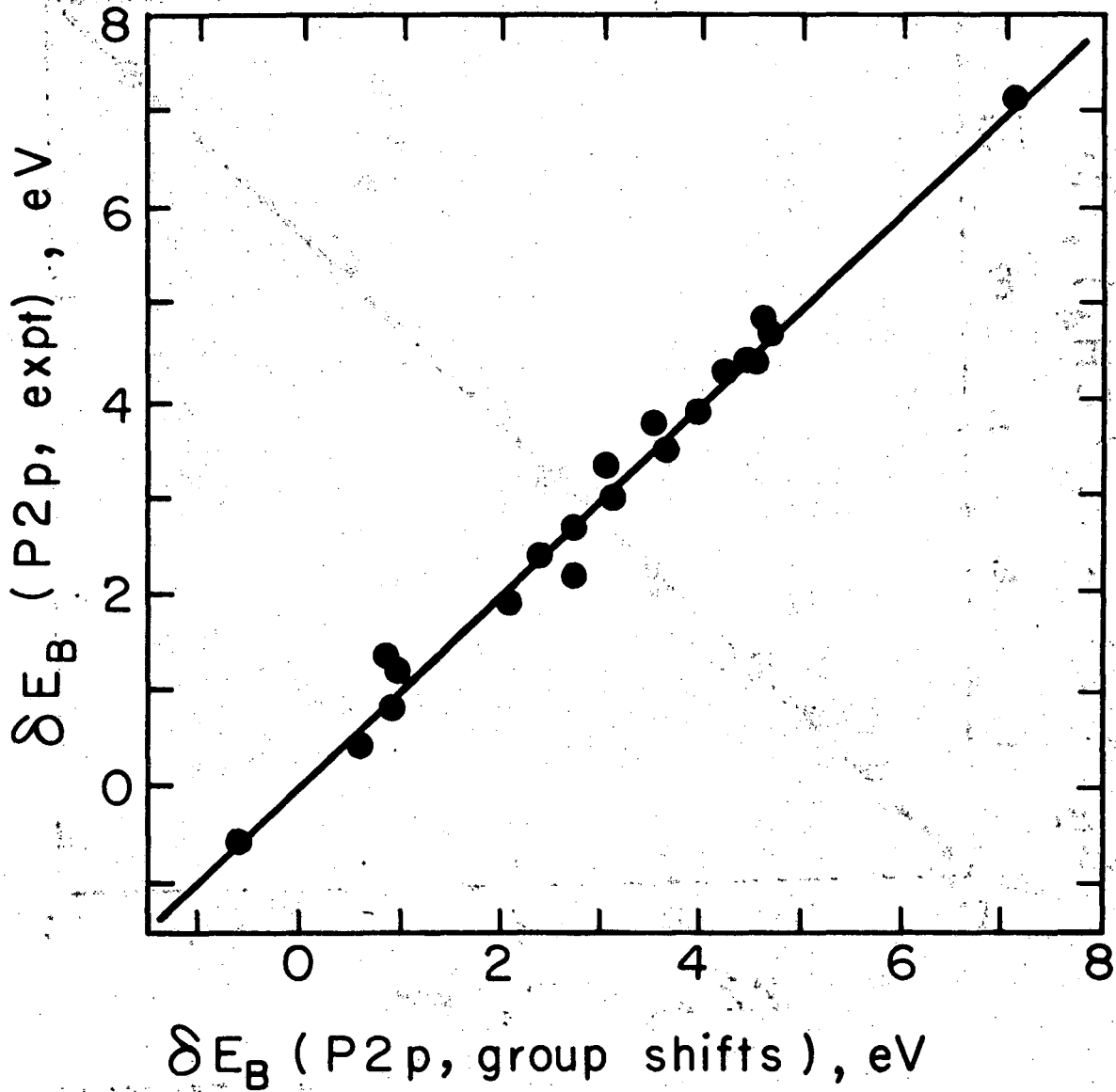
In fact this equation can be obtained by rearranging terms in Eq. (52). The coordinates along the abscissa of Fig. 18 can be reproduced with the values $\Delta E_X - \Delta E_H = 1.033$ eV, 1.362 eV, and 2.725 eV respectively, for X = Br, Cl, and F. Gelius et al.⁸ have exploited the concept of group shifts to correlate Cls shifts in a number of carbon compounds in the solid state, but excluding ionic compounds. They found a very good correlation for compounds involving a total of 34 different functional groups. For the above three cases their least-squares procedures gave values of 0.88 eV, 1.55 eV, and 2.78 eV (the shifts in solids are slightly different from those in gases).

Another very impressive example of the use of group shifts has been given by Hedman, et al.⁶⁹ These workers correlated the phosphorous 2p shifts in a large number of phosphorous compounds with excellent results. Figure 19 shows about half of their data. The success of the group shift approach for carbon and phosphorous shifts indicates that this empirical procedure may ultimately prove the best way for predicting core-level shifts, especially for relatively large molecules and in cases for which large amounts of core-level shift data are already available.



XBL 721-2243

Fig. 18. Binding energy shifts in halomethanes versus predictions of a potential model based on Eqs. (51) and (52).



XBL721-2244

Fig. 19. Experimental P2p core-level shifts versus group shifts, after Hedman, et al., Ref. 69. These workers showed 23 additional points between 2 and 5 eV.

III. VALENCE SHELL STRUCTURE STUDIES

III.A. Introduction

The lower binding energies of valence-shell orbitals makes them accessible to lower-energy photons in the ultraviolet (UV) region. Valence orbitals may also be studied by various methods other than photoelectron spectroscopy. Thus, while XPS can make certain unique contributions to valence-shell studies, it is only one of several complementary techniques, and a relatively new one at that. Furthermore, XPS is at present a relatively low-resolution technique. In this section the main objective will be to point out the ways in which XPS can contribute to the elucidation of valence-shell structure. The approach that will be used is to cite specific examples of contemporary valence-shell studies, without making an exhaustive coverage of the literature. Effective use of XPS for valence-shell studies is only beginning, but these examples show that the method holds considerable promise. Applications to the valence shells of metals, molecules, and salts are discussed separately.

III.B. Valence Bands in Metals

Many metallic properties are attributable to the itinerant electrons in the valence shells. The valence orbitals form bands, and electrons fill these bands essentially up to the Fermi energy E_F . As fermions, electrons fill bands according to the Fermi-Dirac distribution function

$$f = \frac{1}{e^{(E-E_F)/kT} + 1}$$

For $(E_F - E) \gg kT$, f is essentially unity, while for $(E - E_F) \gg kT$, f is essentially zero. Thus at $T = 0$ f is 1 below E_F and 0 above. At room temperature

$kT = 0.026$ eV, so on the 0.1 - 1 eV scale of x-ray photoemission the function f is still quite sharp. The number of states available varies with energy according to a function $N(E)$, which is termed the density of states. The occupied density of states is then

$$\rho(E) = f(E) N(E) .$$

Often no clear distinction is made between $\rho(E)$ and $N(E)$ as it is usually clear from context which is meant. A distinction is usually made between valence bands (below E_F) and conduction bands (above E_F). We shall use this nomenclature.

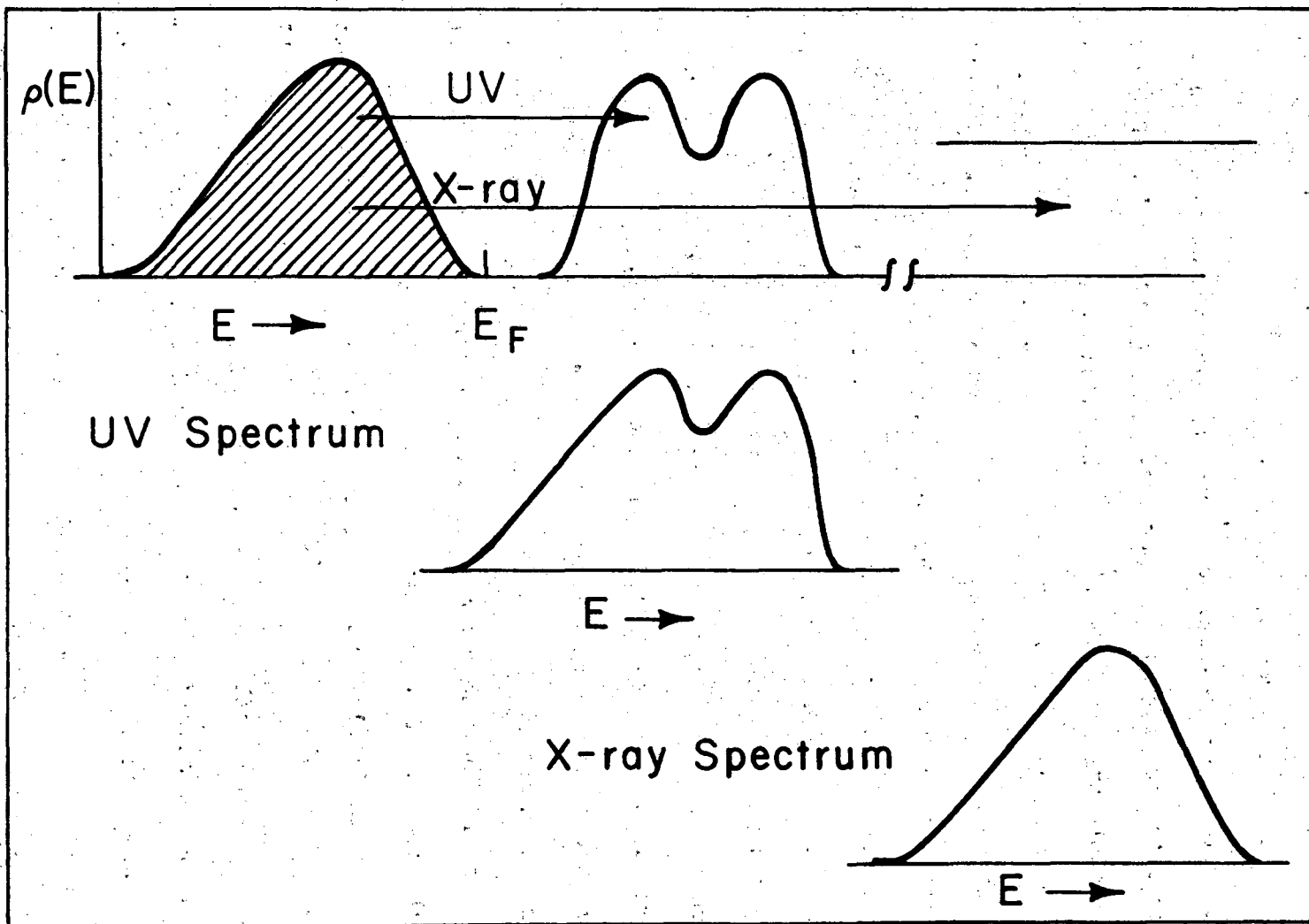
The nature of Fermi statistics has two consequences for studying valence bands. First, transport properties of metals and many of their other properties can be understood in terms of electronic states very near E_F , and those states farther down in the "Fermi-sea" can be ignored. For this reason nearly all the research done on metals to date has in fact studied $N(E_F)$. This approach has obvious merits, particularly in predicting one transport property from another, but even a very detailed knowledge of $N(E_F)$ is totally inadequate for understanding band structure in a fundamental way.

The second consequence of Fermi statistics is that $N(E)$ can never really be studied directly, because the act of studying $N(E)$ disrupts it. This also follows from Fermi statistics. For $(E_F - E) \gg kT$ there are no vacant states nearby in energy, and an electron must be entirely removed, to above E_F at least, in order to be observed. When a hole is thus created, relaxation toward this hole will change $N(E)$. This relaxation can be (and apparently is) small, but it may set a limit on the subtlety of information about $N(E)$ that can be obtained from photoemission.

X-ray and UV photoemission should be compared, because the superior resolution of the latter method would seem to obviate the need for the former. There are some rather strong arguments in favor of x-rays. The greater mean depth from which electrons can be ejected by x-rays implies that this method comes closer to studying bulk properties. In situ monitoring of the surface is also feasible by this method.⁷⁰ Finally with x-rays the final-state energy of the ejected electron is so high that this state can be treated as a continuum state which is essentially unaffected by the crystal potential and therefore structureless. Hence the x-ray photoemission spectrum is a relatively accurate representation of the valence band density of states. By contrast UV spectra are strongly modulated by final state structure in the conduction band, as illustrated in Fig. 20.

Another source of modulation in the XPS spectrum is the variation of the radial wave function of the initial d-band state with $E-E_F$. This is important because the transition matrix element $\langle 5d | \vec{r} | \text{free electron} \rangle$ would vary with energy, and the spectrum would not resemble $\rho(E)$ closely. The extent of modulation is difficult to estimate, but the rather close resemblance between $\rho(E)$ and XPS spectra suggests that it is not very great.

Fadley and Shirley showed the utility of XPS in early valence-band studies of Fe, Co, Ni, Cu, and Pt.⁷⁰ At that time even the general features of $\rho(E)$ were experimentally still in doubt for the 3d bands. To achieve clean surfaces in the relatively poor vacuum then available in electron spectrometers, the samples were heated and gaseous hydrogen was passed over them continuously during the experiments. This work was later extended to the 4d and 5d group analogues of Fe, Co, Ni, and Cu.⁷¹ The same cases were also studied by Baer,



XBL721-2245

Fig. 20. Illustration of the relationship of UV and X-ray photoemission spectra to band structure. For x rays the ejected electron's final-state density-of-states varies slowly with energy, and the spectrum closely resembles the valence-band $\rho(E)$. The UV spectrum is affected by conduction-band structure.

et al.⁷² Their results were in good agreement. Although the early work on these metals was of low resolution, the $\rho(E)$ results gave d band widths and positions. In addition some systematic variations in $\rho(E)$ were observed.⁷¹

Hagström and co-workers⁷³⁻⁷⁶ studied rare-earth metals under better vacuum conditions. They found peaks that could be attributed to the 4f electrons. This confirms the expectation⁷⁷ that higher orbital angular momentum electron bands should be prominent in XPS spectra. Thus the 4f peak in Eu is prominent in the XPS spectrum, while low-energy UV photoemission spectra of Eu on Ba (which differs from Eu in having no 4f electrons) are similar.⁷⁸

These workers found narrow 4f bands in those rare earths with filled shells (Yb, Lu) and those with half-filled shells (Eu, Gd). Single peaks were found in Eu and Gd, consistent with the $4f^7 8s$ structure, while both Yb and Lu showed double peaks, which were assigned to the $4f_{5/2}^6, 4f_{7/2}^8$ doublet. In the rest of the rare-earth metals very complex structure was observed. This was attributed to the rather complicated multiplet structure that is possible in all but the simplest cases (i.e., filled or half-filled shells). The rare earth metals are of special interest because the 4f shell provides both well-defined localized magnetic moments and (presumably) also conduction electrons. Comparison of XPS spectra of ionic salts and metals should lead ultimately to an understanding of the valence-band structures of these elements.

An illustration of the power of XPS for solving valence-band problems is given by its application to the AuX_2 -type intermetallic compounds $AuAl_2$ and $AuGa_2$, by Chan and Shirley.⁷⁹ For some time a "AuGa₂ dilemma" had existed, making the explanation of certain Knight shifts elusive.⁸⁰ Switendick and Narath⁸¹ resolved this enigma by a band-structure calculation that located

the 5d bands of gold about 7 eV below the Fermi energy. This was contrary to the then-common belief that the 5d bands in these compounds lay close to E_F and were responsible for their interesting optical properties. This "d-band dilemma" was settled by the measurements of Chan and Shirley, which showed the d bands centered about 6 eV below E_F , thus confirming the band-structure results.

Recent improvements in resolution, signal-to-background ratio, and particularly vacuum quality, exemplified by the Hewlett-Packard ESCA Spectrometer, with a monochromatic x-ray source, promise to yield much better valence-band information. A comparison⁸² of the gold valence-band spectrum with theoretical density-of-states results (shown in Fig. 21)⁸³⁻⁸⁹ gives the first example of the power of the newer, second-generation spectrometers. This comparison establishes the necessity of relativistic band-structure calculations for gold. It also appears to favor calculations with full (rather than fractional) Slater exchange. Finally, the good agreement of the spectral shape with both high-energy UV spectra^{90,91} and theory shows that matrix-element modulation does not distort the spectrum appreciably and that at the He II resonance energy (40.8 eV) the spectral shape already resembles the XPS spectrum closely. A detailed comparison of the XPS spectrum with theory is given in Table XVII.

III.C. Valence Orbitals in Gases: Cross Sections

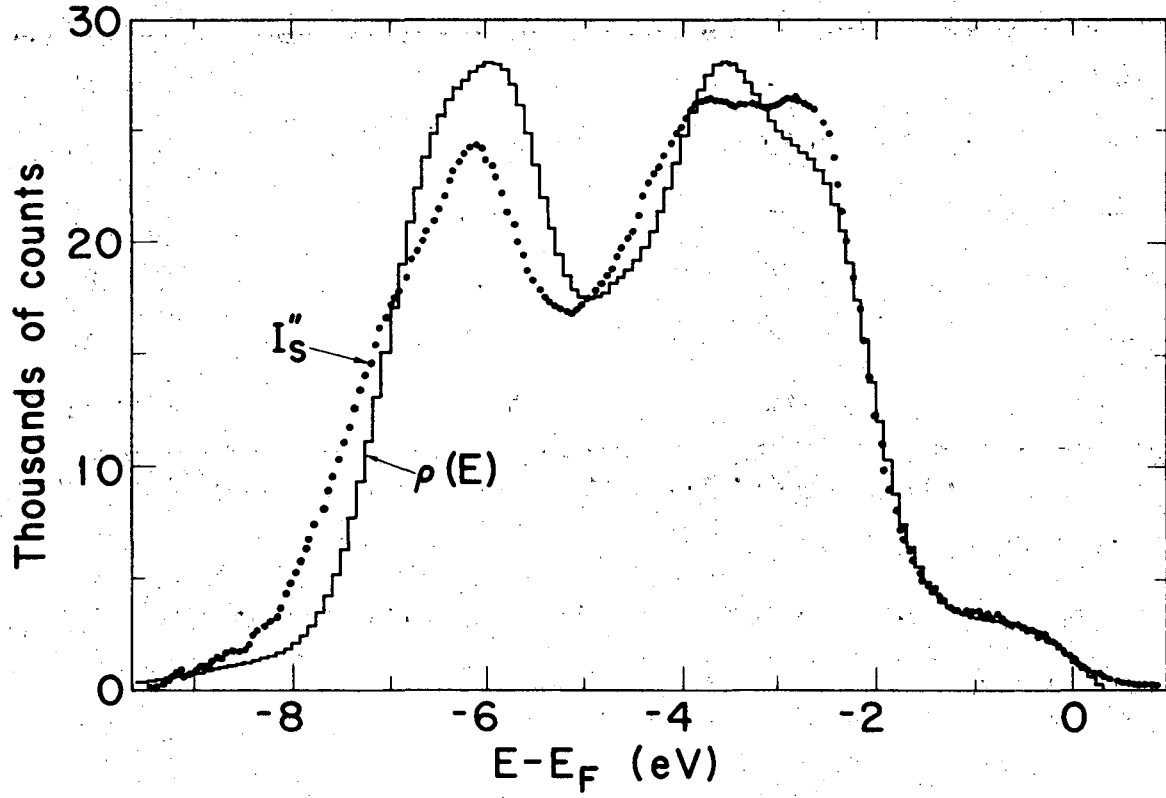
This important topic will be treated briefly because there are available both comprehensive discussions of experimental spectra³ and recent reviews of the implications of cross-section studies.^{92,93} The reader is referred to these sources, and references therein, for detailed discussion. The comments below are confined to a few major points, especially in cross-section studies.

Table XVII. Experimental XPS parameters for gold valence bands and broadened density-of-states parameters

Reference	ΔE_B^a	d-band FWHM	$E_F - E_d^b$
82(expt)	--	5.24 eV	2.04 eV
86	0.79 eV	5.25	1.89
87	0.54	5.54	1.56
89	0.78	4.90	2.21
85	0.85	5.07	2.17
83	0.92	5.67	2.34

^aFWHM of Poisson broadening function by which theoretical band-structure histograms were multiplied.

^bEnergy difference from Fermi level to a point half way up the higher-energy d-band peak.



XBL 7111-4857

Fig. 21. Comparison of the high-resolution valence-band spectrum of gold (points) with density-of-states function from Ref. 85 (broadened).

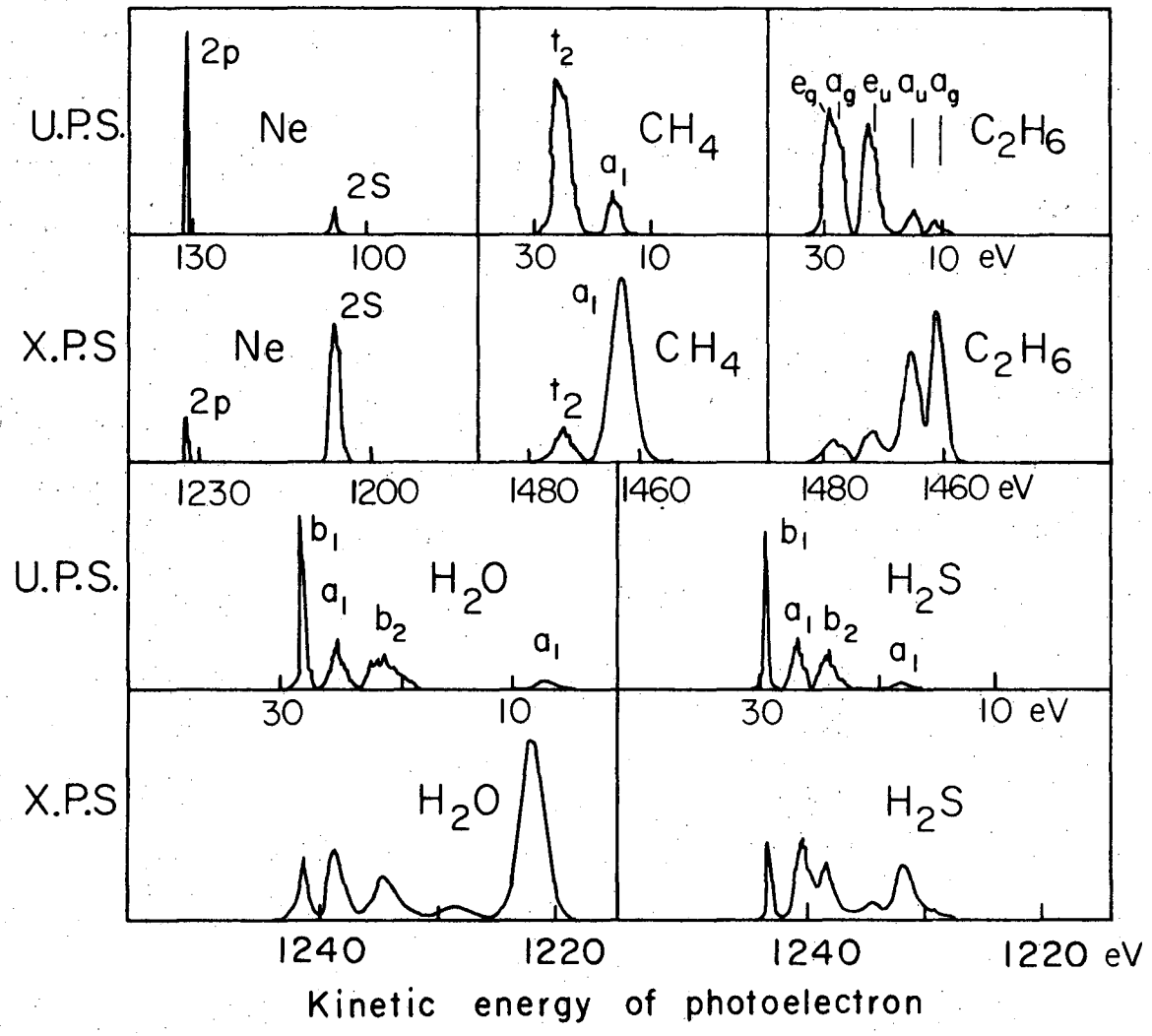
For ten years molecular photoelectron spectroscopy of valence orbitals has been mainly identified with UV excitation, primarily with He I or He II resonance lines, at 21.2 and 40.8 eV respectively.⁹⁴ The resulting spectra show resolution in the 10^{-2} eV range. Final-state vibrational structure can be observed, and very detailed interpretations can be made. Siegbahn and co-workers³ have shown that molecular-orbital spectra can also be studied by x-ray photoemission. They have studied a number of small molecules, identifying most or all of the valence-shell molecular orbitals in each case. Typical results are given in Table XVIII.

The low inherent energy resolution of the x-ray photoemission spectra obviates direct competition with UV spectra in making energy assignments for molecular orbitals. However, the x-ray method has considerable value as a complementary technique that can be used to clarify certain assignments. In addition it has great potential as a method for assigning atomic-orbital parentage to molecular orbitals. These advantages are derived from the variation of photoemission cross section with energy and angular momentum.

Price, et al.⁹² considered the energy variation of photoemission cross section for 2s and 2p electrons. They presented straightforward overlap arguments that show how the cross-section ratio $\sigma(2s)/\sigma(2p)$ should increase, for valence orbitals, from UV photoemission to x-ray photoemission energies. The consequent effect on molecular orbital photoemission spectra can be dramatic, as indicated in Fig. 22. Here Price, et al. have compared UV and x-ray photoemission spectra of the valence orbitals of several small molecules. In both H_2S and H_2O the molecular orbitals b_1 , a_1 , and b_2 , which are derived from p atomic orbitals, retain their relative intensities for the two photon energies, while the a_1 orbital (with s character) shows a relative

Table XVIII. Some Molecular Orbital Binding Energies (after Ref. 3)

H ₂ O		H ₂ S		CF ₄	
orbital	E _B (eV)	orbital	E _B (eV)	orbital	E _B (eV)
1b ₁	12.6	1b ₁	10.3	3t ₂	16.1
2a ₁	14.7	2a ₁	13.2	1t ₁	17.4
1b ₂	18.4	1b ₂	15.1	1e	18.5
1a ₁	32.2	1a ₁	22	2t ₂	22.2
				2a ₁	25.1
				1t ₂	40.3
				1a ₁	43.8



XBL721-2227

Fig. 22. Comparison of ultraviolet and x-ray photoelectron spectra, from Ref. 92, for neon and four small molecules, showing the increase with energy of $\sigma(s)/\sigma(p)$.

increase in intensity from low to high photon energy. The potential value of this approach in assigning atomic s or p character to molecular orbitals is obvious. Price et al. also indicated how subtler phase information can be derived from cross-section studies.

Gelius et al.^{93,95,96} have made quantitative predictions of XPS spectra from valence orbitals of several small molecules. They gave an argument for the constancy of the photoemission cross section σ of an atomic orbital from one molecule to another. The de Broglie wavelength of a photoelectron ejected from a molecular orbital by $\text{MgK}\alpha_{12}$ x-rays is 0.35\AA . Therefore only the innermost regions of the atomic orbitals, where the orbital amplitude varies appreciably over 0.35\AA , can contribute significantly to σ . Hence σ should be nearly independent of the shape of the interatomic portion of the molecular orbital. By assuming that the cross section of the j^{th} molecular orbital could be expressed as a sum over atomic orbitals,

$$\sigma_j^{\text{MO}} = \sum_A \sigma_{Aj}$$

and expanding the molecular orbitals in terms of atomic orbitals,

$$\phi_j = \sum_{A\lambda} C_{A\lambda j} \phi_{A\lambda}$$

where λ labels atomic orbital symmetry, Gelius⁹³ derived the relation

$$\sigma_{Aj} = \sum_{\lambda} P_{A\lambda j} \sigma_{A\lambda}$$

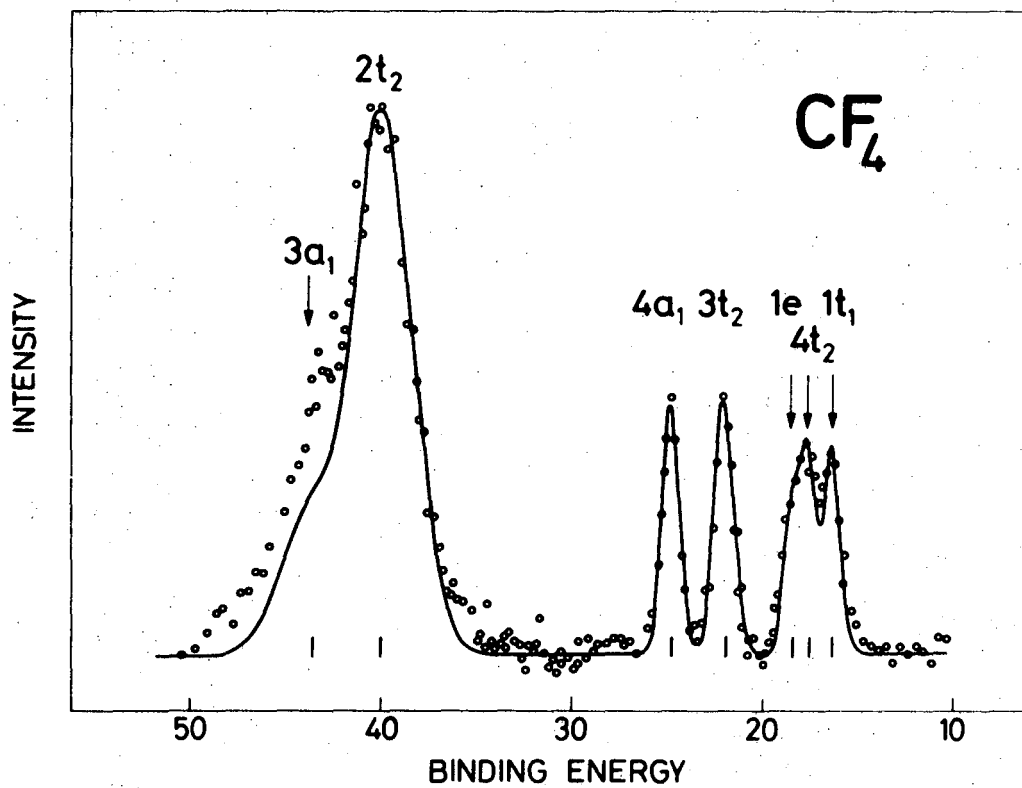
Here $P_{A\lambda j}$ is the gross atomic population on atom A of the atomic orbital $A\lambda$ in molecular orbital j. Gelius et al. worked with relative, rather than absolute, cross sections which they determined by careful studies of the rare gases. Spectra were then fitted using gross atomic populations from ab initio calculations. The results for CF_4 are shown in Fig. 23. The cross-section ratios $\sigma(F2s)/\sigma(F2p) = 10$ and $\sigma(F2s)/\sigma(C2s) = 2.0$ were used by Gelius for the theoretical curve. The fit is generally excellent, with the extra intensity in the $3a_1$ region perhaps arising from two-electron effects. Although this was one of the best fits, good results were obtained for a number of molecules. This approach consequently appears to have great potential in elucidating molecular-orbital structure in terms of atomic-orbital composition.

III.D. Valence Orbitals in Inorganic Anions

Prins and Novakov⁹⁷ studied molecular-orbital spectra of perchlorate and sulfate anions in anhydrous salts of lithium and other metals. They observed six peaks and assigned them to seven molecular orbitals. Their results for $LiClO_4$ and Li_2SO_4 are given in Table XIX. Qualitative assignments of peak intensities as strong, medium or weak have been made by the reviewer. Prins and Novakov observed that theoretical descriptions of the molecular orbital structure of these isoelectronic anions tended to yield three groups of orbitals. The lowest-energy group consists of two levels-- a_1 and t_2 --formed from the ligand oxygen 2s orbitals. The high intensities of the two highest-binding-energy peaks, their relative intensities, and the constancy of their intensities from one salt to another all support this assignment. The next two peaks have been assigned to a_1 and t_2 orbitals derived from the central

Table XIX. Valence-Orbital Binding Energies in LiClO_4 and Li_2SO_4 ,
after Prins and Novakov (Ref. 97)

Orbital	$E_B(\text{LiClO}_4)$	$E_B(\text{Li}_2\text{SO}_4)$	Intensity
$t_1(02p\pi)$	6.3 eV	5.8 eV	weak
$e, t_2(02p\pi)$	9.0	7.7	weak
$t_2(3p)$	13.4	11.4	medium
$a_1(3s)$	16.5	14.3	medium
$t_2(02s)$	27.0	25.3	strong
$a_1(02s)$	34.4	(29.0)	medium



XBL 723-503

Fig. 23. Experimental photoemission spectrum of CF_4 molecular orbitals, using $\text{MgK}\alpha$ radiation, and theoretical curve (after Gelius, Ref. 93).

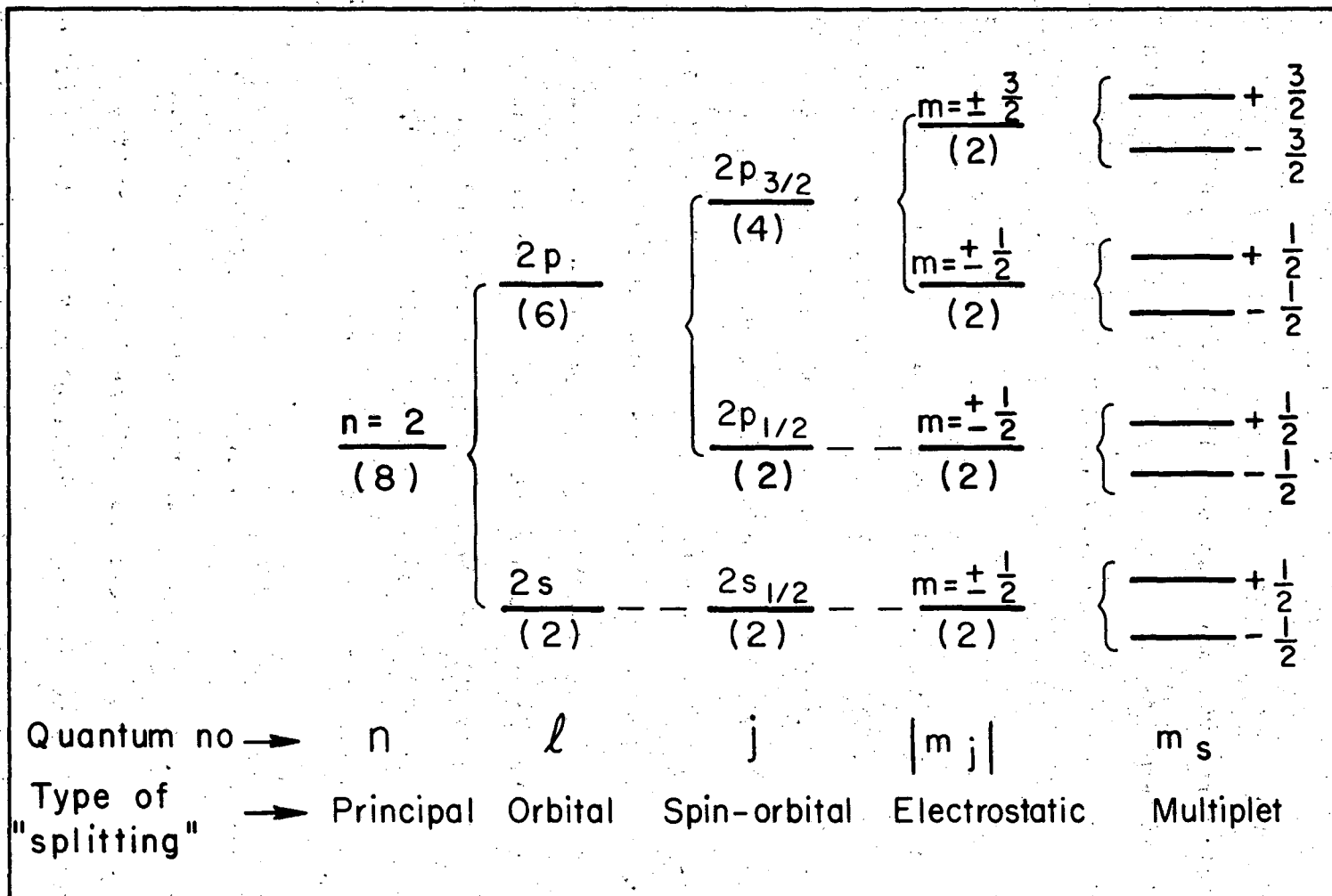
atom 3s and 3p orbitals plus the oxygen 2s and 2p σ orbitals. The intensities of these lines in ClO₄⁻ were about equal to those of the 3s and 3p lines of Cl⁻, thus supporting this assignment. The least-bound group of three orbitals--e, t₂, and t₁--is formed from oxygen 2p π orbitals, and the low intensity of these peaks is a consequence of the low photoemission cross section of the oxygen 2p orbitals. Again the power of intensity-ratio arguments in making spectral assignments is clearly illustrated in the work of Prins and Novakov.

IV. MULTIPLET SPLITTING

IV.A. Introduction

When substances with unpaired electrons in their valence orbitals are studied, their core-level peaks may be split by exchange interaction. This effect has been termed multiplet splitting to distinguish it from other effects that can give rise to extra peaks (e.g., Auger peaks, "shake-off" peaks, "shake-up" peaks, multiple valence states, etc.). In order to identify multiplet splitting it is necessary to eliminate these other effects convincingly. Long experience in the reviewer's laboratory has shown that this can be an extremely tricky problem. Since 1966 a very large number of extra peaks have been identified, but not reported, either because confirmatory experiments showed them to be irreproducible or because they were found to be of different or ambiguous origin. The main difficulty is that the surfaces of most oxides and salts will decompose or at least acquire structural and/or chemical characteristics different from the bulk when placed in a good vacuum, let alone the vacua that prevail in most photoelectron spectrometers.

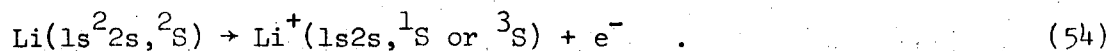
Multiplet splitting may be conveniently categorized by reference to a diagram such as that shown for an atomic $n = 2$ shell in Fig. 24. This one-electron diagram is conceptually imprecise in that it refers to the initial state (and to atomic levels), but it gives a qualitative idea of the types of splitting that are possible. Electrostatic splitting is splitting that arises through the angular dependence of Coulombic interactions between electrons bound in different orbitals. Both Coulomb and exchange integrals contribute to this effect. The absolute value of m_j is indicated in Fig. 24 to emphasize that the electric "field" cannot lift the twofold degeneracy associated with the sign of m_j . Electrostatic splitting was discussed in more detail by Hollander and Shirley.⁵⁴



XBL 721-2246

Fig. 24. Classification of core-level splittings, in the one-electron approximation.

In multiplet splitting the final spin degeneracy of a core level is lifted through interaction with an unpaired spin in the valence shell. This interaction is mainly attributable to exchange, as discussed below, although correlation effects and (to a very slight extent, through differences between radial wave functions for spin-up and spin-down core orbitals) even Coulomb integrals can make finite contributions. Leaving the oversimplified one-electron diagram shown in Fig. 24 and considering the final states that are accessible in a photoemission process, we can write for the simple case of atomic lithium



The final states can be described by products of symmetric space and anti-symmetric spin functions, or vice-versa. The energies of each two states may be estimated by adding to E_0 , the sum of the one-electron energies (which is the same for the 1S and 3S states), the electron repulsion term, given by the expectation value of e^2/r_{12} . This leads to the Coulomb and exchange integrals

$$H_c = \int 1s(1) 2s(2) (e^2/r_{12}) 1s(1) 2s(2) dv_1 dv_2$$

$$H_x = \int 1s(1) 2s(2) (e^2/r_{12}) 1s(2) 2s(1) dv_1 dv_2$$

The resultant energies are

$$E(^1S) = E_0 + H_c + H_x$$

$$E(^3S) = E_0 + H_c - H_x$$

and the final-state splitting is given by

$$\Delta E = E(^1S) - E(^3S) = 2H_X \quad (55)$$

The relative intensities of the multiplet peaks is given by the statistical (multiplet) ratio,

$$I(^3S)/I(^1S) = 3 \quad (56)$$

The generalization of this discussion to an arbitrary case is complicated, but we can easily generalize to the case of any spin S in the valence shell, provided that photoemission only from a core level of s character is considered. Thus we are interested in the process

$$M^Z(\dots ns^2 \dots, ^{2S+1}X) \rightarrow M^{Z+1}(\dots ns \dots, ^{2S}X \text{ or } ^{2S+2}X) \quad (57)$$

The generalization of Eq. (55) is

$$\Delta E = E(^{2S}X) - E(^{2S+2}X) = (2S+1)H_X \quad (58)$$

where H_X is the exchange integral between an ns orbital and a valence-shell orbital. The intensity ratio is

$$I(^{2S+2}X)/I(^{2S}X) = (S+1)/S \quad (59)$$

from the multiplicities.

IV.B. Multiplet Splitting in Atoms

Fadley and Shirley first suggested multiplet splitting in x-ray photoemission, and they reported an unsuccessful search for splitting in the 3p photopeak of metallic iron.⁷⁰ Later they attempted to study high spin atomic systems⁹⁸ in order to clarify the reason for this negative result. With the technique and apparatus then available only atomic europium could be studied, as a vapor at 600°C. Poor counting statistics dictated that only the intense $4d_{3/2} - 4d_{5/2}$ doublet could be used. This doublet was significantly perturbed, presumably because of interaction with the valence configuration $4f^7; 8s$. Careful least-squares curve fitting yielded a value of 2.44 ± 0.15 for the intensity ratio $I(4d_{5/2})/I(4d_{3/2})$, in contrast to an expected unperturbed ratio of 3/2. Auxiliary experiments on gaseous Xe, which has no 4f electrons, gave 1.47 for this ratio, while with gaseous Yb (with a filled 4f shell) the ratio was 1.49. Thus a multiplet effect is clearly present. A quantitative interpretation would require a rather large configuration interaction calculation because of the large angular momenta involved. Further work on atomic gases would be desirable as a means of testing atomic structure calculations. Advances currently underway in spectrometer design should permit studies of atomic systems that are theoretically more tractable.

IV.C. Multiplet Splitting in Molecules

Hedman, et al.⁹⁹ first reported splitting in core levels of molecular O_2 and NO. In oxygen they found two lines, of relative intensity 1:2, and spaced by 1.1 eV, with the higher-intensity line having the lower binding energy. The electronic ground state of O_2 is ${}^3\Sigma_g^-$. Ejection of a 1s electron

therefore leads to states of $^2\Sigma^-$ and $^4\Sigma^-$ character, with the remaining 1s electron on the oxygen atom from which an electron was ejected coupling anti-parallel or parallel to the valence-orbital spin $S = 1$. For NO the splitting was 1.5 eV in the N 1s line, with an intensity ratio of 1:3 for the two components. The O 1s line was broadened to 1.2 eV, as compared to 0.9 eV FWHM for O 1s in O_2 , and a splitting of 0.7 eV was derived. Theoretical estimates of the splittings were in reasonably good agreement with these results^{100,101} (Table XX).

Recently theoretical estimates of the core-level splitting based on hole-state calculations by Bagus and Schaefer^{29,30} have become available. Davis and Shirley^{102,103} remeasured the splittings in both O_2 and NO, taking care to obtain good statistical accuracy and making extensive least-squares fits of their spectra. These spectra are shown as part of Fig. 25, and the derived splittings are given in Table XX. Also given are theoretical estimates by Bagus and Schaefer and by Schwartz.¹⁰⁴

The results are intriguing. For NO the hole-state calculations and the more precise experimental results show very good agreement. In O_2 , however, the most approximate theoretical estimates of splitting actually agrees better with experiment than the hole state calculation. This is probably fortuitous, because the latter show a very substantial transfer of electronic charge toward the hole state³⁰ (see Section II.B.1.c). Such an effect is totally absent in frozen orbital calculations that involve the initial state alone.

The NO results of Hedman, et al. showed that the unpaired spin density resides mainly on the N atom in NO, as expected from molecular-orbital calculations. Davis and Shirley¹⁰² studied the N1s and O1s lines from di-tertbutyl

Table XX. Binding Energies of 1s Electrons in NO and O₂ (in eV)

Case ^a	Binding Energy	Measured Splitting, ΔE	ΔE from Final State Calculations	ΔE from Frozen Orbital Estimates			ΔE (expt) Hedman, <u>et al.</u> (Ref. 99)
<u>NO</u> (¹ Π)	411.5(5) ^b						
		1.412(16) ^c	1.35 ^e	1.23 ^e	1.26 ^g	0.88 ^h	1.5
<u>NO</u> (³ Π)	410.1(5)						
		0.530(21) ^c	0.48 ^e	0.73 ^e	0.77 ^g	0.68 ^h	0.7
<u>NO</u> (¹ Π)	543.6(5)						
		0.530(21) ^c	0.48 ^e	0.73 ^e	0.77 ^g	0.68 ^h	0.7
<u>NO</u> (³ Π)	543.1(5)						
		0.530(21) ^c	0.48 ^e	0.73 ^e	0.77 ^g	0.68 ^h	0.7
<u>O₂</u> (² Σ)	544.2(5)						
		1.115(9) ^d	0.61 ^f	1.68 ^f	1.20 ^h		1.1
<u>O₂</u> (⁴ Σ)	543.1(5)						
		1.115(9) ^d	0.61 ^f	1.68 ^f	1.20 ^h		1.1

^aThe atom losing a 1s electron is underlined. Assumed final-state symmetry is denoted parenthetically.

^bStandard deviation in the last digit is given parenthetically.

^cRef. 102.

^dRef. 103.

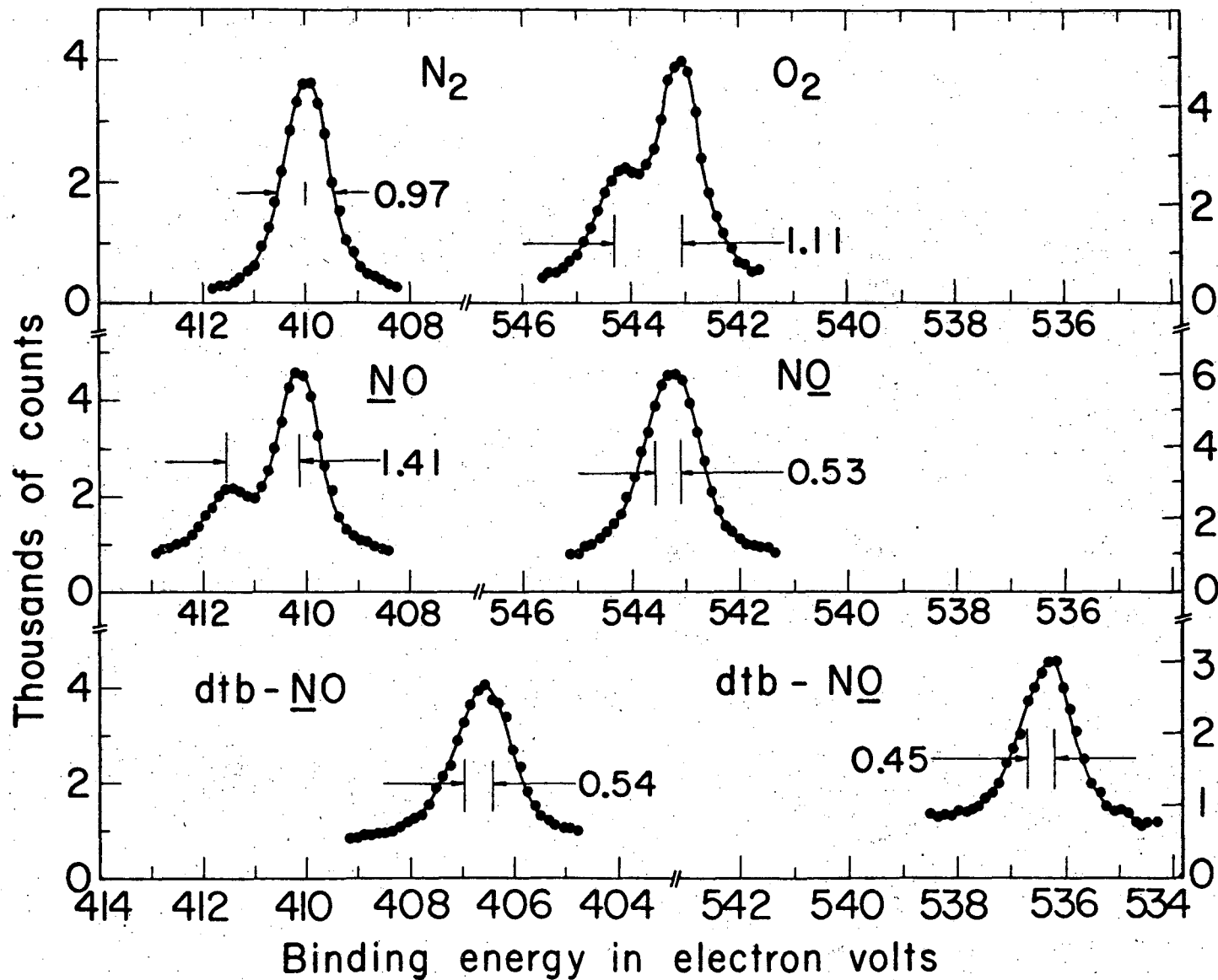
^eRef. 29.

^fRef. 30.

^gRef. 104.

^hRef. 100.

0 0 0 0 5 7 0 0 0 0 7



-124-

Fig. 25. Nitrogen and oxygen 1s peaks in (from top): diamagnetic N_2 and paramagnetic O_2 (showing multiplet splitting; paramagnetic NO , showing that the spin is mostly on the N atom; paramagnetic di-tertbutyl nitroxide, showing spin migration to alkyl group and, from decrease in binding energies, charge migration to NO group. From Refs. 3, 99, 102, 103.

XBL722-2312

nitroxide. They found a "splitting" of 0.448 ± 0.026 eV in the oxygen 1s line, only slightly smaller than the NO result. For the nitrogen line, however, the splitting was reduced from 1.412 ± 0.016 eV to only 0.530 ± 0.021 eV. Since to first approximation the splitting goes as $(2S+1)H_x$ (Eq. (58)), these authors noted that an atom i upon which a fraction f_i of the unpaired spin resides will show a splitting of approximately

$$\Delta E^i \approx f_i H_x^i (2S+1) \quad (60)$$

They therefore interpreted the di-tertbutyl nitroxide results as indicating that the $p\pi$ antibonding orbital of NO (in which the unpaired spin resides) expands from nitrogen over the alkyl groups in the larger molecule, while the oxygen atom retains most of its population in this orbital. At the same time the decreased N1s binding energy (406.5 eV in dtb-NO vs 410.5 eV in NO) and O1s binding energy (536.3 eV in dtb-NO vs 543.2 eV in NO) indicate considerable electron transfer from the alkyl groups to the NO group. Thus core level binding energies can provide useful information about spin and charge migration in free radicals. In comparison with ESR studies, ESCA is much less sensitive but also less ambiguous.

IV.D. Multiplet Splitting in Salts

Fadley, et al.¹⁰⁵ first observed multiplet splitting in transition-metal ions in salts. Fadley and Shirley⁹⁸ discussed this work in more detail. In Mn^{2+} or Fe^{3+} the outer electrons have the configuration d^5 and form a 6S ground state with 5 unpaired spins coupled to $S = 5/2$. The exchange integral H_x between a 3d electron and a core $n\ell$ electron depends on n but is nearly independent

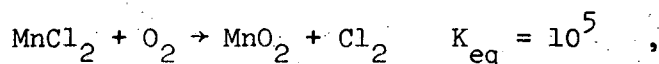
of ℓ . The factor $(2S+1)H_x(3d;n\ell)$ would give splittings of ~ 12 eV for $n = 3$ orbitals and ~ 3 eV for $n = 2$ orbitals. Linewidths and the expectation that both correlation effects and spin migration to anions would reduce the splitting from this figure dictated that early experiments should concentrate on the $n = 3$ orbitals. The a priori obvious choice was the more intense 3p peak, but it showed a complicated spectrum, with no clearly-defined, simple splitting. The reason for this result is straightforward. After ejection of a 3p electron the remaining open-shell configuration $3p^5[3d^5(^6S)]$ can couple to form a 7P final state in only one way (since the spin configuration is "stretched", with all six spins parallel). The complementary 5P state can be formed in three ways, however, from d^5 terms of 6S , 4P , and 4D . Thus the less intense 5P "peak" intensity is in fact distributed among the three eigenstates formed from these levels. These eigenstates are spread over 20 eV, and their intensities are low enough to obviate the immediate advantages of studying the 3p peaks on the basis of total intensity. The 3s peaks are simpler, however: there are two final states, 5S and 7S , split by $6H_x(3d,3s)$. The splitting of these peaks was observed in several materials,^{98,105} with results given in Table XXI.

In interpreting these results several points were made. First, the splittings in MnF_2 and FeF_3 were smaller by half than estimates based on free atom spin-unrestricted Hartree-Fock, on restricted Hartree-Fock, or on multiplet hole theory estimates.¹⁰⁵ Agreement was good with estimates based on unrestricted Hartree-Fock calculations on MnF_6^{4-} clusters, however, suggesting that spin migration to ligands is important. The slightly smaller splitting in MnO_2 than in MnF_2 may be a consequence of the fact that Mn^{4+} has only three 3d electrons. The single 3s lines in $K_4Fe(CN)_6$ and $Na_4Fe(CN)_6$ may be attributed to covalent bonding in these compounds.

Table XXI. Multiplet Splitting in 3s peaks (after Fadley and Shirley⁹⁸)

Atom	Compound	Electron configuration	3s(1)-3s(2) Separation (eV)	3s(1):3s(2) Intensity ratio
Mn	MnF ₂	3d ⁵ 6s	6.5	2.0:1.0
	MnO	3d ⁵ 6s	5.7	1.9:1.0
	MnO ₂	3d ³ 4f	4.6	2.3:1.0
Fe	FeF ₃	3d ⁵ 6s	7.0	1.5:1.0
	Fe	(3d ⁶ 4s ²)	(4.4)	(2.6:1.0)
	K ₄ Fe(CN) ₆	(3d ⁶)	...	> 10:1
	Na ₄ Fe(CN) ₆	(3d ⁶)	...	> 10:1
Ni	Ni	(3d ⁸ 4s ²)	(4.2)	(7.0:1.0)
Cu	Cu	(3d ¹⁰ 4s ¹)	...	> 20:1

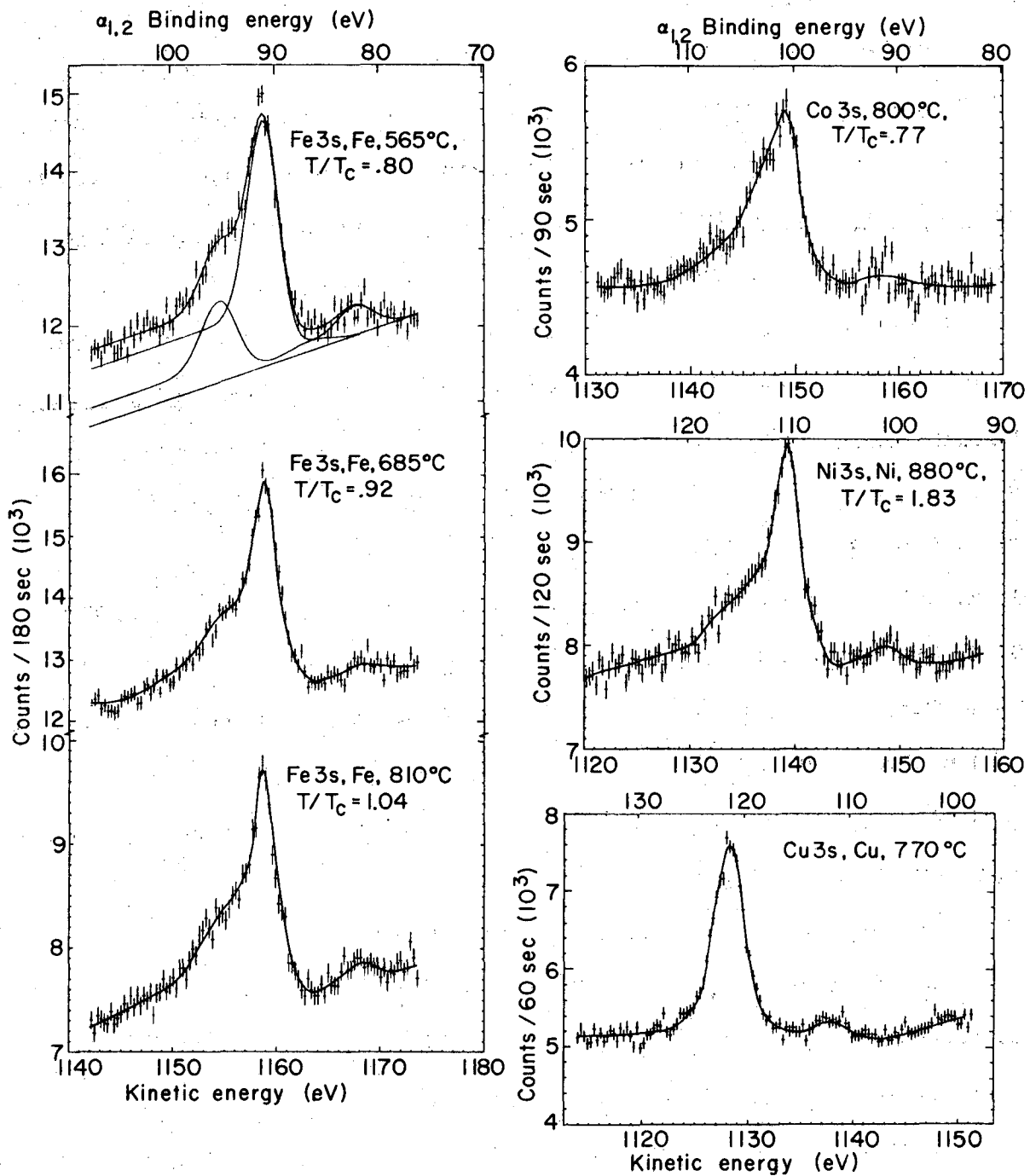
At first sight, multiplet-splitting studies in transition metals appears to be a powerful diagnostic tool for elucidating spin distributions, and this may yet prove to be true. There is, however, a very severe technical problem. Many compounds are not stable in a vacuum at room temperature. Oxides can lose oxygen, hydrates can lose water, and halides can undergo reactions of the type



by reacting with residual oxygen. Only fluorides appear to possess adequate thermodynamic stability for such studies at room temperature.⁹⁸ In spite of these limitations a number of studies of multiplet splitting in the 3d group have been reported.¹⁰⁶⁻¹⁰⁸ Recently Wertheim et al.¹⁰⁹ have reported a very definitive multiplet splitting of over 8 eV in the 4s peak of Gd in GdF₃. In this case seven unpaired f electrons in the ⁸S state couple to the 4s electrons to produce ⁷S and ⁹S components.

IV.D. Multiplet Splitting in Metals

The effects of multiplet structure on valence-band spectra, as reported by Hägstrom et al.,⁷³⁻⁷⁶ was discussed in Section III.B. Fadley and Shirley⁹⁸ showed that core-level splittings can serve as a diagnostic tool for detecting localized magnetic moments. Their results for the 3d ferromagnets are shown in Fig. 26. The unique power of photoemission for this kind of work lies in its speed. Because the photoemission process takes only $\sim 10^{-16}$ sec, multiplet splitting can detect localized moments that are relaxing too fast to be observed by any other process, or in iron above its Curie point (Fig. 26). Thus ESCA appears to have significant potential for studies in magnetism.



XBL703-2536

Fig. 26. Multiplet structure of the 3p line in 3d ferromagnets above and below the Curie point, and the unsplit line of copper.

FOOTNOTES AND REFERENCES

* Work performed under the auspices of the U. S. Atomic Energy Commission.

1. S. B. M. Hagström, C. Nordling, and K. Siegbahn, *Z. Physik* 178, 433 (1964).
2. K. Siegbahn, C. Nordling, A. Fahlman, R. Nordberg, K. Hamrin, J. Hedman, G. Johansson, T. Bergmark, S.-E. Karlsson, I. Lindgren, and B. J. Lindberg, ESCA - Atomic, Molecular and Solid State Structure by Means of Electron Spectroscopy, Nova Acta Regiae Soc. Sci. Upsaliensis Ser. IV, Vol. 20 (1967).
3. K. Siegbahn, C. Nordling, G. Johansson, J. Hedman, P. F. Hedén, K. Hamrin, U. Gelius, T. Bergmark, L. O. Werme, R. Manne, and Y. Baer, ESCA Applied to Free Molecules, North-Holland Publishing Co., Amsterdam, 1969.
4. D. A. Shirley, editor, "Electron Spectroscopy" (North-Holland, 1972).
5. T. A. Carlson, Ref. 4, p. 53.
6. J. M. Hollander and D. A. Shirley, *Ann. Rev. Nucl. Sci.* 20, 435 (1970).
7. G. D. Mateescu, Ref. 4, p. 661.
8. U. Gelius, P. F. Hedén, J. Hedman, B. J. Lindberg, R. Manne, R. Nordberg, C. Nordling, and K. Siegbahn, *Physica Scripta* 2, 70 (1970).
9. C. S. Fadley, S. B. M. Hagström, M. P. Klein, and D. A. Shirley, *J. Chem. Phys.* 48, 3779 (1968).
10. T. D. Thomas, *J. Am. Chem. Soc.* 92, 4184 (1970).
11. A. Veillard and E. Clementi, *J. Chem. Phys.* 49, 2415 (1969).
12. T. Koopmans, *Physica* 1, 104 (1933).
13. J. K. L. McDonald, *Phys. Rev.* 43, 830 (1933).
14. P. S. Bagus, *Phys. Rev.* 139, A619 (1965).
15. G. Verhaegen, J. J. Berger, J. P. Desclaux, and C. M. Moser, *Chem. Phys. Letters* 2, 479 (1971).
16. A. Rosén and I. Lindgren, *Phys. Rev.* 176, 114 (1968).

17. F. A. Gianturco and C. A. Coulson, *Molecular Physics* 14, 223 (1968).
18. I. Oksuz and O. Sinanoğlu, *Phys. Rev.* 181, 42 (1969).
19. R. K. Nesbet, *Phys. Rev.* 175, 2 (1968).
20. M. E. Schwartz, *Chem. Phys. Letters* 5, 50 (1970).
21. C. L. Pekeris, *Phys. Rev.* 112, 1649 (1958).
22. Schwartz suggested 1.2 eV for correlation following Clementi (Ref. 17).
The figure 1.4 is obtained from the estimate for neon (Ref. 14) plus the constancy of the $1s^2$ correlation energy with Z (Ref. 18).
23. E. Clementi, *IBM J. Res. Development* 9, 2 (1965).
24. I. H. Hillier, V. R. Saunders, and M. H. Wood, *J. Chem. Phys.* 7, 323 (1970).
25. C. R. Brundle, M. B. Robin, and H. Basch, *J. Chem. Phys.* 53, 2196 (1970).
26. F. A. Gianturco and C. Guidotti, *Chem. Phys. Letters* 9, 539 (1971).
27. R. Moccia and M. Zandomenighi, *Chem. Phys. Letters* 11, 221 (1971).
28. P. F. Franchini and C. Vergani, *Theoret. Chim. Acta.* 13, 46 (1969);
P. F. Franchini, R. Moccia, and M. Zandomenighi, *Intern. J. Quantum Chem.* 4, 487 (1970).
29. P. S. Bagus and H. F. Schaefer III, *J. Chem. Phys.* 55, 1474 (1971).
30. P. S. Bagus and H. F. Schaefer III, *J. Chem. Phys.* 56, 224 (1972).
31. L. C. Snyder, *J. Chem. Phys.*, in press.
32. P. Siegbahn, *Chem. Phys. Letters* 8, 245 (1971).
33. L. Hedin and G. Johansson, *J. Phys. B* 2, 1336 (1969).
34. P. Liberman, *Bull. Am. Phys. Soc. Ser. II* 9, 731 (1964).
35. S. Brenner and G. E. Brown, *Proc. Roy. Soc. (London)* A218, 422 (1953).
36. R. Manne and T. Aberg, *Chem. Phys. Letters* 7, 282 (1970).

37. M. O. Krause, T. A. Carlson, and R. D. Dismukes, Phys. Rev. 170, 37 (1968).
38. C. Zener, Phys. Rev. 36, 51 (1930).
39. J. C. Slater, Phys. Rev. 36, 59 (1930).
40. H. Basch and L. C. Snyder, Chem. Phys. Letters 3, 333 (1969).
41. D. W. Davis, J. M. Hollander, D. A. Shirley, and T. D. Thomas, J. Chem. Phys. 52, 3295 (1970).
42. M. E. Schwartz, Chem. Phys. Letters 6, 631 (1970).
43. T. K. Ha and L. C. Allen, Int. J. Quantum Chemistry 15, 199 (1967).
44. D. W. Davis, D. A. Shirley, and T. D. Thomas, J. Chem. Phys. 56, 671 (1972).
45. Ref. 2; also C. S. Fadley, S. B. M. Hagstrom, J. M. Hollander, D. A. Shirley, and M. P. Klein, Lawrence Radiation Laboratory Report UCRL-17299, January, 1967, p. 233 (unpublished).
46. H. Basch, Chem. Phys. Letters 5, 3371 (1970).
47. C. Edmiston and R. Ruedenberg, Rev. Mod. Phys. 35, 457 (1963).
48. J. A. Pople, D. P. Santry, and G. P. Segal, J. Chem. Phys. 43, S129 (1965).
49. F. O. Ellison and L. L. Larcom, Chem. Phys. Letters 10, 580 (1971).
50. D. W. Davis, Lawrence Berkeley Laboratory, private communication, December, 1971.
51. R. S. Mulliken, J. Chem. Phys. 23, 1833 (1955).
52. U. Gelius, B. Roos, and P. Siegbahn, Chem. Phys. Letters 4, 471 (1970).
53. D. W. Davis, D. A. Shirley, and T. D. Thomas, J. Chem. Phys. 56, 671 (1972).
54. J. M. Hollander and D. A. Shirley, Ann. Rev. Nucl. Sci. 20, 435 (1970).
55. M. E. Schwartz, Chem. Phys. Letters 7, 78 (1971).
56. W. L. Jolly and D. N. Hendrickson, J. Am. Chem. Soc. 92, 1863 (1970).
57. J. M. Hollander and W. L. Jolly, Accounts Chem. Res. 3, 193 (1970).
58. P. Furin, R. K. Pearson, J. M. Hollander, and W. L. Jolly, Inorg. Chem. 10, 378 (1971).

59. W. L. Jolly, in "Electron Spectroscopy", ed. by D. A. Shirley (North-Holland, 1972).
60. A full discussion by the reviewer is in preparation.
61. J. A. Hashmall, B. E. Mills, D. A. Shirley, and A. Streitwieser, Jr., "A Comparison of Valence Shell and Core Ionization Potentials of Alkyl Iodides" (to be published).
62. F. Brogli, J. A. Hashmall, and E. Heilbronner, *Helv. Chim. Acta.*, in press.
63. J. B. Mann, "Atomic Structure Calculations I. Hartree Fock Energy Results for the Elements Hydrogen to Lawrencium", LA-3690, TID 4500.
64. See, for example, R. E. Block, *J. Mag. Res.* 5, 155 (1971).
65. W. H. Flygare and Jerry Goodisman, *J. Chem. Phys.* 49, 3122 (1968).
66. R. Ditchfield, D. P. Miller, and J. A. Pople, *Chem. Phys. Letters* 6, 537 (1970).
67. L. Pauling, The Nature of the Chemical Bond, 3rd Edition (Cornell University Press, Ithaca, New York, 1960).
68. W. Gordy, *Discussions Faraday Soc.* 19, 14 (1955).
69. J. Hedman, M. Klasson, C. Nordling, and B. J. Lindberg, University of Uppsala Institute of Physics Report UUIP-744 (1971).
70. C. S. Fadley and D. A. Shirley, *Phys. Rev. Letters* 21, 980 (1968).
71. C. S. Fadley and D. A. Shirley, *J. Rev. Natl. Bur. Stds.* 74A, 543 (1970).
72. Y. Baer, P.-F. Hedén, J. Hedman, M. Klasson, C. Nordling, and K. Siegbahn, *K. Phys. Scripta* 1, 55 (1970).
73. G. Brodén, S. B. M. Hagström, P.-O. Hedén, and C. Norris, *Proc. 3rd IMR Symposium Nat. Bur. Stand. Spec. Publ.* 323 (1970).
74. P.-O. Hedén, H. Löfgren, and S. B. M. Hagström, *Phys. Rev. Letters* 26, 432 (1971).

75. G. Brodén, S. B. M. Hagström, and C. Norris, Phys. Rev. Letters 24, 1173 (1971).
76. S. B. M. Hagström, Ref. 4, p. 515.
77. F. Combet Farnoux, J. de Physique 30, 521 (1969).
78. J. G. Endriz and W. W. Spicer, Phys. Rev. B 2, 1466 (1970).
79. Dorothy P.-Y. Chan and D. A. Shirley, Proceedings of the Density of States Symposium, National Bureau of Standards, November, 1969 (to be published).
80. V. Jaccarino, M. Weber, J. W. Wernick, and A. Menth, Phys. Rev. Letters 21, 1811 (1968).
81. A. C. Switendick and Albert Narath, Phys. Rev. Letters 22, 1423 (1969).
82. D. A. Shirley, "High-Resolution X-Ray Photoemission Spectrum of the Valence Bands of Gold", Lawrence Berkeley Laboratory Report LBL-277, November, 1971 (submitted to Phys. Rev.).
83. N. V. Smith and M. U. Traum, "Spin Orbit Coupling Effects in the Ultraviolet and X-Ray Photoemission Spectra of Metallic Gold", Ref. 4, p. 541.
84. C. B. Sommers and H. Amar, Phys. Rev. 188, 1117 (1969).
85. N. E. Christensen and B. O. Seraphin, Phys. Rev. B4, 3321 (1971).
86. J. W. D. Connolly and K. H. Johnson, MIT Solid State and Molecular Theory Group Report No. 72, page 19 (1970) (unpublished), and private communication.
87. M. G. Ramchandani, J. Phys. C, Solid State Phys. 3, S1 (1970).
88. M. G. Ramchandani, J. Phys. F, Metal Phys. 1, 109 (1970).
89. S. Kupratakuln, J. Phys. C, Solid State Phys. 2, S109 (1970).
90. D. E. Eastman and J. K. Cashion, Phys. Rev. Letters 24, 310 (1970).
91. D. E. Eastman, Phys. Rev. Letters 26, 1108 (1971).
92. W. C. Price, A. W. Potts, and D. G. Streets, Ref. 4, p. 187.
93. U. Gelius, Ref. 4, p. 311.
94. D. W. Turner, C. Baker, A. D. Baker, and C. R. Brundle, "Molecular Photoelectron Spectroscopy" (Wiley-Interscience, 1970).

95. U. Gelius, C. J. Allan, G. Johansson, H. Siegbahn, D. A. Allison, and K. Siegbahn, *Physica Scripta* 3, 237 (1971).
96. U. Gelius, C. J. Allen, D. A. Allison, H. Siegbahn, and K. Siegbahn, *Chem. Phys. Letters*, in press.
97. R. Prins and T. Novakov, *Chem. Phys. Letters* 2, 593 (1971).
98. C. S. Fadley and D. A. Shirley, *Phys. Rev.* 2A, 1109 (1970).
99. J. Hedman, P.-F. Hedén, C. Nordling, and K. Siegbahn, *Phys. Letters* 29A, 178 (1969).
100. Ref. 3, pages 59-61. Integrals from Ref. 101 were used in these estimates.
101. H. Brion, C. Moser, and M. Yamazaki, *J. Chem. Phys.* 30, 673 (1959).
102. D. W. Davis and D. A. Shirley, *J. Chem. Phys.* 56, 669 (1972).
103. D. W. Davis and D. A. Shirley, unpublished data (1971).
104. M. E. Schwartz, *Theoret. Chim. Acta.* 19, 396 (1970).
105. C. S. Fadley, D. A. Shirley, A. G. Freeman, P. S. Bagus, and J. V. Mallow, *Phys. Rev. Letters* 23, 1397 (1969).
106. T. Novakov, private communication, March, 1970. Reported at Uppsala Conference on Electron Spectroscopy, September, 1970.
107. G. K. Wertheim, reported at Uppsala Conference on Electron Spectroscopy September, 1970.
108. J. C. Carver, T. A. Carlson, L. C. Cain, and G. K. Schweitzer, Ref. 4, p. 803.
109. G. K. Wertheim, R. L. Cohen, A. Rosencwaig, and H. J. Guggenheim, Ref. 4, p. 813.

LEGAL NOTICE

This report was prepared as an account of work sponsored by the United States Government. Neither the United States nor the United States Atomic Energy Commission, nor any of their employees, nor any of their contractors, subcontractors, or their employees, makes any warranty, express or implied, or assumes any legal liability or responsibility for the accuracy, completeness or usefulness of any information, apparatus, product or process disclosed, or represents that its use would not infringe privately owned rights.

TECHNICAL INFORMATION DIVISION
LAWRENCE BERKELEY LABORATORY
UNIVERSITY OF CALIFORNIA
BERKELEY, CALIFORNIA 94720